--37. (New) The method of claim 34, wherein the molecule is selected from the group consisting of a lipid, carbohydrate, protein and nucleic acid.--

A marked-up version of the amended claims showing the changes made is attached hereto as **Exhibit A**.

REMARKS

Claims 1-32 were pending in the subject application. Claims 29-32 have been withdrawn from consideration by the Examiner as drawn to non-elected subject matter. By this amendment, applicants have canceled claims 29-32 without prejudice or disclaimer; amended claims 1, 7, 10, 11, 17-21, 27, and 28; and added new claims 33-37. Accordingly, upon entry of this amendment, claims 1-28, as amended, and new claims 33-37 will be pending and under examination.

Applicants maintain that the amendments to claims 1, 7, 10, 11, 17-21, 27, and 28 and the addition of claims 33-36 raise no issue of new matter. Support for amended claim 1 can be found *inter alia* in the specification as original filed on page 8, lines 13-18; page 16, line 24 through page 17, line 32; and page 18, line 26 through page 22, line 4. Support for amended claims 7 and 10 can be found *inter alia* in the specification as original filed on page 9, lines 16-23. Support for amended claim 11 can be found *inter alia* in the specification as original filed on page 9, lines 27-33. Support for amended claims 17-20 can be found *inter alia* in the specification as original filed on page 10, lines 1-3 and 14-22. Support for amended claim 21 can be found *inter alia*

in the specification as original filed on page 10, line 24 through page 11, line 30; page 16, line 24 through page 17, line 32; page 21, line 21 through page 22, line 4; and page 3, lines 4-5. Support for amended claims 27 and 28 can be found *inter alia* in the specification as original filed on page 11, lines 21-30. Support for new claims 33 and 35 can be found *inter alia* in the specification as original filed on page 2, line 33 through page 3, line 13. Support for new claim 34 can be found *inter alia* in the specification as original filed on page 2, line 19 through page 3, line 13; page 4, lines 9-24; page 10, line 24 through page 11, line 30; and page 21, line 21 through page 22, line 10. Support for new claims 36 and 37 can be found *inter alia* in the specification as original filed on page 9, lines 1-5 and page 22, lines 4-10.

Accordingly, applicants respectfully request that the Amendment be entered.

Rejection Under 35 U.S.C. §112, first paragraph

On page 3 of the February 7, 2002 Office Action, the Examiner rejected claims 1-28 under 35 U.S.C. §112, first paragraph, allegedly because the specification, while being enabling for amine-specific dyes and sulfhydryl-specific dyes, does not reasonably provide enablement for all second harmonic-active moieties. The Examiner alleged that the specification does not enable any person skilled in the art to which it pertains, or with which it is most nearly connected, to make and use the invention commensurate in scope with these claims.

The Examiner stated that enablement requires that the

specification teach those in the art to make and use the invention without undue experimentation and that the factors that must be considered in determining undue experimentation are set forth in *In re Wands* USPQ2d 14000. Factors to be considered in determining whether a disclosure would require undue experimentation include (1) the nature of the invention, (2) the state of the prior art, (3) the predictability or lack thereof in the art, (4) the amount of direction or guidance present, (5) the presence or absence of working examples, (6) the quantity of experimentation necessary, (7) the relative skill of those in the art, and (8) the breadth of the claims.

The Examiner stated that the instant claims are directed to labeling a molecule with a second harmonic-active moiety and detecting the labeled molecule at the interface using a surface selective technique and that while the specification on page 16, lines 24-26, discloses the use of amine-specific dyes and sulfhydryl-specific dyes for second-harmonic active moieties, it does not disclose the use of all second-harmonic active moieties. The Examiner alleged that second-harmonic active moieties are not well known in the art and thus one of ordinary skill in the art would have a low level of predictability in the art.

The Examiner further stated that the working examples in the specification are limited to the use of two specific dyes: (1) the sulfhydryl-specific dye 1-(2,3-epoxypropyl)-4-(5-(4-methoxyphenyl) oxazol-2-yl)pyridinium trifluoromethanesulfonate (PyMPO epoxide), and (2) the amine-specific dye 1-(3-(succinimidyloxycarbonyl)benzyl)-4-(5-(4-methoxyphenyl)oxazol-2-yl) pyridiniumbromide (PyMPO, SE). The Examiner alleged that at best, the detection of the molecule can be determined only by

using amine-specific dyes or sulfhydryl-specific dyes and not all second-harmonic active moieties. The Examiner concluded that such is not seen as sufficient to support the breath of the claims and that one skilled in the art cannot practice the claimed invention without undue experimentation, because in order to select an appropriate second harmonic active moiety, one skilled in the art would have to have a high level of predictability, in order to successfully select a second-harmonic active moiety without undue experimentation.

In response, applicants respectfully traverse this ground of rejection for the following reasons. Applicants maintain that there are numerous known examples of second-harmonic active molecules and materials in the art. In addition, general theoretical principles are known to guide the selection of a second-harmonic-active moiety or molecule. Furthermore, there are standard experimental protocols for measuring the degree of nonlinear optical activity. Applicants direct the Examiner's attention to the following references which are exemplary of the art; copies of which are attached hereto as **Exhibits 1-5**:

> Barlow S. et al. Studies of the electronic structure of metallocene-based second-order nonlinear optical dyes. J. Am. Chem. Soc. 121: 3715-3723, 1999 (**Exhibit 1**);
>
> Cheng L. et al. Experimental investigations of organic molecular nonlinear optical polarizabilities. 1. Methods and results on benzene and stilbene derivatives. J. Phys. Chem. 95: 10631-10643, 1991 (**Exhibit 2**);

Cheng L. et al. Experimental investigations of organic molecular nonlinear optical polarizabilities. 2. A study of conjugation dependences. J. Phys. Chem. 95: 10643-10652, 1991 (**Exhibit 3**);

Elshocht S. Van et al. Chiral 1,1-binaphthyl-based helical polymers as nonlinear optical materials. Chem. Phys. Lett. 309: 315-320, 1999 (**Exhibit 4**); and

Suslick, K.S. et al. Push-pull porphyrins as nonlinear optical materials J. Am. Chem. Soc. 114: 6928-6930, 1992 (**Exhibit 5**).

In addition applicants respectfully point out that there are well known methods for attaching labels to molecules which do not depend on amine or sulfhydryl groups. One reference which is exemplary of the art is:

Hermanson, G.T. Bioconjugate Techniques, Academic Press, San Diego, 1996; a compendium of synthetic techniques and references for coupling synthetic molecules to biomolecules. The Table of Contents and the first 125 pages are attached hereto as **Exhibit 6**.

Applicants maintain that the skilled artisan would know how to select an appropriate second harmonic active label and that the teachings of the specification enable the skilled artisan to practice the claimed invention without undue experimentation. Accordingly, applicants respectfully request that the Examiner reconsider and withdraw this ground of rejection.

Rejections Under 35 U.S.C. §112, second paragraph, and 35 U.S.C. §101

On page 4 of the February 7, 2002 Office Action, the Examiner rejected claims 17-28 under 35 U.S.C. §112, second paragraph, as being indefinite for failing to particularly point out and distinctly claim the subject matter which applicants regard as the invention.

Claims 17-20

The Examiner stated that claims 17-20 provide for the use of a second harmonic-active moiety, but alleged that since the claims do not set forth any steps involved in the method/process, it is unclear what method/process applicants are intending to encompass. The Examiner stated that a claim is indefinite where it merely recites a use without any active, positive steps delimiting how this use is actually practiced.

On page 5 of the February 7, 2002 Office Action, the Examiner also rejected claims 17-20 under 35 U.S.C. §101 because the claimed recitation of a use, allegedly without setting forth any steps involved in the process, results in an improper definition of a process, i.e., results in a claim which is not a proper process claim under 35 U.S.C. §101. See for example *Ex parts Dunki*, 153 USPQ 678 (Bd.App. 1967) and *Clinical Products, Ltd. v. Brenner*, 255 F. Supp. 131, 149 USPQ 475 (D.D.C. 1966).

In response, in order to expedite the prosecution of the subject application, but without conceding the correctness of the Examiner's position, applicants have amended claims 17-20 to

recite: "The method of claim 1, wherein the molecule is [as specified] and the interface is [as specified]." Applicants maintain that the steps of the methods of amended claims 17-20 are clear.

In view of the amendments and remarks made hereinabove, applicants respectfully request that the Examiner reconsider and withdraw these grounds of rejection.

Claims 21-28

On page 5 of the February 7, 2002 Office Action, the Examiner alleged that in claim 21, line 27, the recitation "exposing" is vague, and that it is unclear if exposing means that the surface physically contacts the medium or if the surface is brought in close proximity to the medium.

In response, in order to expedite the prosecution of the subject application, but without conceding the correctness of the Examiner's position, applicants have amended claim 21 to recite: "contacting the surface with a medium...". Applicants maintain that amended claim 21 is clear. Applicants note that claims 22-28 depend from claim 21.

In view of the amendments and remarks made hereinabove, applicants respectfully request that the Examiner reconsider and withdraw this ground of rejection.

Rejection Under 35 U.S.C. §102(b)

On page 5 of the February 7, 2002 Office Action, the Examiner rejected claims 1-4, 7, 8, 12, 13, 21, 23, 27 and 28 under 35

U.S.C. §102(b) as being anticipated by Quinn et al. (European Patent Application No. 0 740 156).

The Examiner stated that Quinn et al. disclose the following: (1) use of nonlinear optical methods of surface second-harmonic and sum-frequency generation to detect and quantify antibody-antigen interactions, polynucleotide hybridization and enzyme-substrate complexes (column 1, lines 7-11); (2) that antibodies, antigens, polynucleotides or enzymes are attached to a sensor surface (column 4, lines 1 and 2); (3) that a reporter molecule (label) which possess a molecular excitation close to 2f may be attached by covalent or other means to the antibody, antigen, or enzyme thereby producing a condition of resonance enhancement (column 2, lines 46-57); and (4) that the surface is into contact with a solution which may contain the complementary species. The Examiner further stated that formation of a complex between the complementary species will result in a modification of the surface nonlinear optical properties and that measurement of the magnitude, angular dependence or any other parameter dependent on changes of nonlinear optical properties such as surface second-harmonic generation can be used to determine the amount of complex formation at the surface (column 4, lines 39-49).

In response, in order to expedite the prosecution of the subject application, but without conceding the correctness of the Examiner's position, applicants have amended claims 1, 7, 21, 27, and 28.

Claim 1 now recites:

1. A method for detecting a molecule in contact with an interface, which comprises:

(a) contacting an interface with a molecule which comprises a second harmonic-active label attached to the molecule; and

(b) detecting light emitted from the interface using a surface selective technique so as to detect the second harmonic-active labeled molecule in contact with the interface, wherein the molecule is not detectable in contact with the interface using the surface selective technique in the absence of the second harmonic-active label.--

Claim 21 now recites:

21. A method for detecting a molecule in a medium, which comprises:

(a) labeling a surface with a molecule which comprises a second harmonic-active label attached to the molecule, wherein the second harmonic-active label specifically interacts with a second molecule to be detected, and wherein the second harmonic-active labeled molecule is not detectable at the surface using the surface selective technique in the absence of the second harmonic-active label,

(b) contacting the surface with a medium comprising the second molecule, thereby creating an interface at the surface,

(c) detecting the second harmonic-active labeled molecule at the interface by measuring a signal generated using a surface selective technique, and

(d) detecting a change in the signal when the second molecule interacts with the second harmonic-active labeled molecule, thereby detecting the second molecule in the medium.

Applicants note that claims 2-20 depend from claim 1 and that claims 22-28 depend from claim 21.

Applicants note that claim 1 comprises contacting an interface with a molecule which comprises a second harmonic-active label attached to the molecule and detecting the second-harmonic active labeled molecule in contact with the interface using a surface selective technique, wherein the molecule is not detectable at the interface using the surface selective technique in the absence of the second-harmonic active label. Similarly, claim 21 comprises labeling a surface with a molecule which comprises a second harmonic-active label attached to the molecule, wherein the second harmonic-active labeled molecule is not detectable at the surface using a surface selective technique in the absence of the second harmonic-active label, and detecting a change in a signal generated using the surface selective technique when a second molecule in a medium in contact with the surface interacts with the second harmonic-active labeled molecule.

Applicants further note that in Quinn et al., the "[s]econd-order optical processes originate from the field and structural discontinuity at the interface" [Quinn et al., column 2, lines 31-33], and a reporter molecule is used to resonantly enhance the surface nonlinear susceptibility [Quinn et al., column 2, lines 46 to 57]. Thus, Quinn et al. use a reporter molecule to resonantly enhance a signal that is already present. In contrast, the subject invention uses a second harmonic-active label to produce a signal that is not present in the absence of the label.

Applicants maintain that Quinn et al. do not anticipate the subject claimed invention because Quinn et al. do not disclose the use of a second harmonic-active label to detect a molecule at an interface or to detect a molecule in a medium, wherein the

molecule is not detectable using the surface selective technique in the absence of the second-harmonic active label. Accordingly, applicants respectfully request that the Examiner reconsider and withdraw this ground of rejection.

Rejections Under 35 U.S.C. §103(a)

1. Mattingly et al.

On page 6 of the February 7, 2002 Office Action, the Examiner rejected claims 5, 24 and 25 under 35 U.S.C. §103(a) as being unpatentable over Quinn et al. (European Patent Application No. 0 740 156) in view of Mattingly et al. (U.S. Patent No. 5,145,790).

The Examiner referred applicants to the teachings of Quinn et al. described above. The Examiner alleged that Quinn et al. differ from the instant invention in failing to disclose the molecule being a pollutant.

The Examiner stated that Mattingly et al. disclose specific binding reagents, such as antibodies, for detecting the presence or amount of polychlorinated biphenyls in a test sample (column 2, lines 10-34).

The Examiner alleged that it would have been obvious to one of ordinary skill in the art to use the polychlorinated biphenyl specific antibodies taught by Mattingly et al. in the method of Quinn et al. because Quinn et al. is generic with respect to the analyte that is to be detected and one would use the appropriate reagent, i.e. antibody to detect the desired analyte, in this case polychlorinated biphenyls.

In response, in order to expedite the prosecution of the subject application, but without conceding the correctness of the Examiner's position, applicants have amended claims 1 and 21 as described hereinabove. Applicants maintain that Quinn et al. do not teach or suggest the instant claimed invention for the reasons set forth above. Applicants further maintain that Mattingly et al. do not teach or suggest the use of a second harmonic-active label. Finally, even if the teachings of Quinn et al. and Mattingly et al. are combined they do not result in the instant claimed invention because they do not teach or suggest the use of a second harmonic-active label to detect a molecule at an interface or to detect a molecule in a medium, wherein the molecule is not detectable using the surface selective technique in the absence of the second-harmonic active label. Accordingly, applicants respectfully request that the Examiner reconsider and withdraw this ground of rejection.

2. Marshall et al.

On page 7 of the February 7, 2002 Office Action, the Examiner rejected claims 6, 11 and 22 under 35 U.S.C. §103(a) as being unpatentable over Quinn et al. (European Patent Application No. 0 740 156) in view of Marshall et al. (U.S. Patent No. 5,236,826).

The Examiner referred applicants to the teachings of Quinn et al. described above. The Examiner alleged that Quinn et al. differ from the instant invention in failing to disclose (1) detecting analyte molecule on a surface of a nanoparticle or polymer bead and (2) a plurality of individual second harmonic-active labels bound together to increase the overall nonlinear susceptibility of the second harmonic-active moiety.

The Examiner stated that Marshall et al. disclose the use of beads or particles which have bound to their surface a molecule, that these particles increase the surface area of the solid support and that the use of these particles increases favorable reaction kinetics through Brownian motion, thereby establishing equilibrium faster than a system with less available surface for binding.

The Examiner alleged that it would have been obvious to one of ordinary skill in the art to incorporate the use of particles as taught by Marshall et al. into the method of Quinn et al. because Marshall et al. show that these particles increase the surface area of the solid support and the use of these particles increase favorable reaction kinetics through Brownian motion, thereby establishing equilibrium faster than a system with less available surface for binding.

The Examiner also alleged that with respect to the plurality of individual second harmonic-active labels bound together in a fixed and determinate orientation with respect to each other so as to increase the overall nonlinear susceptibility of the second harmonic-active moiety as recited in the instant claims, the optimum overall nonlinear susceptibility of the second harmonic-active moiety can be determined by routine experimentation and thus would have been obvious to one of ordinary skill in the art. The Examiner further stated that it has long been settled to be no more than routine experimentation for one of ordinary skill in the art to discover an optimum value of a result effective variable. The Examiner cited the following: "[W]here the general conditions of a claim are disclosed in the prior art, it is not inventive to discover the optimum of workable ranges by routine

experimentation." Application of Aller, 220 F.2d 454,456, 105 USPQ 233, 235-236 (C.C.P.A. 1955). "No invention is involved in discovering optimum ranges of a process by routine experimentation." *Id.* at 458,105 USPQ at 236-237. The "discovery of an optimum value of a result effective variable in a known process is ordinarily within the skill of the art." Application of Boesch, 617 F.2d 272, 276, 205 USPQ 215, 218-219 (C.C.P.A. 1980).

In response, in order to expedite the prosecution of the subject application, but without conceding the correctness of the Examiner's position, applicants have amended claims 1, 11 and 21 as described hereinabove. Applicants maintain that Quinn et al. do not teach or suggest the instant claimed invention for the reasons set forth above. Applicants further maintain that Marshall et al. do not teach or suggest the use of a second harmonic-active label. Finally, even if the teachings of Quinn et al. and Marshall et al. are combined they do not result in the instant claimed invention because they do not teach or suggest the use of a second harmonic-active label to detect a molecule at an interface or to detect a molecule in a medium, wherein the molecule is not detectable using the surface selective technique in the absence of the second-harmonic active label. Accordingly, applicants respectfully request that the Examiner reconsider and withdraw this ground of rejection.

3. Buechler et al.

On page 8 of the February 7, 2002 Office Action, the Examiner rejected claim 9 under 35 U.S.C. §103(a) as being unpatentable over Quinn et al. (European Patent Application No. 0 740 156) in view of Buechler et al. (U.S. Patent No. 6,194,222).

The Examiner referred applicants to the teachings of Quinn et al. described above. The Examiner alleged that Quinn et al. differ from the instant invention in failing to disclose the non-specific interaction being an electrostatic interaction.

The Examiner stated that Buechler et al. disclose labels which are bound to the molecule by electrostatic interactions (column 21, lines 1-10), that these interactions allow for an immunoassay system that is simple, rapid and reliable, and that reliability in an immunoassay system is critical for the accurate measurement of the analyte (column 1, lines 40-43).

The Examiner alleged that it would have been obvious to one of ordinary skill in the art to incorporate electrostatic interactions as taught by Buechler et al. for the binding of the second harmonic-active moiety to the molecule of Quinn et al. because Buechler et al. show that these interactions allow for an immunoassay system that is simple, rapid and reliable.

In response, in order to expedite the prosecution of the subject application, but without conceding the correctness of the Examiner's position, applicants have amended claim 1 as described hereinabove. Applicants maintain that Quinn et al. do not teach or suggest the instant claimed invention for the reasons set forth above. Applicants further maintain that Buechler et al. do not teach or suggest the use of a second harmonic-active label. Finally, even if the teachings of Quinn et al. and Buechler et al. are combined they do not result in the instant claimed invention because they do not teach or suggest the use of a second harmonic-active label to detect a molecule at an

interface, wherein the molecule is not detectable using the surface selective technique in the absence of the second-harmonic active label. Accordingly, applicants respectfully request that the Examiner reconsider and withdraw this ground of rejection.

4. Wang et al.

On page 9 of the February 7, 2002 Office Action, the Examiner rejected claim 10 under 35 U.S.C. §103(a) as being unpatentable over Quinn et al. (European Patent Application No. 0 740 156) in view of Wang et al. (U.S. Patent No. 5,696,157).

The Examiner referred applicants to the teachings of Quinn et al. described above. The Examiner alleged that Quinn et al. differ from the instant invention in failing to disclose that the second harmonic-active moiety is specific for an amine group.

The Examiner stated that Wang et al. disclose labels which are specific for amine groups, that these amine-reactive dyes are of particular relevance as they are commonly used to label proteins and polypeptides (column 13, lines 50-63), and that these labels are able to preferentially label a specific ingredient or component in a sample and enable the researcher to determine the presence, quantity or location of that specific ingredient or component (column 1, lines 11-19).

The Examiner alleged that it would have been obvious to one of ordinary skill in the art to substitute the label as taught by Wang et al. for the label of Quinn et al. because Wang et al. show that these amine labels are of particular relevance as they are commonly used to label proteins and polypeptides and that these labels are able to preferentially label a specific

ingredient or component in a sample and enable the researcher to determine the presence, quantity or location of that specific ingredient or component.

The Examiner alleged furthermore that since the amine-specific dyes of Wang et al. are within the chemical class as disclosed in the instant specification on page 16, line 24 (amine-specific dyes), it is considered that the amine-specific dye of Wang et al. would be a second-harmonic active moiety.

In response, in order to expedite the prosecution of the subject application, but without conceding the correctness of the Examiner's position, applicants have amended claims 1 and 10 as described hereinabove. Applicants maintain that Quinn et al. do not teach or suggest the instant claimed invention for the reasons set forth above. Applicants further maintain that Wang et al. do not teach or suggest the use of a second harmonic-active label. Applicants note that Examiner has not provided any reference which teaches or suggests that all amine-specific dyes are second-harmonic active moieties as alleged by the Examiner. Finally, even if the teachings of Quinn et al. and Wang et al. are combined they do not result in the instant claimed invention because they do not teach or suggest the use of a second harmonic-active label to detect a molecule at an interface, wherein the molecule is not detectable using the surface selective technique in the absence of the second-harmonic active label. Accordingly, applicants respectfully request that the Examiner reconsider and withdraw this ground of rejection.

5. Eisenthal

On page 10 of the February 7, 2002 Office Action, the Examiner

rejected claims 14 and 16 under 35 U.S.C. §103(a) as being unpatentable over Quinn et al. (European Patent Application No. 0 740 156) in view of Eisenthal (Photochemistry and photophysics of liquid interfaces by second harmonic spectroscopy, J. Phvs. Chem 1996, 100: 12997-13006).

The Examiner referred applicants to the teachings of Quinn et al. described above. The Examiner alleged that Quinn et al. differ from the instant invention in failing to disclose an air-water interface and a water-glass interface.

The Examiner stated that Eisenthal discloses the investigation of interface properties using second-harmonic spectroscopy and studies of molecules at the silica/water interface and at the air/water interface, that the study of molecules at these interfaces provide new information and insights into equilibrium and dynamic processes occurring at interfaces, and that these liquid interfaces not only are of great scientific interest but also directly impact many areas of medicine and technology (page 12998).

The Examiner alleged that it would have been obvious to one of ordinary skill in the art to incorporate the interfaces as taught by Eisenthal into the method of Quinn et al. because Eisenthal shows that the study of molecules at these interfaces provide new information and insights into equilibrium and dynamic processes occurring at interfaces and that these liquid interfaces not only are of great scientific interest but also directly impact many areas of medicine and technology.

In response, in order to expedite the prosecution of the subject

application, but without conceding the correctness of the Examiner's position, applicants have amended claim 1 as described hereinabove. Applicants maintain that Quinn et al. do not teach or suggest the instant claimed invention for the reasons set forth above. Even if the teachings of Quinn et al. and Eisenthal et al. are combined they do not result in the instant claimed invention because they do not teach or suggest attaching a second harmonic-active label to a molecule in order to detect the molecule at an interface, wherein the molecule is not detectable using the surface selective technique in the absence of the second-harmonic active label. Accordingly, applicants respectfully request that the Examiner reconsider and withdraw this ground of rejection.

6. Conboy et al.

On page 11 of the February 7, 2002 Office Action, the Examiner rejected claim 15 under 35 U.S.C. §103(a) as being unpatentable over Quinn et al. (European Patent Application No. 0 740 156) in view of Conboy et al. (Studies of alkane/water interfaces by total internal reflection second harmonic generation. J. Phy. Chem. 1994, 98: 9688-9692).

The Examiner referred applicants to the teachings of Quinn et al. described above. The Examiner alleged that Quinn et al. differ from the instant invention in failing to disclose an oil-water interface.

The Examiner stated that Conboy et al. disclose the investigation of oil-water interfaces, that the study of this interface demonstrates the utility of using second harmonic generation to

measure properties of the oil-water interface in the absence of any optical resonances and expand the range of systems which can be examined by second harmonic generation (abstract and introduction), and that Conboy et al. also disclose that there is a high interest in the characterization of oil-water interfaces because of the central role which they play in many areas of chemistry, physics, and biology.

The Examiner alleged that it would have been obvious to one of ordinary skill in the art to incorporate the oil-water interface as taught by Conboy et al. into the method of Quinn et al. because Conboy et al. show that the study of this interface demonstrates the utility of using second harmonic generation to measure properties of oil-water interface in the absence of any optical resonances and expand the range of systems which can be examined by second harmonic generation and because Conboy et al. also show that there is a high interest in the characterization of oil-water interfaces because of the central role which they play in may areas of chemistry, physics, and biology.

In response, in order to expedite the prosecution of the subject application, but without conceding the correctness of the Examiner's position, applicants have amended claim 1 as described hereinabove. Applicants maintain that Quinn et al. do not teach or suggest the instant claimed invention for the reasons set forth above. Even if the teachings of Quinn et al. and Conboy et al. are combined they do not result in the instant claimed invention because they do not teach or suggest attaching a second harmonic-active label to a molecule in order to detect the molecule at an interface, wherein the molecule is not detectable using the surface selective technique in the absence of the

second-harmonic active label. Accordingly, applicants respectfully request that the Examiner reconsider and withdraw this ground of rejection.

7. Buechler et al.

On page 12 of the February 7, 2002 Office Action, the Examiner rejected claim 26 under 35 U.S.C. §103(a) as being unpatentable over Quinn et al. (European Patent Application No. 0 740 156) in view of Tadano et al. (U.S. Patent No. 5,962,248).

The Examiner referred applicants to the teachings of Quinn et al. described above. The Examiner alleged that Quinn et al. differ from the instant invention in failing to disclose the molecule being a chloride ion.

The Examiner stated that Tadano et al. disclose a reagent for detecting chloride ions in a sample (column 1, line 66 - column 2, line 10).

The Examiner alleged that it would have been obvious to one of ordinary skill in the art to use the enzyme substrate specific for chloride ions taught by Tadano et al. in the method of Quinn et al. because Quinn et al. is generic with respect to the analyte that is to be detected and one would use the appropriate reagent, i.e. enzyme substrate to detect the desired analyte, in this case chloride ion.

In response, in order to expedite the prosecution of the subject application, but without conceding the correctness of the Examiner's position, applicants have amended claim 21 as described hereinabove. Applicants maintain that Quinn et al. do

not teach or suggest the instant claimed invention for the reasons set forth above. Applicants further maintain that Tadano et al. do not teach or suggest the use of a second harmonic-active label. Finally, even if the teachings of Quinn et al. and Tadano et al. are combined they do not result in the instant claimed invention because they do not teach or suggest the use of a second harmonic-active label to detect a molecule in a medium, wherein the molecule is not detectable using the surface selective technique in the absence of the second-harmonic active label. Accordingly, applicants respectfully request that the Examiner reconsider and withdraw this ground of rejection.

Supplemental Information Disclosure Statement

This Supplemental Information Disclosure Statement is submitted under 37 C.F.R. §1.97(c)(2) to supplement the Information Disclosure Statement filed on July 10, 2001 in connection with the subject application.

According to 37 C.F.R. §1.97(c), an Information Disclosure Statement shall be considered by the U.S. Patent and Trademark Office if filed before the mailing date of any of a Final Office Action under 37 C.F.R. §1.113, a Notice of Allowance under 37 C.F.R. §1.311, or any other Office Action which closes prosecution in the application, provided that the Information Disclosure Statement is accompanied by either (1) the statement specified in 37 C.F.R. §1.97(e)(1) or §1.97(e)(2) or (2) the fee set forth in 37 C.F.R. §1.17(p). Applicants are filing this Supplemental Information Disclosure Statement before any of a Final Office Action under 37 C.F.R. §1.113, a Notice of Allowance under 37 C.F.R. §1.311, or any other Office Action which closed

prosecution in the application. The fee set forth in 37 C.F.R. §1.17(p) is ONE HUNDRED EIGHTY DOLLARS ($180.00) and a check including this amount is enclosed.

In accordance with their duty of disclosure under 37 C.F.R. §1.56, applicants would like to direct the Examiner's attention to the disclosures which are listed on the attached Form PTO-1449 (**Exhibit B**) and attached hereto as **Exhibits C-E:**

1. Khatchatouriants, A. et al. GFP is a selective non-linear optical sensor of electrophysical processes in *Caenorhabditis elegans*. Biophysical J. 79: 2345-52, November 2000 (**Exhibit C**);

2. Lewis, A. et al. Second-harmonic generation of biological interfaces: probing the membrane protein bacteriorhodopsin and imaging membrane potential around GFP molecules at specific sites in neuronal cells of *C. elegans*. Chemical Physics 245: 133-144, 1999 (**Exhibit D**); and

3. Peleg, G. et al. Nonlinear optical measurement of membrane potential around single molecules at selected cellular sites. Proc. Natl. Acad. Sci. 96: 6700-4, June 1999 (**Exhibit E**).

In summary, in view of the amendments and remarks made hereinabove, applicants respectfully request that the Examiner reconsider and withdraw the various grounds of rejection set forth in the February 7, 2002 Office Action and allow the claims now pending in the subject application.

If a telephone conference would be of assistance in advancing prosecution of the subject application, applicants' undersigned attorney invites the Examiner to telephone the number provided below.

No fee other than the enclosed $649.00 fee ($9.00 for filing an additional claim, plus $460.00 for a three month extension of time plus $180.00 for filing an Information Disclosure Statement) is deemed necessary in connection with the filing of this Amendment and Supplemental Information Disclosure Statement. However, if an additional fee is required, authorization is hereby given to charge the amount of any such fee to Deposit Account No. 03-3125.

Respectfully submitted,

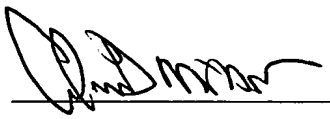

John P. White
Registration No. 28,678
Alan D. Miller
Registration No. 42,889
Attorneys for Applicants
Cooper & Dunham LLP
1185 Ave of the Americas
New York, New York 10036
(212) 278-0400

I hereby certify that this correspondence is being deposited this date with the U.S. Postal Service with sufficient postage as first class mail in an envelope addressed to: Assistant Commissioner for Patents, Washington, D.C. 20231.

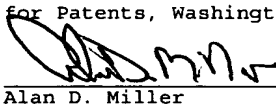

8/6/02

Alan D. Miller Date
Reg. No. 42,889

Marked-up Version of Amended Claims

Additions to the text are indicated by underlining; deletions are indicated by square brackets.

--1. (Amended) A method for detecting a molecule in contact with [at] an interface, which comprises:

[labeling the molecule with a second harmonic-active moiety]
(a) contacting an interface with a molecule which comprises a second harmonic-active label attached to the molecule; and

(b) [detecting the labeled molecule at the interface using a surface selective technique] detecting light emitted from the interface using a surface selective technique so as to detect the second harmonic-active labeled molecule in contact with the interface, wherein the molecule is not detectable in contact with the interface using the surface selective technique in the absence of the second harmonic-active label.--

--7. (Amended) The method of claim 1, wherein the second harmonic-active [moiety] label is bound to the molecule by a specific interaction or a non-specific interaction.--

--10. (Amended) The method of claim 1, wherein the second harmonic-active [moiety] label is specific for an amine group or a sulfhydryl group on the molecule.--

--11. (Amended) The method of claim 1, wherein the second harmonic-active label [moiety] comprises a plurality of individual second harmonic-active moieties [labels] which each have a nonlinear susceptibility and are bound together in a fixed and determinate orientation with respect to each other so as to increase the overall nonlinear susceptibility of the second harmonic-active label [moiety].--

--17. (Amended) [Use of t]The method of claim 1, wherein the molecule is [to detect binding of] a protein and the interface is at [to] a receptor on a membrane.--

--18. (Amended) [Use of t]The method of claim 1, wherein the molecule is on a viral surface [to detect binding of a virus] and the interface is at [to] a cell surface.--

--19. (Amended) [Use of t]The method of claim 1, wherein the molecule is a protein and the interface is at a protein [to study protein-protein interaction at an interface].--

--20. (Amended) [Use of t]The method of claim 1, wherein the molecule is on a cell and the interface is at a cell surface [to study cell-cell interaction].--

--21. (Amended) A method for detecting a molecule in a medium, which comprises:

(a) labeling a surface with a [second harmonic-active

moiety wherein the second harmonic-active moiety specifically interacts with the molecule to be detected,] molecule which comprises a second harmonic-active label attached to the molecule, wherein the second harmonic-active label specifically interacts with a second molecule to be detected, and wherein the second harmonic-active labeled molecule is not detectable at the surface using the surface selective technique in the absence of the second harmonic-active label,

(b) [exposing] contacting the surface with a [to the] medium comprising the second molecule, thereby creating an interface at the surface,

(c) detecting the second harmonic-active [moiety] labeled molecule at the interface by measuring a signal generated using a surface selective technique, and

(d) detecting a change in the signal when the second molecule interacts with the second harmonic-active [moiety] labeled molecule, thereby detecting the second molecule in the medium.--

--27. (Amended) The method of claim 21, wherein the interaction between the second harmonic-active labeled molecule [moiety] and the molecule to be detected is an antibody-antigen interaction.--

--28. (Amended) The method of claim 21, wherein the medium contains an amount of the molecule to be detected, the change in the signal when the molecule interacts with the second harmonic-active labeled molecule [moiety] is a quantitative change, and the amount of the

molecule in the medium can be determined from the change in the signal.--

Studies of the Electronic Structure of Metallocene-Based Second-Order Nonlinear Optical Dyes

Stephen Barlow,[†] Heather E. Bunting,[‡] Catherine Ringham,[‡] Jennifer C. Green,[‡] Gerold U. Bublitz,[#] Steven G. Boxer,[#] Joseph W. Perry,[§] and Seth R. Marder*[,§]

Contribution from the Beckman Institute, 139-74, California Institute of Technology, Pasadena, California 91125, Inorganic Chemistry Laboratory, University of Oxford, South Parks Road, Oxford, OX1 3QR, UK, Department of Chemistry, Stanford University, Stanford, California 94305-5080, Jet Propulsion Laboratory, California Institute of Technology, Pasadena, California 91109, and Department of Chemistry, University of Arizona, Tucson, Arizona 85721

Received August 27, 1998

Abstract: This paper describes a simple orbital picture for understanding the optical transitions and the second-order nonlinear optical response of metallocene-based chromophores of the form metallocene−(π-bridge)−acceptor, and experimental studies to test this model. From a combination of UV photoelectron spectroscopy, cyclic voltammetry, and density functional calculations, it is deduced that the three highest occupied orbitals are little perturbed from the parent metallocenes, that the HOMO-3 is a π-orbital delocalized between the metallocene cyclopentadienyl ring and the unsaturated bridge, and that the LUMO is acceptor based. The lowest energy transition in the UV/visible/near-IR spectra of these compounds is assigned to a metal-to-acceptor transition, while the higher energy transition is attributed to a transition to the acceptor-based LUMO from the delocalized HOMO-3 orbital. The variations in oscillator strength can be rationalized by considering the low-energy transition as borrowing intensity from the high-energy transition. Stark spectroscopy confirms that large dipole moment changes are associated with both transitions, as expected from our assignment. These dipole moment changes indicate that, according to the perturbation theory-derived expression for the first hyperpolarizability, β, both transitions contribute significantly to the observed optical nonlinearity.

Introduction

There has been considerable interest in the second-order nonlinear optical (NLO) properties of organometallic chromophores.[1−3] Powder second harmonic generation (SHG) efficiencies 62 and 220 times that of urea were found for *Z*-1-ferrocenyl-2-(*p*-nitrophenyl)ethylene, **Fc[1]1** (Figure 1),[4] and *E*-1-ferrocenyl-2-(*N*-methylpyridinium-4-yl)ethylene iodide, **Fc[1]3-I** (Figure 1),[5] respectively. These properties arise from the combination of moderate molecular first hyperpolarizabilities, β, with noncentrosymmetric crystal structures. More recent studies of metallocene-based chromophores have focused on the determination and understanding of molecular properties, especially using electric field induced second harmonic generation (EFISH).[6−13] EFISH yields values of $\mu\beta$, the vectorial projection of the hyperpolarizability along the molecular dipole moment direction; $\mu\beta$ is also a figure of merit for the NLO behavior of materials rendered noncentrosymmetric by poling chromophores in a polymer matrix. Ferrocene derivatives with very large values of $\mu\beta$, comparable with the best all-organic chromophores, are now known; 11200 × 10^{-48} esu for **Fc[4]6** (Figure 2a)[12] vs 15000 × 10^{-48} esu for **1** (Figure 2b).[14,15]

The two-level model[16,17] relates the static molecular hyperpolarizability, $\beta(0)$, to characteristics of the molecule's optical

* To whom correspondence should be addressed at the University of Arizona.
† Beckman Institute. Present address: Inorganic Chemistry Laboratory.
‡ Inorganic Chemistry Laboratory.
# Stanford University.
§ Beckman Institute, Jet Propulsion Lab, and University of Arizona.

(1) Marder, S. R. In *Inorganic Materials*, 2nd ed.; Bruce, D. W., O'Hare, D., Eds.; Wiley: Chichester, 1996, and references therein.
(2) Long, N. J. *Angew. Chem., Int. Ed. Engl.* **1995**, *34*, 21−38 and references therein.
(3) Verbiest, T.; Houbrechts, S.; Kauranen, M.; Clays, K.; Persoons, A. *J. Mater. Chem.* **1997**, *7*, 2175−2189 and references therein.
(4) Green, M. L. H.; Marder, S. R.; Thompson, M. E.; Bandy, J. A.; Bloor, D.; Kolinsky, P. V.; Jones, R. J. *Nature* **1987**, *330*, 360−362.
(5) Marder, S. R.; Perry, J. W.; Schaefer, W. P.; Tiemann, B. G. *Organometallics* **1991**, *10*, 1896−1901.
(6) Calabrese, J. C.; Cheng, L.-T.; Green, J. C.; Marder, S. R.; Tam, W. *J. Am. Chem. Soc.* **1991**, *113*, 7227−7232.
(7) Doisneau, G.; Balavoine, G.; Fillebeen-Khan, T.; Clinet, J.-C.; Delaire, J.; Ledoux, I.; Loucif, R.; Pucetti, G. *J. Organomet. Chem.* **1991**, *1991*, 299−304.
(8) Loucif-Saïbi, R.; Delaire, J. A.; Bonazzola, L.; Doisneau, G.; Balavoine, G.; Fillebeen-Khan, T.; Ledoux, I.; Puccetti, G. *Chem. Phys.* **1992**, *167*, 369−375.
(9) Yuan, Z.; Taylor, N. J.; Sun, Y.; Marder, T. B.; Williams, I. D.; Cheng, L.-T. *J. Organomet. Chem.* **1993**, *449*, 27−37.
(10) Blanchard-Desce, M.; Runser, C.; Fort, A.; Barzoukas, M.; Lehn, J.-M.; Bloy, V.; Alain, V. *Chem. Phys.* **1995**, *199*, 253−261.
(11) Alain, V.; Blanchard-Desce, M.; Chen, C. T.; Marder, S. R.; Fort, A.; Barzoukas, M. *Synth. Met.* **1996**, *81*, 133−136.
(12) Alain, V.; Fort, A.; Barzoukas, M.; Chen, C. T.; Blanchard-Desce, M.; Marder, S. R.; Perry, J. W. *Inorg. Chim. Acta* **1996**, *242*, 43.
(13) Alagesan, K.; Chandra-Ray, P.; Kumar-Das, P.; Samuleson, A. G. *Curr. Sci.* **1996**, *70*, 69−71.
(14) Ahlheim, M.; Barzoukas, M.; Bedworth, P. V.; Blanchard-Desce, M.; Fort, A.; Hu, Z.-Y.; Marder, S. R.; Perry, J. W.; Runser, C.; Staehelin, M.; Zysset, B. *Science* **1996**, *271*, 335−337.
(15) These $\mu\beta(2\omega)$ values were obtained by EFISH at 1.907 μm in chloroform (**Fc″[4]6**) or dichloromethane (**1**). The dispersion-corrected $\mu\beta(0)$ values are substantially lower: a value of 5000 × 10^{-48} esu is estimated for **1**.
(16) Oudar, J. L.; Chemla, D. S. *J. Chem. Phys.* **1977**, *66*, 2664−2668.
(17) Oudar, J. L. *J. Chem. Phys.* **1977**, *67*, 446−457.

10.1021/ja9830896 CCC: $18.00
Published on Web 04/02/1999

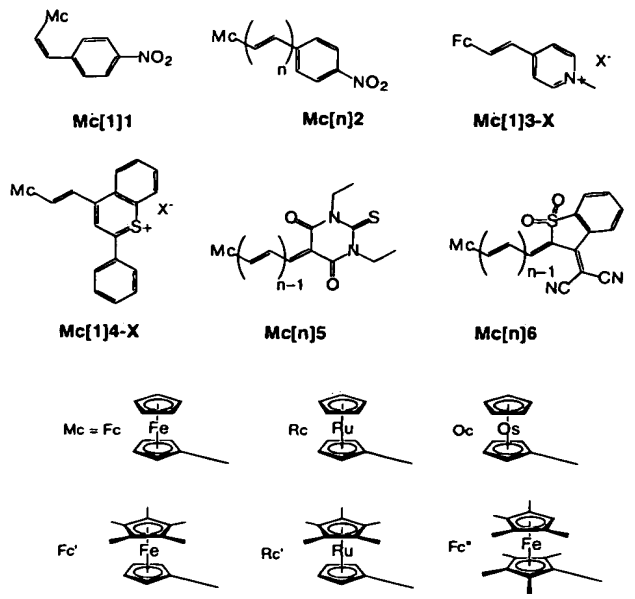

Figure 1. Structures of metallocene-based NLO chromophores discussed in this work.

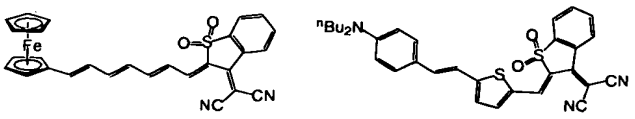

$\mu\beta(2\omega) = 11200 \times 10^{-48}$ esu

$\mu\beta(2\omega) = 15000 \times 10^{-48}$ esu

$\mu\beta(0) = 5000 \times 10^{-48}$ esu

Figure 2. Structures of highly efficient (a) organometallic[12] and (b) organic[14] NLO chromophores, together with $\mu\beta(2\omega)$ values determined by EFISH at 1.907 μm in chloroform (**Fc[4]6**) or dichloromethane (**1**). The dispersion-corrected static $\mu\beta(0)$ value for **1** was estimated by using the two-level model.[17]

transitions through the equation:

$$\beta(0) \propto (\mu_{ee} - \mu_{gg})\frac{\mu_{ge}^2}{E_{ge}^2} \quad (1)$$

where μ_{ee} and μ_{gg} are excited and ground-state dipole moments, respectively, μ_{ge} is the transition dipole moment, and E_{ge} is the transition energy. Thus, to a first approximation, trends in β can be inferred from knowledge of these parameters. Molecules with intense low-energy charge-transfer transitions will have large β.

In the case of organic donor–acceptor dyes such as *E*-4-(dimethylamino)-4′-nitrostilbene, a single low-energy charge-transfer transition is observed and dominates the NLO response.[17] However, the ultraviolet/visible/near-infrared (UV–vis–NIR) spectra of analogous molecules with metallocene donors show *two* low-energy transitions. To develop design guidelines for metallocene dyes, it is helpful to know which transitions contribute significantly to the NLO response and to understand the molecular origin of these transitions. We previously suggested assignments for the two transitions (model I) based upon the spectral trends observed with variation of chromophore structure, and upon extended Hückel calculations for **Fc[1]2**.[6] In this model, the highest occupied orbitals were the essentially nonbonding $d_{z^2}/d_{x^2-y^2}/d_{xy}$ orbitals of the metal (**M**), while the next highest orbital (HOMO-3, π) had mainly cyclopentadienyl and conjugated bridge, with little metal, character. The LUMO (**A**) was localized on the acceptor, while higher in energy was an orbital (LUMO+1) largely localized on the conjugated bridge, but with a small degree of acceptor and metal d character, hereafter referred to as π^*. The lower energy (LE) of the two transitions was assigned to a charge-transfer transition between the HOMO and the bridge-localized LUMO+1; the possibility of a direct HOMO–LUMO transition was considered less likely owing to the small spatial overlap between these orbitals. The higher energy (HE) transition was assigned to a transition from π to LUMO. The substantial dipole moment changes expected for both transitions, together with their low energies and high oscillator strengths, suggested *both* transitions should contribute to the observed NLO response. A more quantitative analysis of the spectra of these compounds was described by Kanis, Ratner, and Marks,[18–20] using Zerner intermediate neglect of differential overlap (ZINDO) calculations. The calculations were able to predict the energies of the HE transitions for a series of ferrocene derivatives within 0.3 eV, but were somewhat less accurate in predicting the energies of the LE transitions (a discrepancy of ca. 0.8 eV being obtained between calculation and experiment for **Fc[1]1**) and consistently significantly underestimated the intensities of the LE transitions. Sum over states (SOS) calculation of β gave rather good agreement with experiment. The LE transition was assigned as a metal-localized ligand-field (d–d) transition with little contribution to β, while the HE transition was identified as the major contributor to β and was described as a metal–acceptor transition. Hereafter, these assignments are referred to as model II. The previous assignments discussed above (models I and II) are approximations of the true electron redistributions associated with the two transitions. Such a simplified model is useful if it allows one to develop a chemically intuitive picture of the relationship between a chromophore's structure and its linear and nonlinear optical properties, and if the model has predictive power. Full computation of the optical properties of this class of molecules would be interesting; however, accurate reproduction of the *linear* optical properties of these molecules has not been achieved with any computational method.

Recently, additional examples of metallocene–bridge–acceptor dyes have been synthesized;[11,12] these have greater structural variation than within the series available when models I and II were proposed, and, most notably, include molecules with considerably stronger acceptor groups. Neither model I nor II is fully satisfactory in rationalizing the observed spectral trends in this expanded class of metallocene dyes. We have, therefore, attempted to develop a more refined description of the transitions (model III), building upon models I and II. Here we describe model III and compare its predictions with observed trends in UV–vis–NIR spectra. We also present additional data—photoelectron spectroscopy, electrochemistry, and Stark spectroscopy—for both previously reported and new compounds, which are consistent with model III and which yield additional insight into the orbital structure of metallocene–(π-bridge)–acceptor chromophores, and thus, into the origin of the NLO response of this class of compounds.

(18) Kanis, D. R.; Ratner, M. A.; Marks, T. J. *J. Am. Chem. Soc.* **1990**, *112*, 8203–8204.
(19) Kanis, D. R.; Ratner, M. A.; Marks, T. J. *J. Am. Chem. Soc.* **1992**, *114*, 10338–10357.
(20) Kanis, D. R.; Ratner, M. A.; Marks, T. J. *Chem. Rev.* **1994**, *94*, 195–242.

Table 1. Ionization Energies (eV) for *p*-Nitrostyrene

assignment	π_4	π_3	π_2	NO_2						
I.E.	9.29	10.05	10.75	11.15	12.42	12.86	13.8	14.8	15.6	16.5

Results and Discussion

Model for the Origin of the Spectra. The spectroscopic properties of this class of molecules can largely be accounted for as follows. The highest occupied molecular orbitals correspond to the predominately nonbonding, nearly degenerate $d_{z^2}/d_{x^2-y^2}/d_{xy}$ orbitals (**M**) of the metal. The next highest orbital (HOMO-3, π) is formed from a combination of the highest occupied cyclopentadienyl orbital and the highest occupied π-bridge orbital. The LUMO (which we will refer to as **A**) is largely localized on the acceptor, but also has a small bridge contribution. The LE absorption is a **M**→**A** transition, while the HE absorption is a π→**A** transition.[21] The assignment of the HE transition is, therefore, equivalent to that in model I, but the present model differs in the identification of the acceptor orbital of the LE transition. Model I invoked the π-bridge based LUMO+1, owing to the low spatial overlap between **M** and **A**; however, some of the spectral data (vide infra) are in conflict with that assignment while the observed intensities may be accounted for in terms of "intensity borrowing". Specifically, mixing of the π→**A** excited state (e') into the ground state (g) and mixing between **M**→**A** (e) and π→**A** (e') excited states allows both ground and **M**→**A** states to gain bridge character and thus experience greater spatial overlap with one another. Perturbation theory dictates that the degree of this mixing, and hence the **M**→**A** oscillator strength, will depend inversely upon the energetic separations between the ground and π→**A** excited state, $\Delta E_{ge'}$, and between the **M**→**A** and π→**A** excited states, $\Delta E_{ee'}$. Thus, it should be possible to use the present model (model III) to make qualitative predictions of trends in both transition energies and transition intensities.

Kanis, Ratner, and Marks also suggested that the LE transition could borrow intensity from the HE transition and that neglect of the vibrational coupling responsible for this borrowing in the ZINDO calculations could account for the underestimation of the LE transition intensity. In their model (model II) this corresponds to a d−d transition borrowing **M**→**A** character; in contrast, the present model (model III) considers a **M**→**A** transition borrowing from a π→**A** transition.

The three models are summarized pictorially for **Mc[1]2** in Figure 3. In the following sections we present experimental evidence in support of model III. The structures of the compounds discussed are shown in Figure 1; the compounds were prepared as described previously,[4-6,11,12,22,23] or as described in the Supporting Information.

UV Photoelectron Spectroscopy (UV-PES). He I and He II photoelectron (PE) spectra were recorded for **Fc[1]1**, **Fc[1]2**, **Rc[1]1**, and **Oc[1]2**, together with the model compound *p*-nitrostyrene. The ionizations observed for *p*-nitrostyrene are summarized in Table 1,[24] together with assignments made by comparison with the PE spectra of styrene[25] and nitrobenzene.[26]

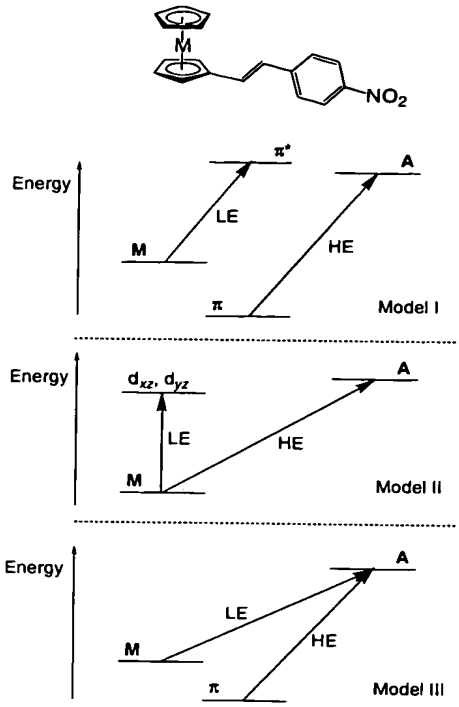

Figure 3. Schematic representation of the orbitals identified by the three models as most important in the low (LE) and high (HE) energy transitions for the spectra of metallocene−(π-bridge)−acceptor chromophores. The horizontal scale represents the approximate spatial location of the orbitals along the molecule.

The spectra of the metallocene−bridge−acceptor dyes (Figure 4; Table 2)[24] can be assigned by comparison with the spectra of *p*-nitrostyrene and the appropriate parent metallocenes.[27-29] The lowest energy ionizations of metallocenes correspond to removal of electrons from the occupied $d_{x^2-y^2}/d_{xy}$ (e_2') and d_{z^2} (a_1') orbitals. For ferrocene two distinct transitions are observed, while in ruthenocene the energy difference cannot be resolved and in osmocene three transitions are seen owing to spin−orbit splitting of the $^2E_2$ ion state. The lowest energy ionizations, A, for the 1-metallocenyl-2-(*p*-nitrophenyl)ethylenes closely resemble those of the respective parent metallocenes, both in terms of the splitting of the bands and their relative enhancement in the He II spectra, but are all shifted by ca. 0.1 eV to higher energy. The magnitude of this shift, coupled with the constant splittings, suggests very little perturbation of the d-levels by the substituent, i.e., that the HOMO in these molecules can be regarded as metal-based.

The next lowest ionization energy (IE) band in the parent unsubstituted metallocenes is due to ionization of the e_1' orbitals; these are a combination of the e_1 orbitals of the two cyclopentadienyl rings, possibly with some contribution from the p_x and p_y orbitals of the metal. The variation in the IE of this band between ferrocene, ruthenocene, and osmocene is much less than

(21) We also expect d−d transitions to be present in the visible part of the spectrum. However, we expect these to be very weak compared to the two charge-transfer transitions and to make negligible contribution to the observed optical nonlinearity. Therefore, they are not considered further in our discussion.

(22) Toma, S.; Gáplovsky, A.; Elecko, P. *Chem. Pap.* **1985**, *39*, 115−124.

(23) Bunting, H. E.; Green, M. L. H.; Marder, S. R.; Thompson, M. E.; Bloor, D.; Kolinsky, P. V.; Jones, R. J. *Polyhedron* **1992**, *11*, 1489−1499.

(24) He I and He II PE spectra for *p*-nitrostyrene, **Fc[1]1**, **Fc[1]2**, **Rc[1]1**, and **Oc[1]2** are presented as Supporting Information.

(25) Rabalais, J. W.; Colton, R. J. *J. Electron Spectrosc.* **1972**, *1*, 83.

(26) Rabalais, J. W. *J. Chem. Phys.* **1972**, *57*, 960.

(27) Evans, S.; Green, M. L. H.; Jewitt, B.; Orchard, A. F.; Pygall, C. F. *J. Chem. Soc., Faraday Trans. 2* **1972**, *68*, 1847−1865.

(28) Cauletti, C.; Green, J. C.; Kelly, M. R.; Robbins, J.; Smart, J. C. *J. Electron Spectrosc. Rel. Phenom.* **1980**, *19*, 327−353.

(29) Cooper, G.; Green, J. C.; Payne, M. P. *Mol. Phys.* **1988**, *63*, 1031.

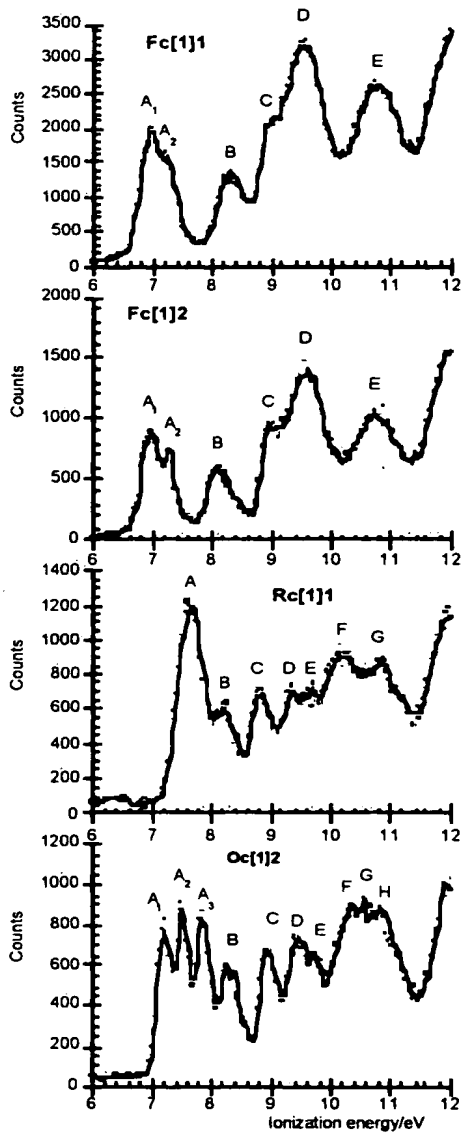

Figure 4. He I photoelectron spectra of *Z*-1-ferrocenyl-2-(*p*-nitrophenyl)ethylene, **Fc[1]1**, *E*-1-ferrocenyl-2-(*p*-nitrophenyl)ethylene, **Fc[1]2**, *Z*-1-ruthenocenyl-2-(*p*-nitrophenyl)ethylene, **Rc[1]1**, and *E*-1-osmocenyl-2-(*p*-nitrophenyl)ethylene, **Oc[1]2**.

Table 2. Ionization Energies (eV) for Four Metallocene-Based NLO Chromophores

Fc[1]1	Fc[1]2	Rc[1]1	Oc[1]2	assignment
6.98 A_1	6.97 A_1	7.57 A	7.22 A_1	$d_{z^2}/d_{x^2-y^2}/d_x$
7.26 A_2	7.31 A_2		7.50 A_2	
			7.85 A_3	
8.36 B	8.20 B	8.15 B	8.30 B	$e_1' - \pi_4$
9.08 C	9.05 C	8.72 C	8.96 C	e_1'
9.59 D	9.56 D	9.30 D	9.47 D	$e_1' + \pi_4$
		9.70 E	9.69 E	π_3
		10.15 F	10.32 F	e_1''
			10.58 G	e_1''
10.76 E	10.79 E	10.82 G	10.82 H	NO_2
12.98	12.7	12.4	12.6	
13.5	13.7	13.6	13.8	
16.6	16.6	16.5	17.0	

the variation in the $d_{x^2-y^2}/d_{xy}/d_{z^2}$ band IE. The other combination of the ring e_1 orbitals can combine with the metal d_{xz}/d_{yz} orbitals to give the e_1'' orbitals associated with the next band in the metallocene spectra. The IE of the e_1'' band increases substantially as the metal is changed from iron to ruthenium to osmium. The PE spectra of the nitrostyrene metallocene derivatives all show a band, B, at ca. 8.3 eV. This band cannot be accounted for by the superposition of the spectrum of the appropriate metallocene, where the e_1' ionizations occur in the range 8.51–8.72 eV, and that of *p*-nitrostyrene, the lowest energy ionization of which is at 9.29 eV. Thus, the presence of the nitrostyrene substituent leads to a substantial perturbation of the metallocene electronic structure. We assign band B to an orbital resulting from an antibonding combination of the HOMO of *p*-nitrostyrene and one of the pair of e_1' orbitals on the cyclopentadienyl ring to which the substituent is bound. Band B shows no relative intensity increase in the He II spectra, indicating that the corresponding orbital has little metal d-character. The variation in the energy of band B ionizations between iron, ruthenium, and osmium mirrors that in the e_1' ionizations of the parent metallocenes and is small relative to the variation in the band A IEs.[30] Therefore, the PES provides evidence for the delocalized orbital (labeled π), which in model III is the donor orbital in the HE optical transition (vide supra). The assignments of the remaining bands are summarized in Table 2.

Density functional (DF) calculations were carried out for **Fc[1]1** and **Fc[1]2** (using the Amsterdam Density Functional package version 2.3.[31]) in order to provide an independent orbital picture for these compounds, thus helping us to determine the validity of the orbital picture deduced above from the PE spectra. The orbital structure given by the DFT calculation is similar to that previously produced with extended Hückel calculations.[6] The HOMO is largely localized on the metal, as are the HOMO-1 and the HOMO-2, while the HOMO-3 has the delocalized π structure inferred from the position of band B in the PE spectrum. Iso-surfaces for the HOMO-3 and the principally acceptor-based LUMO of **Fc[1]2** are shown in Figure 5. The ionization energies for the HOMO and HOMO-3 of **Fc[1]2** were calculated explicitly by the ΔSCF method. The values found were 7.0 and 7.7 eV, in good agreement with the experimental values of 7.0 and 8.2 eV, respectively.

In summary, the most important results from UV–PES are as follows. First, the three highest occupied orbitals of the 1-metallocenyl-2-(*p*-nitrophenyl)ethylenes are similar to those of the appropriate parent metallocenes. Second, these molecules have a π-orbital that is delocalized over the cyclopentadienyl ring and the π-bridge, which is higher in energy than either the highest occupied cyclopentadienyl-based orbitals of the parent metallocene or the HOMO of *p*-nitrostyrene, and which is relatively unaffected by the identity of the metal.

Electrochemistry. Electrochemistry offers the possibility to examine trends in LUMO energies, as well as providing an alternative probe to the UV–PES of the trends in HOMO energies. We studied a range of metallocene–(π-bridge)–acceptor compounds using cyclic voltammetry in tetrahydrofuran (0.1 M $[^nBu_4N]^+[PF_6]^-$). Processes attributable to the $[m]^+/[m]$ couple, as reversible as the ferrocenium/ferrocene couple under the same conditions, were observed for all the ferrocenyl and octamethylferrocenyl compounds studied. Ruthenocene itself

(30) Interestingly, the PE spectra of **Fc[1]1** and **Fc[1]2** are virtually superimposable, except that band B occurs at lower IE in the *E*-isomer, **Fc[1]2**. This effect can be attributed to the nonplanar π-system of the *Z*-isomer leading to a weaker interaction between cyclopentadienyl and *p*-nitrostyrene π-orbitals; this nonplanarity is evident in the crystal structure reported in ref 4.

(31) Baerends, E. J.; te Velde, G. ADF, version 2.0.1; Department of Theoretical Chemistry, Vrije Universiteit, Amsterdam, 1996.

Table 3. Half-Wave Potentials (in mV) vs Ferrocenium/Ferrocene for Selected Metallocene-Containing Chromophores, Measured with Use of Cyclic Voltammetry in THF (0.1 M $[^nBu_4N]^+[PF_6]^-$)

	Mc[*n*]2		Mc[*n*]5	Mc[*n*]6		Mc[1]3-Cl
	$E_{1/2}([m]^+/[m])$	$E_{1/2}([m]/[m]^-)$	$E_{1/2}([m]^+/[m])$	$E_{1/2}([m]^+/[m])$	$E_{1/2}([m]/[m]^-)$	$E_{1/2}([m]^+/[m])$
Fc, $n = 1$	+25	−1670	+260	+325	−1090	+85
Fc, $n = 2$	+25	−1635	+180	+200	−950	
Fc, $n = 3$			+95	+110	−880	
Fc″, $n = 1$	−270	−1685				
Fc″, $n = 3$			−205	−183	−960	
Rc, $n = 1$	*a*	−1665				
Rc, $n = 3$			*a*	*a*	−880	

[a] Irreversible.

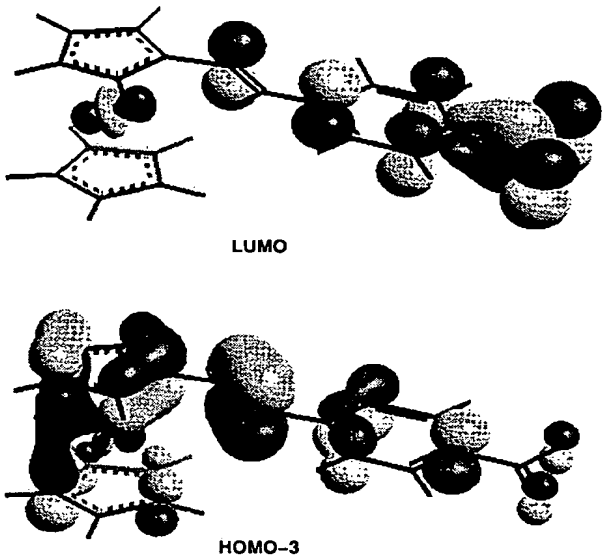

Figure 5. Representations of the HOMO-3 and the LUMO of **Fc[1]2** according to DF calculations.

shows an electrochemically irreversible two-electron oxidation;[32] the ruthenocenyl dyes also showed no reversible process assignable to the $[m]^+/[m]$ couple. The compounds with *p*-nitrophenyl acceptors (**Mc[*n*]2** series) all showed features attributable to the $[m]/[m]^-$ couple with reversibility comparable to that of ferrocenium/ferrocene, while compounds with *N,N*′-diethylthiobarbituric acid acceptors (**Mc[*n*]5** series) showed irreversible $[m]/[m]^{n-}$ processes; no reversible molecular reduction was observed for **Fc[1]3-Cl**. The $[m]/[m]^-$ features for the **Mc[*n*]6** series were characteristic of situations in which the electron transfer itself is reversible, but where the reduced species undergoes a chemical reaction on a time scale comparable with that of the electron transfer.[33,34] Half wave potentials are summarized in Table 3.

In the series **Mc[*n*]2**, the potentials for the $[m]/[m]^-$ couple occur in the range −1635 to −1685 mV; $[m]/[m]^-$ potentials of −1670 and −1730 mV were found, under the same conditions, for the model compounds *p*-nitrostyrene[35] and nitrobenzene, respectively. These data suggest a LUMO that is largely localized on the nitrophenyl group, with some contribution from the π-bridge, and thus, consistent with model III and with the results of DF calculations (Figure 5). **Fc[2]2** is slightly easier to reduce than **Fc[1]2**, indicative of a larger bridge contribution in the more extended species where empty bridge-based and acceptor-based orbitals will be closer in energy, leading to a stronger in-phase interaction and, thus, to a lower energy LUMO. Recently the ESR spectrum of the **Fc[1]2** radical anion has been reported.[36] The hyperfine coupling clearly shows the unpaired electron to be largely localized on the nitrophenyl ring, also consistent with **Fc[1]2** having a nitrobenzene-like LUMO.[37]

The $[m]^+/[m]$ couples for **Fc[1]2** and **Fc[2]2** occur at experimentally identical potential, +25 mV vs ferrocene (a single methyl substituent would have a somewhat larger effect of ca. 55 mV[38]), implying the HOMO to be principally localized on the ferrocene moiety and having even less π-character than the LUMO. This result is clearly consistent with the UV−PES and DF results discussed above. The $[m]^+/[m]$ couples for *E*-4-Fc-C_6H_4-CH=CH-C_6H_4-4-NO_2 and 4-Fc-C_6H_4-N=N-C_6H_4-4-NO_2 have been previously reported to be +20 and +70 mV, respectively, vs ferrocene in CH_2Cl_2.[39] The octamethylferrocenyl complex, **Fc″[1]2**, is considerably easier to oxidize than its ferrocene analogue, consistent with the well-known effect of methylation upon ferrocene oxidation potentials.[38,40−42]

For compounds with stronger acceptors (**Mc[*n*]5** and **Mc[*n*]6**) the trends in redox behavior are more complex due to more effective coupling of donor and acceptor in these compounds, the degree of coupling decreasing with increasing bridge length. This coupling is equivalent to the incorporation of more charge-transfer character into the ground state of the molecule, equivalent to increased contributions to the ground state from resonance structures such as those shown in the right-hand portion of Figure 6.[43]

UV−Vis−NIR Spectra. Trends in UV−vis−NIR spectra have been reported previously for a number of compounds. Here we compare qualitative predictions based upon the three models with these results and with additional data. We will examine in turn the effect of changing acceptor strength, changing the

(32) Diaz, A. F.; Mueller-Westerhoff, U. T.; Nazzar, A.; Tanner, M. *J. Organomet. Chem.* **1982**, *236*, C45−C48 and references therein.

(33) Evans, D. H.; O'Connell, K. M.; Peterson, R. A.; Kelly, M. J. *J. Chem. Educ.* **1983**, *60*, 290−293.

(34) Mabbot, G. A. *J. Chem. Educ.* **1983**, *60*, 697−701.

(35) Low concentrations had to be employed to avoid polymerization on the electrode.

(36) Pedulli, G. F.; Todres, Z. V. *J. Organomet. Chem.* **1992**, *439*, C46−C48.

(37) The unusually large g-factor (2.0056 vs 2.00479 in the nitrobenzene radical anion) and the small hyperfine couplings ($a = 0.213$ G) to the protons in the 2-position of the ferrocen-1-yl unit also indicate some (very limited) delocalization of spin density onto the ferrocene donor.

(38) Gassman, P. G.; Macomber, D. W.; Hershberger, J. W. *Organometallics* **1983**, *2*, 1470−1472.

(39) Coe, B. J.; Jones, C. J.; McCleverty, J. A.; Bloor, D.; Cross, G. *J. Organomet. Chem.* **1994**, *464*, 225−232.

(40) Hoh, G. L. K.; McEwen, W. E.; Kleinberg, J. *J. Am. Chem. Soc.* **1961**, *83*, 3949−3953.

(41) Robbins, J. L.; Edelstein, N.; Spencer, B.; Smart, J. C. *J. Am. Chem. Soc.* **1982**, *104*, 1882−1893.

(42) Interestingly, the difference in ease of oxidation between **Fc″[1]2** (−270 mV vs ferrocenium/ferrocene) and the parent octamethylferrocene (−360 mV) is somewhat larger than that between **Fc[1]2** (+25 mV) and ferrocene (0 mV). This reflects the greater contribution of charge-transferred resonance structures to the ground state in the stronger donor (octamethylferrocenyl) case.

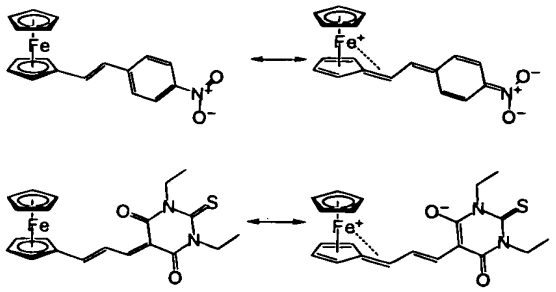

Figure 6. Neutral (left) and charge-transfer (right) resonance structures for **Fc[1]2** (top) and **Fc[2]5** (bottom).

conjugation length between donor and acceptor, changing iron for ruthenium or osmium, and varying degrees of methylation of the cyclopentadienyl rings. We will begin by briefly restating these models. In model I,[6] the LE transition is **M**→π^* and the HE transition is π→**A**. In model II,[18-20] the LE transition is d−d and the HE transition is **M**→**A**. In model III (the present model), the LE transition is **M**→**A** and the HE transition is π→**A**. The models are summarized diagrammatically in Figure 3.

(a) Effect of a Stronger Acceptor. All three models predict a red-shift of the HE transition on increasing acceptor strength, since in all three models this transition involves charge transfer to an empty acceptor-based orbital. However, the models disagree over the behavior of the LE transition. In model I, this is **M**→π^*; since π^* has only a small acceptor contribution, this transition is predicted to be relatively insensitive to acceptor strength. In model II the LE transition is a d−d ligand field transition; if it were a pure d−d transition it should be insensitive to acceptor strength. The observed variable energy of the LE transition and its large extinction coefficient (compared to that of a typical d−d transition) were previously attributed to borrowing of intensity from charge-transfer transitions via coupling through vibrational modes.[19] If this coupling is a minor perturbation then the description of the transition as a ligand-field transition remains valid. However, if the coupling is large it is necessary to account for this when describing the transition, which will become increasingly important as a contributor to the nonlinearity. Model III predicts a red-shift for the LE (**M**→**A**) transition of similar magnitude to that for the HE transition since both transitions involve charge transfer to the same empty orbital.

When the *p*-nitrophenyl acceptor (**Fc[1]2**) is replaced by a stronger acceptor such as *p*-*N*-methylpyridinium (**Fc[1]3-X**), or by an even stronger acceptor such as the 2-phenylthioflavone derivative shown in Figure 1 (**Fc[1]4-ClO$_4$**), *both* transitions show red-shifts of similar magnitude (1.04 and 0.99 eV red-shifts for HE and LE transitions, respectively, on moving from **Fc[1]2** to **Fc[1]4-ClO$_4$**), most consistent with model III (see Figure 2 in ref 12). Another comparison can be made by examining the spectra of **Fc[1]2** and **Fc[1]6** (Figure 7). Again the shifts are similar in magnitude (0.50 eV for the HE transition, 0.60 eV for the LE transition).[44] These shifts are also of similar magnitude to the difference of 580 mV between the [m]/[m]$^-$ potentials of the two compounds (vide supra). Furthermore, there

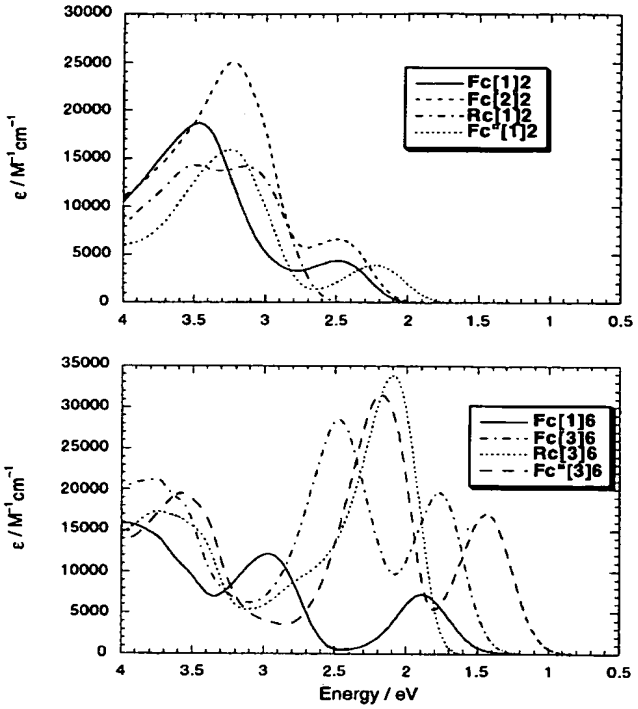

Figure 7. UV−vis spectra of metallocene chromophores containing nitrobenzene (**Mc[*n*]2** series) and 1-dioxothia-3-(dicyanomethylene)-indane (**Mc[*n*]6** series) acceptors in 1,4-dioxane.

is a marked tendency for the oscillator strength of the LE transition to increase relative to that of the HE transition with increasing acceptor strength. For example, in the series **Fc[1]2**, **Fc[1]3-Br**, and **Fc[1]4-ClO$_4$**, the oscillator strength for the LE transition changes from 0.10 to 0.11 to 0.25, while that for the HE transition decreases from 0.60 to 0.51 to 0.43.[12] The same effect is seen by comparing some of the compounds in Figure 7.[44] This is consistent with increased intensity borrowing in the stronger acceptor species; this arises from the increased mixing of states brought about by the lowering in energy of the two excited states (decrease in $\Delta E_{ge'}$). However, different spatial orbital extents, and therefore varying overlap with donor orbitals, of the LUMOs of the different acceptors may also be a contributory factor to the observed variations in intensities.

Toma and co-workers found that, although the LE transitions for a wide range of arylferrocenes[45] and 1-ferrocenyl-2-arylethylenes[22] were similar to the d−d transition of ferrocene itself[46] and showed a weak dependence upon the Hammett parameters of the substituents, the LE transitions of derivatives with strongly electron-withdrawing substituents (*p*-CHO, *p*-CN, and *p*-NO$_2$) could not readily be correlated with Hammett parameters. Thus, their data suggest the LE transitions of the strong acceptor compounds are not typical d−d transitions, consistent with the present hypothesis (model III) that they are better described as charge-transfer transitions.

(b) Effect of a Longer Conjugated Bridge. Simple Hückel arguments predict that an increase in conjugation length will

(43) Evidence for the contribution of this type of resonance structure may be found in the ^{1}H NMR spectra of species with strong acceptors, where ^{1}H−^{1}H couplings across formally double C−C bonds are reduced. Thus, in the strong acceptor compounds **Fc″[3]5** and **Fc″[3]6** ^{1}H−^{1}H coupling constants of ca. 13 Hz (in CD_2Cl_2) are seen across both single and double bonds, whereas, in the parent aldehyde, Fc″(CH=CH)$_2$CHO, the coupling constants alternate between ca. 15 Hz for formally double bonds and ca. 10 Hz for formally single bonds (C_6D_6).

(44) The two molecules in this comparison have somewhat different π-bridges and consequently the orbitals π are not so comparable as in the **Fc[1]2/Fc[1]4-ClO$_4$** comparison; therefore, it is not surprising that the two bands do not show as similar shifts to one another as in that comparison.

(45) Toma, S.; Gáplovsky, A.; Hudecek, M.; Langfelderová, Z. *Monatsh. Chem.* **1985**, *116*, 357−364.

(46) Sohn, Y. S.; Hendrickson, D. N.; Gray, H. B. *J. Am. Chem. Soc.* **1971**, *93*, 3603−3612.

lead to an increase in the energy of the highest occupied orbitals associated with the π-backbone and a decrease in the lowest unoccupied π-backbone orbitals. Metallocene- and acceptor-localized orbitals should be little affected by the nature of the conjugated bridge. Thus, in model I, the lowering of π^* will lead to a red-shift of the LE transition, while the raising of π will red-shift the HE transition. Model II predicts the energies of both transitions will be only weakly affected by the change in conjugation length as the LE and HE transitions involve substantially metal-localized orbitals or metal- and acceptor-localized orbitals, respectively. In model III, as in model I, the combination of e_1' and π-bridge orbitals (π, HOMO-3), should rise in energy with increased conjugation length. Thus, the HE transition is expected to red-shift, while the energy of the LE transition, involving only metal- and acceptor-localized orbitals, should be insensitive to conjugation length.

The experimental results are best explained with use of model III. We have previously compared spectra for the **Fc[n]6** series (see Figure 2 in ref 12); those for **Fc[1]6** and **Fc[3]6** are also shown in Figure 7, together with those for **Fc[1]2** and **Fc[2]2**. The HE transition of **Fc[n]6** red-shifts by ca. 0.70 eV as n is increased from 1 to 4. The LE transition is much less sensitive to chain length, the small variation (0.22 eV) observed between the extreme cases probably reflecting deviation from the idealized model, i.e., in molecules with stronger acceptors **A** can mix more strongly with π-levels. Excepting **Fc[4]6**, both transitions are observed to increase in intensity with increasing chain length. It is well-known that the intensity of polyene $\pi-\pi^*$ transitions increases with chain length.[47] The increase in intensity of the low-energy transition may also reflect increased intensity borrowing, owing to the decreased separations ($\Delta E_{ge'}$, $\Delta E_{ee'}$) between states. The intensity of both transitions of α,ω-diferrocenylpolyenes has also been found to increase with increasing chain length.[48,49]

(c) Effect of Exchanging Fe for Ru. The first ionization potential of ruthenocene is substantially greater than that of ferrocene.[27-29] The e_1' cyclopentadienyl orbitals (which combine with polyene bridge orbitals to give the HOMO-3, labeled π, in models I and III) of ruthenocene are, however, quite similar in energy to those of ferrocene. The acceptor orbitals should also be insensitive to the identity of the metallocene; the reduction potentials in Table 3 support this hypothesis. Hence, model I predicts a blue shift for the **M**$\rightarrow\pi^*$ LE transition, while the higher energy $\pi\rightarrow$**A** transition should be only slightly blue-shifted from that of the corresponding ferrocene analogue. Model II predicts that both transitions will undergo large blue-shifts: the LE transition due to the greater ligand field splittings characteristic of the heavier transition metals (indeed, the lowest energy spin-allowed d−d transition of ruthenocene is blue-shifted by 0.96 eV relative to that of ferrocene[46]), and the HE transition due to the higher ionization energy of ruthenocene. In the case of exchanging Fe for Ru, model III makes equivalent predictions to model I.

Experimentally, the LE transition is blue-shifted by ca. 0.3 to 0.6 eV, while the HE transition is shifted by less than 0.2 eV. In molecules with fairly weak acceptors, such as nitrophenyl, to which model III is most successfully applied, the blue shift of the LE transition is comparable with that expected by comparing first IEs of either the parent metallocenes or the dyes themselves. Thus, in **Rc[1]2** the LE transition (in *p*-dioxane) is blue-shifted by ca. 0.65 eV relative to **Fc[1]2** (Figure 7); the ionization potentials of the parent metallocenes differ by 0.57 eV. Other comparisons of spectra may be found in refs 5, 11, and 12. Also noteworthy is the dramatic increase in the intensity of the LE transition at the expense of that of the HE transition when iron is exchanged for ruthenium. One factor is presumably that the decreased energy difference between **M** and π levels, and thus decreased $\Delta E_{ee'}$, leads to increased mixing of first and second excited states, and thus increased intensity borrowing by the nominally **M**$\rightarrow$**A** transition from the $\pi\rightarrow$**A** transition. A second factor may be the increased d-orbital extent of ruthenium, leading to increased direct or indirect spatial overlap with **A**. Evidence for this increased extent may be found in the crystal structures of metallocenyl carbocations; ruthenocenyl compounds are best described as [(η^6-fulvene)(η^5-cyclopentadienyl)ruthenium] cations,[50,51] while the corresponding iron compounds are perhaps best regarded as distorted ferrocenes.[52,53] For *E*-1-osmocenyl-2-(*p*-nitrophenyl)ethylene, **Oc[1]2**, only a single transition is observed, at similar energy to the HE transition of its iron and ruthenium analogues; presumably the blue-shift of the LE transition is sufficiently large that the two transitions overlap in this case.

(d) Effect of Metallocene Methylation. Methylation of both metallocene cyclopentadienyl rings (**Fc″** derivatives) will raise the energy of both the metal d-orbitals and the highest filled π orbitals, as evidenced by comparison of the photoelectron spectra of ferrocene and decamethylferrocene.[28] Model I predicts the HE ($\pi\rightarrow$**A**) transition will red-shift on replacing a metallocene with the corresponding methylated metallocene; the effect on the LE transition depends on the relative magnitudes of the effects of methylation on **M** and π^*. Model II also predicts a red-shift for the HE (**M**$\rightarrow$**A**) transition, but a *blue*-shift for the LE (d−d) transition on methylation; methylated cyclopentadienyl ligands are known to lead to *greater* ligand-field splittings than their unmethylated analogues.[41,54] Model III predicts red-shifts for both transitions; both donor levels will be raised in energy, while the common acceptor level will be unchanged. The predictions are broadly similar for the case of methylating the cyclopentadienyl ring not bearing the π-bridge (**Mc′** derivatives), the details of the predictions for models I and III depending on the Cp* orbital contribution to π.

We have previously reported UV−vis absorption maxima for the 1′,2′,3′,4′,5′-pentamethylmetallocen-1-yl derivatives, **Fc′[1]2** and **Rc′[1]2**.[6] In the iron case, shifts of 0.095 and 0.17 eV were observed relative to the unmethylated analogue for the high- and low-energy transitions, respectively, while in the ruthenium case, shifts of 0.19 and 0.23 eV were found. In the new compound **Fc″[1]2**, containing the 2,3,4,5,1′,2′,3′,4′-octamethylferrocen-1-yl group, the shifts are 0.21 and 0.26 eV for high- and low-energy transitions, respectively (see Figure 7). Interestingly, the shift of the energy of the low-energy transition of the ferrocene compound observed with eight methyl groups

(47) Klessinger, M.; Michl, J. *Excited States and Photochemistry of Organic Molecules*; VCH: New York, 1995.

(48) Ribou, A. C.; Launay, J.-P.; Sachtleben, M. L.; Li, H.; Spangler, C. W. *Inorg. Chem.* **1996**, *35*, 3735−3740.

(49) A related issue is that of *E*/*Z* isomerism. On moving from **Fc[1]2** (*E*) to **Fc[1]1** (*Z*), a blue shift of 0.33 eV is found for the HE UV−vis−NIR transition, for which we propose the planarity dependent cyclopentadienyl/nitrostyrene combination (π, HOMO-3) as donor, while the LE transition blue shifts by only 0.08 eV, consistent with a transition originating from the metal $d_{z^2}/d_{x^2-y^2}/d_{xy}$ orbitals (**M**), which are unaffected by the bridge planarity. These results are also consistent with the UV−PES data for **Fc[1]1** and **Fc[1]2**.

(50) Kreindlin, A. Z.; Petrovskii, P. V.; Rybinskaya, M. I.; Yanovskii, A. I.; Struchkov, Y. T. *J. Organomet. Chem.* **1987**, *319*, 229−237.

(51) Sato, M.; Kudo, A.; Kawata, Y.; Saitoh, H. *Chem. Commun.* **1996**, 25−26.

(52) Cais, M.; Dani, S.; Herbstein, F. H.; Kapon, M. *J. Am. Chem. Soc.* **1978**, *100*, 5554−5558.

(53) Sime, R. L.; Sime, R. J. *J. Am. Chem. Soc.* **1974**, *96*, 892−896.

(54) Robbins, J. L.; Edelstein, N. M.; Cooper, S. R.; Smart, J. C. *J. Am. Chem. Soc.* **1979**, *101*, 3853−3857.

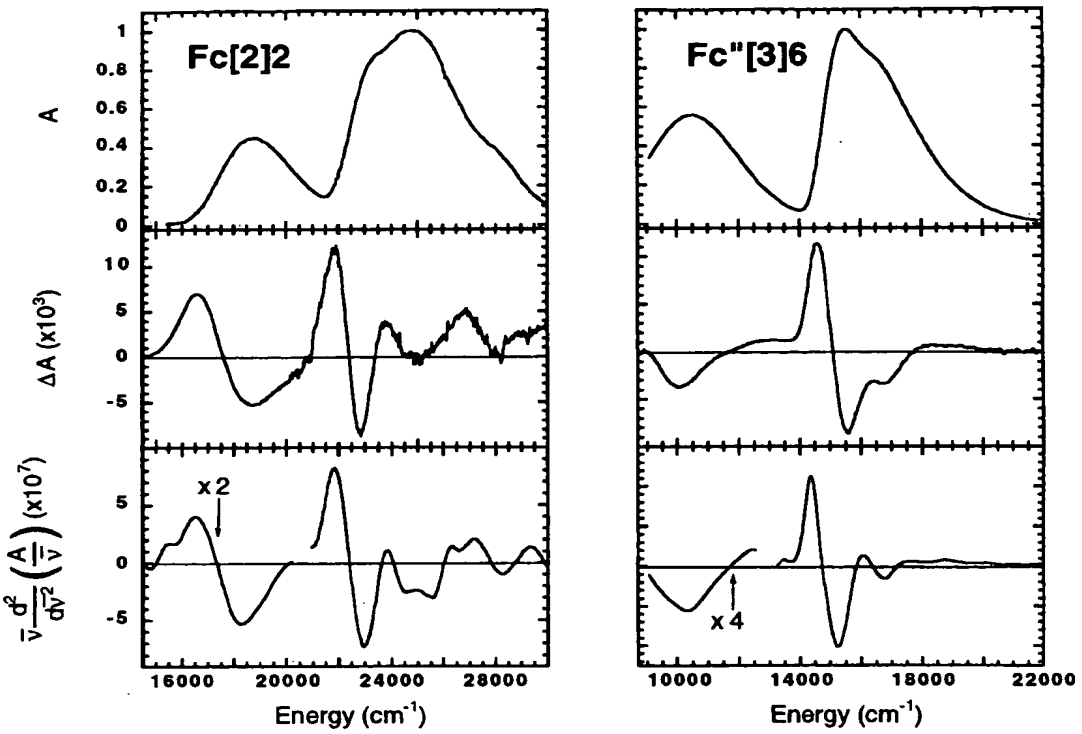

Figure 8. Absorption spectra (top panels), ΔA (Stark) spectra (center panels), and $\bar{\nu}$-weighted second derivatives of the absorption spectra (bottom panels) for **Fc[2]2** (left) and **Fc"[3]6** in frozen 2-methyltetrahydrofuran. The absorption of the samples was scaled so both are equal to unity at the absorption maximum and for an applied field strength of 1 MV cm^{-1} in order to facilitate comparisons. The second derivatives of the low-energy bands have been multiplied by factors of 2 and 4, respectively, to simulate their importance in the Stark spectra.

is ca. 8/5 times that observed with five methyl groups. This is in accordance with the well-documented additive effect of alkyl groups upon ferrocene oxidation potentials[38,40] and is entirely in agreement with the present model of a donor orbital resembling that of the parent metallocene and an acceptor orbital relatively unaffected by the metallocene. The shift in the high-energy transition with eight methyl groups is, however, ca. 2.2 times that with five methyl groups. This reflects the greater contribution of the cyclopentadienyl ring directly bound to the π-bridge (methylated in the octamethyl compound, unmethylated in the pentamethyl example) to the HOMO-3, π. Shifts of similar magnitude are also seen in octamethylated species with longer π-bridges and stronger acceptors (Figure 7). These results appear to exclude the possibility that the low-energy transition is a d−d transition. Of course, it may be argued that sufficient charge-transfer character is mixed into the transition such that the lower charge-transfer energy expected on methylation outweighs the higher ligand-field splitting, but if this is the case, then the transition is more appropriately described in terms of a charge-transfer transition.

In summary, the present model (model III) is best able to account for the effects of structural changes upon the transition energies and intensities.

Solvatochromism and Stark Spectroscopy. The three models make different qualitative predictions about the dipole moment changes, $\Delta\mu$, associated with the two transitions in the neutral dyes. Charge transfer (M→A, M→π^*, π→A) transitions are expected to be associated with large $\Delta\mu$ values. For a ligand-field transition, however, the charge redistribution is spatially very limited and, therefore, $\Delta\mu$ will be small.

Both transitions in the UV−vis−NIR of all the neutral metallocene−bridge−acceptor molecules considered in this paper show positive solvatochromism (cationic species such as **Mc[*n*]4-X**[12] show negative solvatochromism, since in these species the ground-state dipole moments are opposite in sign to those of the neutral species, due to the acceptor-localized positive charges, but the charge transfer is in the same direction as in the neutral species). The LE and HE transitions of **Fc[1]2** show bathochromic shifts of 0.16 and 0.23 eV, respectively, on moving from heptane to DMF.[4] For **Fc"[3]6**, red-shifts of 0.11 and 0.30 eV are seen for LE and HE energy transitions, respectively, between cyclohexane and DMSO.[55] Analogous solvatochromism has previously been reported for a variety of ferrocene donor−acceptor compounds with different types of π-bridges or acceptors.[8,39,56] Positive solvatochromism is generally taken as an indication of an increase in dipole moment with photoexcitation; thus, solvatochromism of both bands is consistent with both models I and III. In principle, $\Delta\mu$ can be estimated from solvatochromism data by using the McRae equation;[57] however, the analysis requires assumptions to be made about molecular shape. Some other problems of this type of analysis have recently been discussed.[58]

Electroabsorption, or Stark spectroscopy, of frozen solutions provides an alternative method to determine $|\Delta\mu|$; the method, its application to merocyanine dyes, and its limitations have recently been discussed.[59] Frozen 2-methyltetrahydrofuran solu-

(55) Spectra showing the solvatochromism of **Fc"[3]6** are presented in the Supporting Information.

(56) Houlton, A.; Jasim, N.; Roberts, R. M. G.; Silver, J.; Cunningham, D.; McArdle, P.; Higgins, T. *J. Chem. Soc., Dalton Trans.* **1992**, 2235−2241.
(57) McRae, E. G. *J. Phys. Chem.* **1957**, *61*, 562−572.
(58) Lombardi, J. R. *J. Phys. Chem. A* **1998**, *102*, 2817−2823.
(59) Bublitz, G. U.; Ortiz, R.; Marder, S. R.; Boxer, S. G. *J. Am. Chem. Soc.* **1997**, *119*, 3365−3376.

tions of **Fc[2]2** and **Fc″[3]6** were investigated by Stark spectroscopy; Figure 8 shows the absorption spectra, Stark spectra, and the $\bar{\nu}$-weighted second derivatives of the absorption spectra. In both cases the Stark spectra show overall second-derivative line shapes. First-derivative contributions to Stark spectra arise from polarizability changes, $\Delta\alpha$, associated with transitions; second-derivative contributions reflect dipole moment changes, $|\Delta\mu|$, associated with transitions. In the figure, the second derivatives of the LE transitions have been multiplied by factors of 2 or 4 for **Fc[2]2** and **Fc″[3]6**, respectively, in order to replicate the relative magnitudes of the two transitions in the appropriate Stark spectra. The result indicates that, for each compound, a larger dipole moment change is associated with the LE transition. For **Fc[2]2**, $|\Delta\mu|$ for the LE transition is ca. $\sqrt{2}$ times that of the HE transition, while $|\Delta\mu|$ for the LE transition of **Fc″[3]6** is approximately twice that for the HE transition. For **Fc″[3]6**, the data quality allowed quantitative anlaysis: $|\Delta\mu|$ for the LE is ca. 18 D, that for the HE transition is ca. 9 D.

The observation of large dipole moment changes of similar magnitude for *both* transitions indicates *both* transitions have considerable charge-transfer character. Moreover, given the relative transition energies and transition dipole moments, large $|\Delta\mu|$ terms for both transitions mean that both transitions will make significant contributions to the observed values of β. The relative two-level contributions can be estimated according to eq 1. For **Fc[2]2**, 63% of the two-level contribution is from the HE transition, while the LE transition contributes 37%. For **Fc″[3]6**, the HE transition is responsible for ca. 25% of the two-level contributions, while the LE transition contributes 75%. Assuming the validity of the two-level model, these results demonstrate, *independently of the spectral assignment*, that *both* transitions make contributions of comparable magnitude to the observed optical nonlinearity.

Summary

We have described a simple orbital model (model III) for understanding the spectra of metallocene−(π-bridge)−acceptor NLO-chromophores. We have tested the model by making qualitative predictions about the dependence of the UV−vis−NIR spectra of these molecules upon changes in chromophore structure; these predictions are in better agreement with experiment than the predictions of two previously published models.[6,19] While none of the models is adequate to explain all the data for the wide range of compounds considered, UV−PES, DF calculations, and cyclic voltammetry are generally consistent with model III. Stark spectroscopy confirms that large dipole moment changes are associated with both low-energy transitions in these molecules; together with the energies and intensities of the transitions, this indicates that the two transitions make comparable contributions to the observed nonlinear optical properties. Although there is still room for improvement in model III, it is more robust in its predictive capabilities than the previous models and should, therefore, be a helpful guide to chemists seeking to intuitively understand the spectroscopy and NLO responses of this class of molecules.

Acknowledgment. Support from the National Science Foundation (Chemistry Division), Office of Naval Research, Air Force Office of Scientific Research (AFOSR) at Caltech is gratefully acknowledged. The research described in this paper was performed in part by the Jet Propulsion Laboratory (JPL), California Institute of Technology, as part of its Center for Space Microelectronics Technology and was supported by the Ballistic Missile Defense Initiative Organization, Innovative Science and Technology Office through an agreement with the National Aeronautics and Space Administration (NASA). Support from the North Atlantic Treaty Organization (NATO) Grant No. 910903 is also gratefully acknowledged. Work at Stanford was supported in part by grants from the NSF Chemistry Division. H.E.B. thanks the Science and Engineering Research Council (SERC) for a studentship. We thank Arjun Mendiratta for technical assistance and Professors S. Toma, H. B. Gray, and M. Ratner for helpful comments.

Supporting Information Available: Experimental details for synthesis of new compounds, instrumental methods, and DF calculations. He(I) and He(II) PE spectra for *p*-nitrostyrene, **Fc[1]1**, **Fc[1]2**, **Rc[1]1**, and **Oc[1]2**; figure comparing cyclic voltmmograms of **Fc″[1]2**, octamethylferrocene and nitrobenzene; figure illustrating solvatochromism of **Fc″[3]6** (PDF). This material is available free of charge via the Internet at http://pubs.acs.org.

JA9830896

Experimental Investigations of Organic Molecular Nonlinear Optical Polarizabilities. 1. Methods and Results on Benzene and Stilbene Derivatives

Lap-Tak Cheng,* Wilson Tam,* Sylvia H. Stevenson, Gerald R. Meredith,

Central Research and Development Department, E. I. Du Pont de Nemours & Co. (Inc.), Experimental Station, P.O. Box 80356, Wilmington, Delaware 19880-0356

Geert Rikken,

Philips Research Laboratories, P.O. Box 80000, 5600JA, Eindhoven, The Netherlands

and Seth R. Marder

Jet Propulsion Laboratory, California Institute of Technology, 4800 Oak Grove Drive, Pasadena, California 91109 *(Received: May 13, 1991; In Final Form: August 5, 1991)*

In a series of two contributions, we present results of our systematic effort in the investigation of organic molecular hyperpolarizabilities using solution-phase dc electric field induced second-harmonic generation (EFISH) and third-harmonic generation (THG) experiments. In the present contribution, the experimental details, theoretical models, and data analysis scheme of a relatively precise and efficient EFISH/THG characterization method are described. Measurement results on donor–acceptor-substituted benzene and stilbene derivatives are presented. Structure–property relationships concerning intrinsic molecular nonlinearities are discussed, including issues concerning the electronic biasing strengths of various donor and acceptor groups, charge-transfer enhancement, substitution pattern, and multiple substituents. Correlations between hyperpolarizability (β) and substituent constants as well as property trade-off between nonlinearity and optical transparency are established. The observed relations are compared with the prediction of a widely accepted two-state model. The influences of heteroatom and various additional side-group substitutions on hyperpolarizability and the charge-transfer band position are examined. Structural dependencies of the cubic polarizability are also discussed.

Introduction

Organic materials have been extensively investigated for their large optical nonlinearities.[1] Owing to their molecular nature, properties such as the optical nonlinearity of organic solids can often be addressed at the molecular level. The different orders of linear and nonlinear responses of the molecular dipole polarization, $\mathbf{p}^{NLO}$, under external electric fields, $\mathbf{E}$, is expressed as follows:

$$p_i^{NLO} = \mu + \alpha_{ij}E_j + \beta_{ijk}E_jE_k + \gamma_{ijkl}E_jE_kE_l + \ldots \quad (1)$$

where μ is the permanent molecular dipole moment, and α_{ij}, β_{ijk}, and γ_{ijkl} are tensor elements of the molecular linear polarizability, quadratic, and cubic hyperpolarizabilities, respectively. The electric fields E_i are defined as the sum of complex conjugates. The latter three microscopic polarizabilities, when properly modified to account for intermolecular interactions and statistical ensemble averages, determine the macroscopic optical properties of the bulk refractive indexes, electrooptic and three-wave mixing processes such as second-harmonic generation and four-wave mixing processes such as third-harmonic generation and nonlinear refractive indices. β, which is the principal concern of the present study, represents the lowest order asymmetric response. It vanishes for molecules with inversion symmetry. Intuitively, to achieve large asymmetric polarizability, chemists have relied on the opposing electron affinities of various chemical substituents, commonly known as electron donors and acceptors, to bias the ground-state distribution and the response to optical perturbations of the highly polarizable π electrons in a variety of conjugated structures. This simple approach has led to successful activities in engineering molecules with enhanced nonlinearities.

The fundamental law governing molecular polarizability is given by quantum mechanics through time-dependent perturbation theory[2] in which all orders of polarizability are expressed as sums of transition matrix products with energy denominators involving the full electronic structure of a molecule. Tensorial components β_{ijk} for second-harmonic generation, neglecting excited-state lifetimes, are expressible as sums of terms of the following form[1]

$$\sum_n \sum_{n'} \frac{\mu_{gn}^i \mu_{nn'}^j \mu_{n'g}^k}{(\omega_n^2 - 4\omega^2)(\omega_{n'}^2 - \omega^2)} \quad (2)$$

where i, j, and k are coordinates; μ's are transition dipole moments; ω_n and $\omega_{n'}$ are energy gaps; and ω is the perturbation frequency. Simplification of such an expression shows that quadratic optical response is largely determined by strong, low-lying, and charge-transferring electronic excitations.

Given the theoretical formulation, at various levels of approximations, full scale calculations of molecular hyperpolarizabilities can be performed.[3] The advantage of the theoretical approach is that it permits inquiry of structure–property relationships without the undertaking of elaborate synthesis and experimental characterization. It also affords information which is not accessible to measurements. However, because of the uncertainty in molecular geometry and the often drastic approximations needed for reasonable efficiency, the success of various computational approaches must be evaluated with experimental data. Approximate theories can also be parametrized with measurement results. Measurements of some components of the quadratic and cubic hyperpolarizability tensors of organic molecules are commonly accomplished by dc electric field induced second-harmonic generation (EFISH)[4] and third-harmonic generation (THG)[5] experiments in solution. In principle, these

(1) See, for example: *Nonlinear Optical Properties of Organic Molecules and Crystals*; Chemla, D. S., Zyss, J., Eds.; Academic Press: New York, 1987; Vol. 1 and 2.

(2) (a) Butcher, P. N.; McLean, T. P. *Proc. Phys. Soc., London* **1963**, *81*, 219. (b) Ward, J. F. *Rev. Mod. Phys.* **1965**, *37*, 1. (c) Flytzanis, C. In *Quantum Electronics: A Treatise*; Rabin, H., Tang, C. L., Eds.; Academic Press: New York, 1975; Vol. 1, Part A, pp 9–207.

(3) (a) Zyss, J. *J. Chem. Phys.* **1979**, *70*, 3333–3340, 3341–3349; **1979**, *71*, 909–916. (b) Lalama, S. J.; Garito, A. F. *Phys. Rev. A.* **1979**, *20*, 1179–1194. (c) Teng, C. C.; Garito, A. F. *Phys. Rev. B* **1983**, *28*, 6766. (d) Waite, J.; Papadopoulos, M. G. *J. Chem. Phys.* **1985**, *82*, 1427–1434. (e) Docherty, V. J.; Pugh, D.; Morley, J. O. *J. Chem. Soc., Faraday Trans. 2* **1985**, *81*, 1179–1192. (f) Morley, J. O.; Docherty, V. J.; Pugh, D. *J. Chem. Soc., Perkin Trans. 2* **1987**, 1351–1355, 1357–1360. (g) Dirk, C. W.; Twieg, R. J.; Wagniere, G. *J. Am. Chem. Soc.* **1986**, *108*, 5387–5395. (h) Li, D.-Q.; Ratner, M. A.; Marks, T. J. *J. Am. Chem. Soc.* **1988**, *110*, 1707–1715. (i) Ulman, A. *J. Phys. Chem.* **1988**, *92*, 2385–2390. (j) Wagniere, G. H.; Hutter, J. B. *J. Opt. Soc. Am. B* **1989**, *6*, 693–702.

(4) Levine, B. F.; Bethea, C. G. *Appl. Phys. Lett.* **1974**, *24*, 445–447.

0022-3654/91/2095-10631$02.50/0

techniques are capable of yielding precise values. However, as a result of differing experimental and theoretical methodologies, that include differences in laser frequencies, solvents, local field models, and data reduction schemes, widely differing results have been reported for many of the prototypical nonlinear organic compounds.[6] In addition, few systematic investigations covering a diversity of structural classes have been reported. Given the sparsity and inconsistency of the available data, it becomes quite difficult to draw conclusions concerning many important aspects of molecular hyperpolarizability. Detailed comparison with computational results and development of additional guidelines toward optimizing nonlinearity are also seriously hampered. It seems therefore desirable to establish a uniform database from which many of the aforementioned causes of discrepancy have been eliminated.

We have taken such an initiative and have developed a relatively efficient and accurate experimental technique to study molecular nonlinearity in solutions. Our intention is to conduct systematic measurements and obtain an internally consistent data set from which conclusions can be drawn concerning the structural factors which influence optical nonlinearity. In the present contribution, details of our experimental methodology are given. Results on benzene and stilbene derivatives are presented. Structure–property relationships concerning intrinsic molecular nonlinearities are discussed. This includes issues concerning the electronic biasing strengths of various donor and acceptor groups, charge-transfer enhancement, substitution pattern, and multiple substituents. Correlations between hyperpolarizability (β) and substituent constants as well as property trade-off between nonlinearity and optical transparency are established. The observed relations are compared with the prediction of a widely accepted two-state model. The influences of heteroatom and various additional side-group substitutions on hyperpolarizability and the charge-transfer band position are examined. Structural dependences of the cubic polarizability are also discussed.

Experimental Methodology

Molecular hyperpolarizabilities are extracted from a set of observable quantities. A lengthy set of physical and optical measurements are needed for this purpose. These include measurements of density, refractive index at several wavelengths, dielectric constant, and THG and EFISH amplitudes and coherence lengths on a series of solutions of graded concentration. From them a specific volume attributed to a solute molecule in solution, refractive index dispersion, dielectric properties, and THG and EFISH nonlinear susceptibilities are determined for each solution. Except for the THG and EFISH measurements, of which a detailed description of experimental configuration will be given, all measurements are performed according to well-established procedures with sufficient accuracy and precision that they contribute insignificantly to the final uncertainties in the hyperpolarizabilities. With the measured solution properties, the relevant molecular properties including the permanent dipole moment and appropriate tensor projections of all three polarizabilities in eq 1 can be calculated according to well-accepted approximations of liquid dielectric behavior. In addition, absorption spectra are collected for most molecules in solutions and solvatochromic measurements are carried out to assess the CT nature of the low-lying electronic excitations of a selected set of para-disubstituted benzene and stilbene derivatives.

The experimental setup for the EFISH and THG experiments is shown in Figure 1. It consists of a 20-Hz (Quanta RAy) Nd:YAG laser configured as unstable resonator with a filled-in mode. The Q-switched and amplified 1.064-μm wavelength output consists of 8-ns pulses with energies of 0.4 J. A 1-m-long gas Raman cell filled to 120 psi with hydrogen provides up to 120 mW average power of polarized Stokes radiation at 1.91 μm. This radiation serves as the fundamental frequency for both the EFISH and THG experiment, the harmonics occurring then at 954 and

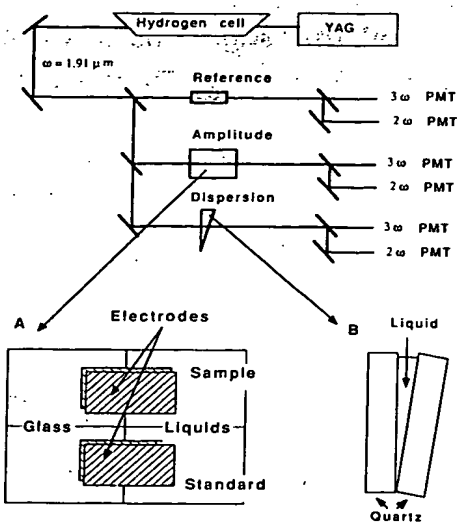

Figure 1. Schematic of optical setup.

636 nm, respectively. For most lightly colored compounds with absorption edges below 500 nm, measurement results are minimally influenced by dispersive enhancement related to approach toward the resonant excitation frequencies of the medium, and can be considered to be approximately the intrinsic (electronic) nonlinearity associated with a specific molecular composition and structure. THG and EFISH experiments are carried out with an unconventional technique in which the harmonic amplitudes and coherence lengths are measured in separate experiments. The advantages of this technique have been elaborated before.[8] They include minimization of possible atmospheric contributions, which are known to be important in THG and, to a lesser extent, EFISH measurements.[9] They also include an increase in the measurement precision by avoidance of the necessity to simultaneously extract several parameters from fitted data[10] as is the case for the conventional Maker's fringe or wedge fringe techniques. The laser beam is divided three ways: a harmonics' intensity normalization reference branch, a coherence length measurement branch, and an amplitude measurement branch. THG and EFISH occur and are detected simultaneously. The second- and third-harmonic signals are separated with dichroic mirrors, detected with photomultiplier tubes, collected through gated integrators, and stored with a small laboratory computer.

A tight-focusing geometry is adopted in the scheme to determine relative harmonic amplitudes. There are two advantages therein: the regions far from the focal region (e.g., external surfaces and exterior of a cell) can be neglected in considering the nonlinear generation of signal; and the complex issue of accumulated phase mismatch between nonlinear polarization waves and harmonic light waves, which gives rise to the well-known nonlinear optical fringes, is functionally simplified. These are important simplifications since poor considerations of these topics has given rise to nonintuitively obvious errors.

Consider a focused Gaussian beam. Relative to an idealized plane wave traveling in the same direction the Gaussian beam accumulates an addition phase of π on propagating between the far-field regions. For normally dispersive media it has been demonstrated that, relating to this, the net THG is zero on

(5) Hermann, J. P.; Ricard, D. *Appl. Phys. Lett.* **1973**, *23*, 178–180.
(6) Nicoud, J. F.; Twieg, R. J. In ref 1, Vol. 2, pp 255–267.

(7) The density is measured with a Mettler digital density meter and the refractive indexes are measured with a prism refractometer provider by Precision Instruments. The solution dielectric constant is determined by measuring the capacitance of a cylindrical capacitance cell at 1 MHz. The cell is calibrated with pure liquids of known dielectric constants.
(8) Meredith, G. R.; Cheng, L.-T.; Hsiung, H.; Vanherzeele, H. A.; Zumsteg, F. C. In *Materials for Nonlinear and Electro-optics*; Lyons, M. H., Ed.; IOP Publishing: New York, 1989; pp 139–150.
(9) (a) Meredith, G. R. *Opt. Commun.* **1981**, *39*, 89–93. (c) Thalhammer, M.; Penzkofer, A.; *Appl. B.* **1983**, *32*, 137–143. (b) Kajzar, F.; Messier, J. *Phys. Rev. A* **1985**, *32*, 2352–2365.
(10) Meredith, G. R.; Buchalter, B.; Hanzlik, C. *J. Chem. Phys.* **1983**, *78*, 1533–1542.

Figure 2. generation beam: (A

traveling intensity cancellat of the inb a transit nonlinear arise as t are depic of the sp curvatur and by d (i.e., the of chang allowing fields by linking represen be prese largest r a result and clos THG in by the d be coinc pieces c a vecto the cen maximi for SH dispersi regions. of the c causes (i.e., n regions the sig of inbc refocus mm), genera Gaussi

(11) Meredi Materi Society

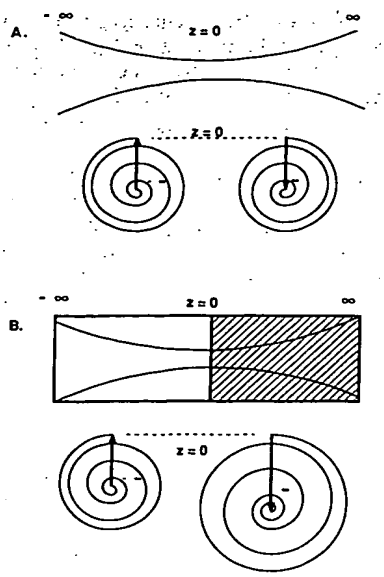

Figure 2. Vibration diagrams of phase-mismatched third harmonic generation in normally dispersive media with tightly focused Gaussian beam: (A) infinite medium; (B) infinite media with a single interface.

traveling between the far fields, though significant harmonic intensity might exist in the focal region.[11] There is a perfect cancellation resulting from fine details of amplitude and phase of the inbound and outbound THG processes. Consequently, when a transition between media with different dispersion and/or nonlinearity occurs in the near field, a nonvanishing net THG will arise as this perfect cancellation is destroyed. These two situations are depicted using vibration diagrams[11] in Figure 2. The centers of the spirals correspond to the far field limits $z \rightarrow \pm\infty$. The curvatures of the spirals are determined by focusing conditions and by dispersion and nonlinearities of the media. Near the focus (i.e., the near field, $z \sim 0$, region), the spiral has the lowest rate of change in curvature. Since these diagrams are constructions allowing integration of the phase specific production of electric fields by polarization density waves, the magnitude of a vector linking the beginning of the diagram ($-\infty$) to any other point represents the magnitude of harmonic electric field which would be present at the corresponding physical location. At focus the largest magnitude vector of harmonic amplitude is observed. As a result of the defocusing, the sense of the spiral reverses there and closes onto the same far-field point, demonstrating the nulled THG in infinite media. (The diagrams in Figure 2 are shifted by the dashed line for clarity; otherwise, the $z \rightarrow \pm\infty$ points would be coincident.) For two media separated by an interface, the two pieces of vibration diagram are different and the magnitude of a vector drawn between the two far-field points is nonzero (i.e., the centers of the two spirals are displaced). Clearly THG is maximized when the focus is placed at the interface. The case for SHG differs in that a finite amplitude will occur in normally dispersive infinite media for propagation between the far-field regions. However, for EFISH in condensed phase media the falloff of the dc fringing fields arising from a finite electrode structure causes a behavior which is functionally similar to that of THG (i.e., no harmonic generated on propagation between far-field regions unless an interface between different media occurs wherein the signal is related to the destruction of the detailed cancellation of inbound and outbound harmonic generation).[11] With tight refocusing (in our case spot size $\sim$50 μm, confocal parameter $\sim$8 mm), the light intensity diminishes rapidly to a level too low to generate observable harmonic radiation. Thus the situation of Gaussian propagation of a tightly focused laser beam across a single interface can be approximated by using a thick glass window (2 cm in our cells) as one medium and a long path length liquid cell (3 cm in our cells) in which organic solution serves as the second medium (see insert A of Figure 1). Harmonic generation from the outer two interfaces of the cell can be ignored due to the rapid beam divergence. To carry out THG and EFISH concurrently, a pair of gold or stainless steel electrodes, spaced by 3 mm, are attached at the glass/liquid interface. A pulsed electric field of a few microseconds duration (used to minimize electrochemical degradation of samples during the EFISH measurement), 7 kV in strength, and synchronized with the laser is applied across the electrodes. Calibration or measurement of the harmonic signal is achieved by comparison to a standard. The liquid cell is partitioned into two chambers, with one chamber containing the organic solution and the other containing a standard liquid such as toluene with known nonlinearity (toluene is used for mere convenience). Comparative measurement is performed by translating alternatively the two liquid chambers into the focal region of the laser beam. Great care is taken to assure that this translation is parallel to the interface and normal to the optical path so that the interface lies always at the same point in the focused fundamental's beam profile. Potential error due to local defects of the interface is minimized by averaging data collected at different positions in the translation. Since the signal arises due to the discontinuities associated with a single interface, no variable or oscillatory interference effects need to be considered (though we note that the interference of incoming and outgoing harmonic generation is an important part of the methodology as it improves the precision of final determinations above the precision of optical signal reproducibility). This is verified by a constant signal level at different window translations across the beam and by the monotonic growth, then decay, of signal as the cell is translated, within reasonable bounds, along the focused beam.

As a result of the tight focusing, laser power is limited by optical damage. About 30 mW average power of the Stokes radiation is used for both the EFISH and THG experiments. Due to the third-order field dependencies, as well as fluctuations in the Raman generation process, shot to shot signal intensities typically show more than 50% variation and are therefore extensively averaged. Over 5000 shots are needed for the experimental value to be stable to 5%, though this is merely 4 min at 20 Hz. The EFISH signal also occurs in a wavelength region where PMT quantum efficiency is very poor ($\sim$0.2%) so that, despite measures to diminish dark noise, the use of this amplitude technique, as opposed to techniques which require fitting of a nonlinear fringing pattern to extract the amplitude, is essential for high precision.

Refractive index dispersion properties of the solution for both THG and SHG, required for the determination of nonlinear susceptibilities, are measured separately with a wedged cell constructed with crystalline quartz windows (see insert B of Figure 1). The quartz windows are matched such that both generate comparable second-harmonic intensities. The interference of THG from air, quartz, and solution is such that good fringe patterns, as described next, indicative of the solution's dispersion are obtained. These well-known interference phenomena arise from the differences in phase velocities of "bound" and "free" harmonic waves, as described in the next section. The accumulated phase mismatches between these waves are continuously varied by translation of the wedged cell which varies the optical path length of the solution. Thus the degree of constructive/destructive interference is altered resulting in these oscillating intensity patterns. The SHG and THG coherence lengths are easily determined from the oscillatory signals. Since the coherence lengths for SHG and EFISH are equal (disregarding the negligible difference due to quadratic electrooptic effects), our method takes advantage of the much stronger SHG signal available to improve precision. Weak focusing (spot size $\sim$200 μm) is used to optimize the fringe contrast ratios.

Figure 3 shows typical EFISH/THG amplitudes (top) and coherence length data (bottom). The amplitude data show the EFISH (○) and THG (◇) signals for an organic solution in the left chamber and for toluene in the right chamber. Clearly, the

(11) (a) Ward, J. F.; New, G. H. C. *Phys. Rev.* 1969, *185*, 57–72. (b) Meredith, G. R. In *Nonlinear Optical Properties of Organic and Polymeric Materials*; Williams, D. J., Ed.; ACS Symposium Series; American Chemical Society: Washington, DC, 1983; Vol. 233, pp 27–56.

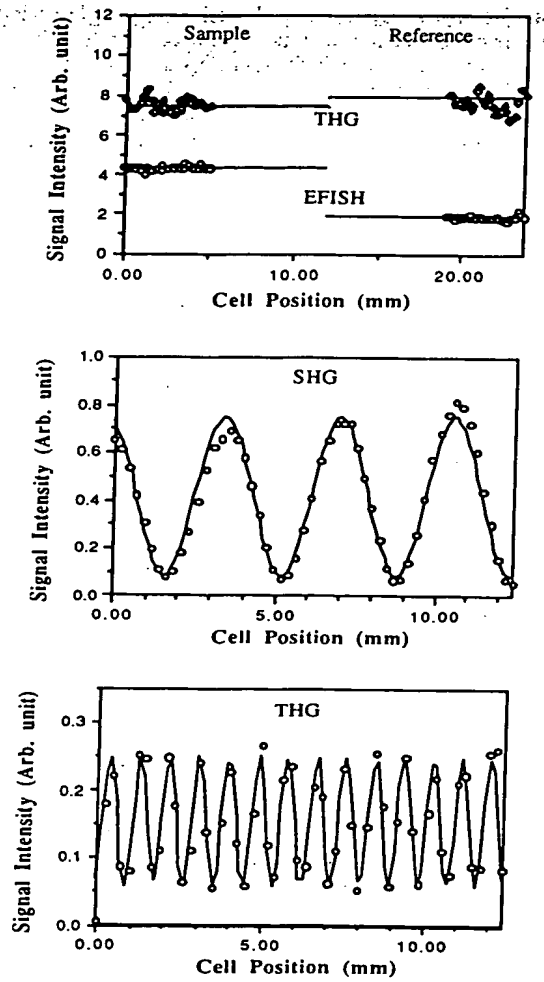

Figure 3. EFISH/THG amplitude (top) and dispersion (middle and bottom) data.

signal level (ordinate) is independent of the cell position (abscissa) within each chamber, demonstrating the lack of interference arising from harmonic generation associated with materials near or beyond other interfaces and verifying the quality of the parallelness of the translation axis and cell window. The solid lines are calculated signal averages. The ratio of the harmonic intensities generated in the two chambers can be precisely determined. The dispersion data show the oscillatory periods from which coherence lengths can be extracted knowing the wedge angle of the liquid cell. The SHG coherence length is much longer than that of THG, as expected. The nonzero background is a result of the focusing and finite spot size of the fundamental beam. The gradual rise in signal is a result of a slight wedge on one of the quartz windows. Solid lines are the best fits under the least-squares criterion from which accurate periods are determined.

Data Analysis

The ratio of the harmonic intensities between the standard liquid and the organic solution and the coherence lengths are the important quantities measured in this experiment. To see how they are related to the solution nonlinearity, one can consider the propagation of plane waves across a single interface between glass (g) and a liquid (l). In glass, due to its nonlinear susceptibility, the fundamental radiation generates a nonlinear polarization wave, $\mathbf{p}_g^{NLS}$. According to Maxwell's equations the presence of this "nonlinear source" polarization requires an accompanying "bound" electric wave,

$$\mathbf{E}_g^b = 4\pi\mathbf{p}_g^{NLS}/(\epsilon_g^b - \epsilon_g^f) \quad (3)$$

The phase velocity of the bound wave, as expressed through a refractive index $n_g^b = (\epsilon_g^b)^{1/2}$, is generally different than that of a normally propagating light wave or "free" wave, $\mathbf{E}_g^f$, at that frequency ($n_g^f = (\epsilon_g^f)^{1/2}$). This difference in phase velocity is often expressed through a coherence length for the qth harmonic

$$l_c = \lambda/2q(n^b - n^f) \quad (4)$$

which is the distance over which a π phase change accumulates, or in other words the distance required for the flow of energy between fundamental and harmonic to reverse. At an isolated interface a reflected wave will be generated and both bound and free harmonic waves, $\mathbf{E}_l^b$ and $\mathbf{E}_l^f$, will arise by transmission in the liquid. At normal incidence, continuity of transverse electric and magnetic fields provide boundary conditions which allow elimination of the reflected wave giving the following familiar result

$$\mathbf{E}_l^f = t_{gl}\mathbf{E}_g^f + (u_{gl}\mathbf{E}_g^b - v_{gl}\mathbf{E}_l^b)e^{i\phi} \quad (5)$$

where

$$t_{gl} = 2n_g^f/(n_g^f + n_l^f) \quad (5a)$$

$$u_{gl} = (n_g^f + n_g^b)/(n_g^f + n_l^f) \quad (5b)$$

$$v_{gl} = (n_g^f + n_l^b)/(n_l^f)/(n_g^f + n_l^f) \quad (5c)$$

are transmission factors due to the differences in refractive indices and ϕ is the accumulated phase mismatch between free and bound waves. Additional phase differences may arise if the material susceptibilities are complex, but to good approximation such is not the case in our experiments. This relation states that the free wave in liquid is the free wave in glass corrected for transmission plus a bound wave discontinuity across the interface. The detected intensity, I_d, is proportional to $n_l^f|E_l^f|^2$.

For a focused Gaussian beam the analysis is more complex.[11] Pictorially, from the vibration diagrams discussed earlier, the field seen by the detector is directly proportional to the nonlinearity (bound wave) difference of the two media:

$$I_d^{1/2} \propto |u_{gl}\mathbf{E}_g^b - v_{gl}\mathbf{E}_l^b| \quad (6)$$

Clearly, without the interface the two bound wave amplitudes would be equal and with $u = v$ (≈ 1), the harmonic field at the detector will be zero. Therefore, the intensity detected strictly comes from the bound wave mismatch at the interface. These conclusions are valid for both THG and EFISH.

The bound wave can be expressed in terms of measured and desired material constants,

$$\mathbf{E}_i^b = \{8q\pi\chi_i^{(3)}l_{ci}/\lambda(n_i^b + n_i^f)\}\mathbf{E}_i\mathbf{E}_i\mathbf{E}_i \quad (7)$$

where i = g or l. Therefore, the bound-wave amplitude is proportional to the nonlinear susceptibility $\chi^{(3)} = \chi^{(3)}(-3\omega,\omega,\omega,\omega)$ or $\chi^{(3)} = \chi^{(3)}(-2\omega,\omega,\omega,0)$ as well as the respective coherence length for THG ($q = 3$) or EFISH ($q = 2$). For linearly polarized radiation, parallel to the dc field for EFISH, the isotropic component of $\chi^{(3)} = \chi^{(3)}_{1111}$ is measured. From eqs 6 and 7, with appropriate transmission factors to account for the reflective losses at interfaces, and the appropriate transmission corrections to the fundamental and harmonic field strengths (t^ω and $t^{3\omega}$), the harmonic intensity reaching the detector for the sample solution (s) and the secondary standard reference liquid (r) can be derived. In a comparative experiment, the ratio ($\mathcal{R}$) of the harmonic intensities from the two chambers is determined. Its relation to the material properties is written concisely as follows

$$\mathcal{R}^{1/2} = (I_s/I_r)^{1/2} = \frac{u_{gs}}{u_{gr}}\frac{t_{sg}^{q\omega}}{t_{rg}^{q\omega}}\left(\frac{1 - R_s}{1 - R_r}\right) \quad (8)$$

where

$$R_s = (t_{gs}^{\omega})^q\frac{v_{gs}}{u_{gs}}\frac{n_g^b + n_g^f}{n_s^b + n_s^f}\frac{\chi_s^{(3)}l_{cs}}{\chi_g^{(3)}l_{cg}}$$

$$R_r = (t_{gr}^{\omega})^q\frac{v_{gr}}{u_{gr}}\frac{n_g^b + n_g^f}{n_r^b + n_r^f}\frac{\chi_r^{(3)}l_{cr}}{\chi_g^{(3)}l_{cg}} \quad (9)$$

So far as the nonlinearities and coherence lengths of the window glass and standard liquid are known, and the signal ratio as well as the organic solution coherence lengths are measured, the nonlinearities of the solution can be extracted. Note that, in the case of weak absorption (negligible within a coherence length) of the fundamental wave by the liquid medium, the harmonic intensity will not be affected. This can be understood by considering the effect of weak absorption on the vibration diagrams. The rate of change in the spiral curvature will increase reflecting the accelerated decrease in field strength, but the vector connecting the focus and far field, which determines the harmonic intensity, will not be affected. All solvents used in the present studies have negligible absorption within a path length of many times the coherence lengths. In addition, since R_s and R_r in eq 8 are given by ratios of the linear (n) and the third-order susceptibilities which have similar temperature dependencies, the heating effect which is always present will not lead to significant error.

For THG, calibration of the standard liquid is determined from its response relative to the window material, whose nonlinearity has been extracted from earlier work employing a different methodology,[10] using a statistical criterion to improve the confidence over that of a single liquid.[12] The glass nonlinearity was referenced to crystalline quartz and the quartz nonlinearity was determined from details of the nonlinear fringe pattern which results from interference of direct THG with two-step, cascaded SHG/THG in the same crystal[13a] for which a value of $\chi^{(2)}_{11}(-2\omega,\omega,\omega) = 2.08 \times 10^{-9}$ esu has been used. For EFISH, calibration is accomplished relative to crystalline quartz. The front window of the cell is replaced with an oriented crystal and consideration of the SHG under variable fields with and without liquids allows calibration.[13b] Following are the values of THG and EFISH nonlinearities and coherence lengths for the window material and the reference liquid at 1.91 μm: BK7-grade A glass: $\chi^{(3)}_{THG} = 4.7 \times 10^{-14}$ esu, $l_{THG} = 16.7$ μm, $\chi^{(3)}_{EFISH} = 3.5 \times 10^{-14}$ esu, and $l_{EFISH} = 38.8$ μm; toluene: $\chi^{(3)}_{THG} = 9.9 \times 10^{-14}$ esu, $l_{THG} = 18.3$ μm, $\chi^{(3)}_{EFISH} = 9.1 \times 10^{-14}$ esu, and $l_{EFISH} = 73.5$ μm.

Measurements of solution density (ρ), refractive indexes at He–Ne ($n_{633} \approx n_{3\omega=636}$) and sodium D line ($n_{589}$), and dielectric constant (ϵ) are carried out with commensurate care and precision. Together with $\chi^{(3)}_{THG}$ and $\chi^{(3)}_{EFISH}$, these measured macroscopic quantities are related to the molecular quantities including the dipole moment (μ), the isotropic component of polarizability ($\alpha = \langle\alpha\rangle_{11}$), the vectorial projection of quadratic hyperpolarizability along dipole direction (β), and the isotropic component of cubic hyperpolarizabilities ($\gamma^{THG} = \langle\gamma^{THG}\rangle_{1111}$, $\gamma^{EFISH} = \langle\gamma^{EFISH}\rangle_{1111}$), in a binary, uncorrelated, and orientationally averaged model,[4,10,14] according to the following relations

$$\frac{n^2(\omega) - 1}{4\pi} = \sum_{i=1}^{2} N_i \alpha_i^{\omega} f_i^{\omega} \tag{10}$$

$$\frac{\epsilon - 1}{4\pi} = \sum_{i=1}^{2} N_i \left(\alpha_i^0 f_i^0 + \frac{\mu_i^2 f_i^*}{3kT} \right) \tag{11}$$

$$\chi^{(3)}_{THG} = \sum_{i=1}^{2} N_i (f_i^{\omega})^3 f_i^{3\omega} \gamma_i^{THG} \tag{12}$$

$$\chi^{(3)}_{EFISH} = \sum_{i=1}^{2} N_i (f_i^{\omega})^2 f_i^{2\omega} f_i^0 \gamma_i^{EFISH} \tag{13}$$

$$\gamma_i^{EFISH} = \gamma_i^{\epsilon} + \gamma_i^{\nu} + \frac{\mu\beta}{5kT} \tag{14}$$

where $i = 1$ and 2 denote the solvent and solute species, N_i's are number densities expressible as inverse specific volume, ω denotes optical frequencies, α^0 is the static polarizability, and $(\gamma^{\epsilon} + \gamma^{\nu})$ is the deformational term summing electronic and hyper-Raman contributions to EFISH. f's are local field factors given by the Onsager treatment of dipolar liquids.[15] The local fields are both species- and frequency-dependent and are given as

$$f_i^0 = \frac{\epsilon(n_i^2 + 2)}{2\epsilon + n_i^2}, \quad f_i^* = \frac{\epsilon(2\epsilon + 1)(n_i^2 + 2)^2}{3(2\epsilon + n_i^2)^2}$$
$$f_i^{\omega} = \frac{n^2(\omega)[n_i^2(\omega) + 2]}{2n^2(\omega) + n_i^2(\omega)} \tag{15}$$

n is the refractive index of the solution which is concentration dependent. n_i is the refractive index of the two species with n_1 given by the pure solvent value. n_2 is the effective refractive index of the solute molecules in solution and is determined by the volume attributable to them and their polarizability. It can be obtained from the solution refractive index and the specific volume that the molecule occupies in solution according to a procedure described previously.[16] To obtain the static polarizability, the polarizability can be treated as a frequency-dependent quantity and calculated at different wavelengths according to eq 10. The long-wavelength limit can than be obtained from an extrapolation. To account for deformational contributions, eq 11 is used to deduce α^0 from dielectric measurements at low frequency (1 MHz) for a range of molecules with zero dipole moments. For one and two rings aromatic molecules, α^0's thus obtained are found to be about 15% higher than the extrapolated long-wavelength limiting value. This percentage is than used for other polar molecules of the same structural classes.

The molecular hyperpolarizabilities are related to the third-order nonlinearities of the solution according to eqs 12, 13, and 14, where $(\gamma^{\epsilon} + \gamma^{\nu})$ is assumed to be proportional to γ^{THG} for lack of a better method. The proportionality constant, with typical values between 0.7 and 0.8, is determined by measurements of centrosymmetric molecules with structure similar to that of the nonlinear molecule in question. This is somewhat arbitrary since the dispersions of the electronic contributions are different and the γ^{ν} term, which is generally believed to be quite small, has no contribution in THG. However, since the deformational contribution is proportionately high (up to 30%) only for low $\mu\beta$ molecules, whose electronic transitions are typically in the UV region minimizing the dispersion discrepancy, this scaling procedure is better than ignoring this term. In addition, such a scaling procedure also takes into consideration possible inconsistencies between the THG and EFISH calibrations. For high β molecules in highly polar or polarizable solvents, second-order local field cascading effects will lead to artificially large third order responses.[17] The measurement of γ^{THG} provides an estimate of the cascade contribution to γ^{EFISH}. The accuracy of such an estimate, however, is uncertain, particularly when different solvents are used. For this and other reasons, we carry out our measurements in the same solvent (*p*-dioxane for its dissolving power, low polarizability, and zero dipole moment) whenever possible and avoid using highly polar or polarizable solvents. However, material solubilities often dictate the use of polar solvents and solvent effects may affect some chromophores more than others. Variation of measurement results in different solvents can be found in tables below.

Following earlier work,[18] the desired molecular quantities are extracted at the infinite dilution limit. (Equations 10–13 are rewritten in terms of mole fractions and all solution properties are assumed to be concentration dependent. The four equations are differentiated with respect to mole fraction and all terms proportional to mole fraction are dropped.) At this limit, the initial slopes and the solvent values of the measured quantities determine

(12) Stevenson, S. H.; Meredith, G. R. *SPIE Proc.* **1986**, *682*, 147–152.
(13) (a) Buchalter, B.; Meredith, G. R. *Appl. Opt.* **1982**, *21*, 3221–3224. (b) Stevenson, S. H. Unpublished result.
(14) (a) Equations 10 and 11 are the well-known Clausius–Mosotti–Debye equations for dielectric constant at high and low frequency. (b) Hauchecorne, F.; Kerherve, F.; Mayer, G. *J. Phys.* **1971**, *32*, 47. (c) Finn, R. S.; Ward, J. F. *J. Chem. Phys.* **1974**, *60*, 454. (d) Keilich, S. *IEEE J. Quant. Electron.* **1969**, *QE-5*, 562. (e) Jerphagnon, J. *Phys. Rev. B* **1970**, *2*, 1091.
(15) See for example Bottcher, C. J. F. *Theory of Electric Polarization*, 2nd ed.; Elsevier: New York, 1973.
(16) Meredith, G. R.; Buchalter, B. *J. Chem. Phys.* **1983**, *78*, 1938–1945.
(17) Meredith, G. R. *Chem. Phys. Lett.* **1982**, *92*, 165–171.
(18) Singer, K. D.; Garito, A. F. *J. Chem. Phys.* **1981**, *75*, 3572–3580.

TABLE I: Results on Monosubstituted Benzenes and Stilbenes (Units in esu)

X	$\gamma^{EFISH} \times 10^{-36}$	$\gamma^{THG} \times 10^{-36}$	$\gamma^{EFISH}/\gamma^{THG}$	$\mu \times 10^{-18}$	$\alpha^0 \times 10^{-23}$	$\beta \times 10^{-30}$
						
H[a]	3.1	3.9	0.80	0.0	1.1	0.0
p-dioxane[a]	1.9	2.5	0.76	0.0	0.9	0.0
p-xylene[a]	4.3	5.2	0.83	0.0	1.5	0.0
CH_3[a]	4.1	4.6	0.88	0.38	1.3	<0.2
OH[b]	4.0	5.0	0.80	1.5	1.2	<0.2
SH[a]	4.6	6.3	0.73	1.4	1.5	<0.2
OMe[a]	3.8	4.8	0.79	1.4	1.4	<0.2
SMe[a]	5.9	7.2	0.82	1.3	1.7	<0.2
NH_2[a]	7.8	5.4	1.45	1.5	1.3	0.55
NMe_2[a]	14.1	8.1	1.70	1.6	1.7	1.1
julolidinamine[b]	16.7	7.8	2.14	1.6	2.4	1.3
F[a]	2.2	3.5	0.63	1.5	1.1	<0.2
Cl[a]	2.0	4.5	0.44	1.6	1.3	<0.2
Br[a]	4.4	5.4	0.81	1.4	1.4	<0.2
I[a]	7.2	7.5	0.96	1.3	1.7	<0.2
SO_2CH_3[b]	3.2	3	1.1	3.9	1.5	<0.2
SO_2F[a]	6.7	4	1.7	4.6	1.5	0.3
CN[a]	10.3	4.3	2.4	3.9	1.3	0.36
COH[a]	14.8	5.3	2.8	2.8	1.3	0.80
$COCF_3$[b]	25.0	5.3	4.7	3.3	1.7	1.3
NO[b]	30.0	6.8	4.4	3.1	1.4	1.7
NO_2[a]	40.8	5.7	7.2	4.0	1.4	1.9
$C_2H(CN)_2$[b]	82.3	12	6.9	4.8	2.0	3.1
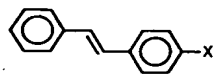						
H (trans)[c]	20	26	0.77	0.0	2.8	0.0
H (cis)[c]	10	12	0.83	0.0	2.6	0.0
NH_2[b]	104	31	3.4	2.2	2.8	7.4
NMe_2[b]	167	64	2.6	2.1	3.3	10
NO_2[b]	276	61	4.5	4.2	2.9	11

[a] Neat. [b] *p*-Dioxane solvent. [c] Chloroform solvent.

the measurement results. Since this method involves long extrapolations, all the measurements need to be of high precision. Figure 4 shows the typical results of concentration-dependent measurements of the relevant solution properties. Data are obtained for up to 1.35 wt % solutions of nitrostilbene which is a moderately nonlinear molecule. For highly nonlinear molecules such as 4-(*N*,*N*-dimethylamino)-4′-nitrostilbene, accurate data can be obtained with less than 0.1 wt % solutions. Solid lines are least-squares fits to linear dependence.

Results and Discussion

The results of our investigations on benzene and stilbene derivatives are given in Tables I–VI. They are organized to facilitate discussion of structure–property trends. These tables should be interpreted as follows:

(1) Where substituents are not specified, hydrogen is implied.

(2) Solution concentrations varied between 0.01 and 0.0005 in mole fraction depending on the nonlinearities and solubilities of the compounds.

(3) Compounds obtained from commercial sources are of the highest purities available and were used without further purification. In-house compounds are all analytically pure. Synthetic procedures for some of these compounds are available upon request.

(4) All nonlinear optical measurements were carried out with 1.91-μm radiation and molecular properties were deduced using Onsager local fields.

(5) λ_{max}, given in nm, denotes the absorption maximum of the lowest energy, prominent transition determined in *p*-dioxane solution. Values given in parentheses were obtained in the same solvent used for EFISH/THG measurements.

(6) The experimental uncertainties of the different measurements and deduced quantities are $\rho < 0.01\%$; $n(\omega = 633, 589$ nm) $< 0.01\%$; $\epsilon < 0.1\%$; I's $< 1\%$; $\mathcal{R} < 5\%$; $\mu < 10\%$; $\alpha^0 < 10\%$; $\mu\beta < 10\%$; and $\gamma < 20\%$. The uncertainties of the last four quantities are additionally dependent on the solubility of the compound and the validity of physical models used.

(7) Results presented in this paper supersede those given in our preliminary report.[19]

1. Donor–Acceptor Strengths. To evaluate the electronic biasing strengths of various donor and acceptor groups, we begin our studies of molecular hyperpolarizability on monosubstituted benzene[20a,b] and stilbene derivatives.[21] A wide range of electron-donating and -withdrawing substituents are examined including the less conventional thioalcohol, thiomethyl, sulfonyl, fluoromethyl ketone, nitroso, and dicyanovinyl groups. Measurement results are tabulated in Table I. For the benzene derivatives, the most striking observation is that, except in *N*,*N*-dimethylaniline and julolidine, all the donors are found to be ineffective in inducing charge and polarizability asymmetry. This is seen in the small μ and β values of the donor-substituted benzenes. Even for anisole and thioanisole, hyperpolarizabilities are too small to be determined by the accuracy of the current theoretical model. Although their γ^{EFISH} and γ^{THG} can be ac-

(19) Cheng, L.-T.; Tam, W.; Meredith, G. R.; Rikken, G.; Meije, E. W. *SPIE Proc.* **1989**, *1147*, 61–72. Occasional discrepancies are, in most cases, due to average of repeated measurements. In cases where compounds are highly colored such as the di- and tricyanovinyl derivatives, the local field factors for the solute molecules were previously overestimated. In one case, the material was found to be of low purity.

(20) Previous measurements of some species performed at 1.06 μm includes: (a) Oudar, J. L.; Leperson, H. *Opt. Commun.* **1975**, *15*, 258–262 (see errata, *Opt. Commun.* **1976**, *18*, 410–411). (b) Levine, B. F.; Bethea, C. G. *J. Chem. Phys.* **1975**, *63*, 2666–2682. (c) See, for example: *Theory and Applications of Ultraviolet Spectroscopy*; Jaffe, H. H., Orchin, M., Eds.; Wiley: New York, 1962; Chapter 12.

(21) Previous measurements of some species includes: at 1.06 μm: (a) Oudar, J. L. *J. Chem. Phys.* **1977**, *67*, 446–457. (b) Huijts, R. A.; Hesselink, G. L. J. *Chem. Phys. Lett.* **1989**, *156*, 209–212. At 1.3 and 1.58 μm: (c) Katz, H. E.; Singer, K. D.; Sohn, J. E.; Dirk, C. W.; King, L. A.; Gordon, H. M. *J. Am. Chem. Soc.* **1987**, *109*, 6561–6563. (d) Singer, K. D.; Sohn, J. E.; King, L. A.; Gordon, H. M.; Katz, H. E.; Dirk, C. W. *J. Opt. Soc. Am. B* **1989**, *6*, 1339–1350. At 1.9 μm: (e) Dulcic, A.; Flytzanis, C.; Tang, C. L.; Pepin, D.; Fetizon, M.; Hoppilliard, Y. *J. Chem. Phys.* **1981**, *74*, 1559–1563.

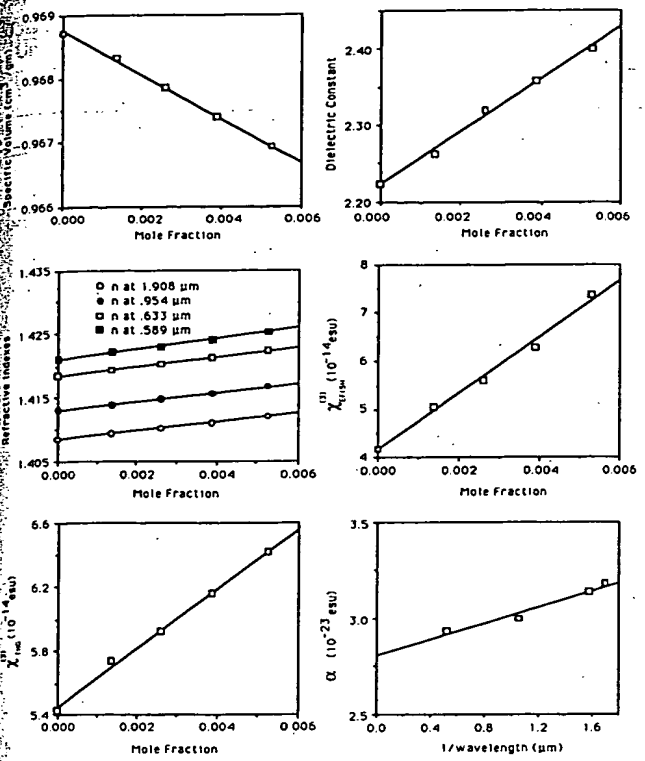

Figure 4. Concentration-dependent data for various macroscopic quantities determined for 4-nitrostilbene in *p*-dioxane.

curately determined (within the Onsager local field model), without performing temperature-dependent studies, separation between the deformational and dipolar contributions to EFISH remains ambiguous (see eq 14). For centric molecules such as benzene, *p*-dioxane, and *p*-xylene, the ratio between γ^{EFISH} and γ^{THG} is around 0.8, which has been used as a crude estimate of the deformational contributions to EFISH signal for benzene derivatives. Examination of the γ^{EFISH} and γ^{THG} values in Table I reveals that for donor-substituted benzenes, both values change in parallel, indicating a limited dipolar contribution to EFISH signal. This is partly due to the small dipole moments. A similar situation is found for the halogen derivatives. Clearly, neglecting the deformational contributions to EFISH would give erroneous results. The ineffectiveness of donors in inducing asymmetry may be attributed to two factors. Other than the dimethylamino group and the bridged structure in julolidine, the connecting atom in all the donors, including the amino, is sp^3 hybridized. The tetrahedral geometry does not allow efficient overlap between the lone pair containing donor orbitals and the π orbitals of the benzene ring. In addition, these donor substitutions only result in minimal extensions of the overall conjugation.[20c]

Accepting groups are found to be much more effective. Their efficacies increase in the order of SO_2CH_3, SO_2F, CN, CHO, $COCF_3$, NO, NO_2, and $CHC(CN)_2$. $(C_2(CN)_3$ is significantly better than $CHC(CN)_2$ as revealed from studies of disubstituted benzenes discussed below.) Nitroso is found to be comparable to nitro while aldehyde is much superior to the cyano group. The proper hybridizations and longer extensions of the benzene conjugation may be reasons for the effectiveness of the accepting groups. This view is supported by the large β of benzylidene malonitrile ($C_6H_5CHC(CN)_2$) and its extended structure. However, the substantially higher dipole moments of the acceptor-substituted benzenes do not mean a greater polarization of the benzene π system since the sulfonyl, cyano, carbonyl, and nitro group dipoles are substantial [e.g. μ(nitrohexane) = 3.6 D, and μ(acetonitrile) = 3.4 D]. Ring polarization contributes less than 0.5 D to the total dipole moments. This point is noteworthy when considering the relationship between substitution pattern and β_{EFISH}.

Results obtained for the stilbene derivatives are quite different. The β values are much higher than their benzene analogous. Clearly, conjugation length is an important factor in determining all orders of polarizability. The higher μ and γ values also indicate that the stilbene entity is more polarizable. The values for 4-nitrostilbene and 4-(*N*,*N*-dimethylamino)stilbene are nearly equal within experimental errors. With the extended stilbene structure, π conjugation extension due to nitro substitution becomes less of a factor than in the case of benzene derivatives.

2. Charge Transfer and Substitution Pattern. The cooperative effects of donor and acceptor groups are investigated by studying para-disubstituted benzene[21b,d,22] and 4,4′-disubstituted silbene[3c,21] derivatives. Measurement results are given in Tables II and III. A significant increase in μ and β values over the sum of the monosubstituted fragments is evident. This is the well-recognized enhancement resulting from the charge-transfer (CT) interactions between the donor and acceptor groups. From simple vector additivity of the monosubstituted fragments, the CT contribution to μ is typically less than 1 D for benzene derivatives. The extended and planar structure makes *trans*-stilbene an effective conjugated backbone for hyperpolarizability. Between the benzene and stilbene structures with the same substituents, typical enhancement of 6–8 times is realized for β. Only modest increases, typically less than 0.5 D, are seen for μ. This may be an indication that only a small fraction of the donor electron is transferred to the acceptor in the ground state, and the polarization of the conjugation may be limited to only the region immediately adjacent to the substituents. Since the molecular dipole is the vectorial sum of these two "local" dipoles, which are often dominated by the group dipole moments of the substituents, increasing their separation does not result in significant increase of the total dipole moment. However, as a result of conjugation extension, the low-energy bands of *trans*-stilbene derivatives are typically 50–60 nm red-shifted in comparison to that of the benzene derivatives when compared in the same solvent. With a given acceptor, the nitro group, for instance, the relative effectiveness of various donors can be established, giving Me, Br, OH, OPh, SMe, N_2H_3, NH_2, NMe_2, and the "julolidine" amine in increasing order. It is interesting to note that the thiomethyl donor, which is found to be significantly more effective than the methoxy group in the benzene system, is slightly less effective than the methoxy group in inducing asymmetric polarizability in the stilbene system. Since the hyperpolarizability of the longer stilbene system is dominated by resonance interaction between donor and acceptor, the lack of propensity for the sulfur atom (and other second-row elements) to form double-bonded resonance structure with carbon may result in the reduced effectiveness of the thiomethyl donor. In all cases, the thiomethyl and thioalcohol donors are found to be inferior to the primary amino group in disagreement with recent report on comparable strengths between thiomethyl and tertiary amino donors.[23] The overall orderings among other donors and acceptors remain unchanged as determined from measurements on monosubstituted benzenes.

Charge-transfer interactions between substituents are often depicted by resonance structures which connect charge-neutral and charge-separated states with alternating single and double bonds. According to this picture, para and ortho substitution patterns allow CT interaction between donor and acceptor groups while meta does not for benzene derivatives. For stilbenes, resonance interactions between substituents are allowed for 2(donor)–2′(acceptor), 4–4′, 2–4′, and 4–2′, and not allowed for 2–3′, 3–2′, 3–3′, 3–4′, and 4–3′ positions. To what extent is such a picture reliable in predicting hyperpolarizability? We examine this question by investigating nitrobenzene and nitrostilbene derivatives. Measurement results are given in Tables IV and V. For benzenes (Table IV), meta and ortho[22a,24] compounds are much

(22) Previous measurements of some species performed at 1.06 μm include: (a) Oudar, J. L.; Chemla, D. S.; Batifol, E. *J. Chem. Phys.* **1977**, *66*, 1626–1635. (b) Dulcic, A.; Sauteret, C. *J. Chem. Phys.* **1978**, *69*, 3453–3457.
(23) Barzoukas, M.; Josse, D.; Zyss, J. *Chem. Phys.* **1989**, *139*, 359–367.
(24) (a) Levine, B. F. *Chem. Phys. Lett.* **1976**, *37*, 516–520. (b) Oudar, J. L.; Chemla, D. S. *J. Chem. Phys.* **1977**, *66*, 2664–2668.

TABLE II: Results on Para-Disubstituted Benzenes (Units in esu)

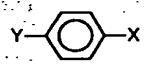

X	Y	solvent	λ_{max}, nm	$\mu \times 10^{-18}$	$\alpha^\circ \times 10^{-23}$	$\beta \times 10^{-30}$	$\gamma \times 10^{-36}$
SO_2Me	OH	*p*-dioxane	290	3.4	1.7	1.3	3
CN	Me	neat		4.4	1.5	0.7	5
CN	Cl	*p*-dioxane		2.3	1.6	0.8	5
CN	Br	*p*-dioxane		2.4	1.8	1.1	7
CN	OPh	*p*-dioxane		4.1	2.6	1.2	9
CN	OMe	*p*-dioxane	248	4.8	1.7	1.9	4
CN	SMe	*p*-dioxane		4.4	2.0	2.8	9
CN	NH_2	*p*-dioxane	270	5.0	1.6	3.1	6
CN	NMe_2	*p*-dioxane	290	5.6	2.1	5.0	10
CHO	Me	neat		3.0	1.6	1.7	7
CHO	OPh	neat	269	2.8	2.5	1.9	12
CHO	OMe	neat	269	3.5	1.7	2.2	8
CHO	SMe	neat	310	3.1	1.9	2.6	13
CHO	NMe_2	*p*-dioxane	326	5.1	2.0	6.3	18
i-$SO_2C_3F_7$	OMe	$CHCl_3$	290	5.4	2.7	3.3	5
$COCF_3$	OMe	*p*-dioxane	292	3.5	2.9	3.6	12
$COCF_3$	OPh	*p*-dioxane	292	4.0	2.0	3.6	7
$COCF_3$	NMe_2	*p*-dioxane	356	5.9	2.4	10	16
NO	NMe_2	*p*-dioxane	407	6.2	2.1	12	
NO_2	Me	*p*-dioxane	272	4.2	1.6	2.1	8
NO_2	Br	*p*-dioxane	274	3.0	1.8	3.3	
NO_2	OH	*p*-dioxane	304	5.0	1.5	3.0	8
NO_2	OPh	*p*-dioxane	294	4.2	2.6	4.0	9
NO_2	OMe	*p*-dioxane	302	4.6	1.5	5.1	10
NO_2	SMe	*p*-dioxane	322	4.4	1.9	6.1	17
NO_2	N_2H_3	*p*-dioxane	366	6.3	1.8	7.6	9
NO_2	NH_2	acetone	365	6.2	1.7	9.2	15
NO_2	NMe_2	acetone	376	6.4	2.2	12	28
NO_2	CN	*p*-dioxane		0.9	1.7	0.6	7
NO_2	CHO	*p*-dioxane	376	2.5	1.7	0.2	7
$CHC(CN)_2$	OMe	*p*-dioxane	345	5.5	2.4	9.8	30
$CHC(CN)_2$	NMe_2	$CHCl_3$	420	7.8	2.8	32	
$CHC(CN)_2$	julolidine	CH_2Cl_2	458	8.0	3.0	44	
$C_2(CN)_3$	NH_2	CH_2Cl_2	498	7.8	3.4	39	
$C_2(CN)_3$	NMe_2	CH_2Cl_2	516	8.2	3.7	50	
$C_2(CN)_3$	julolidine	CH_2Cl_2	556	8.5	3.9	60	

TABLE III: Results on 4,4′-Disubstituted Stilbenes (Units in esu)

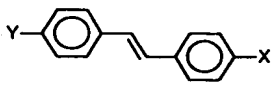

X	Y	solvent	λ_{max}, nm	$\mu \times 10^{-18}$	$\alpha^\circ \times 10^{-23}$	$\beta \times 10^{-30}$	$\gamma \times 10^{-36}$
$SO_2C_5H_{11}$	HOHexO	$CHCl_3$	336	6.5	6.0	10	68
$SO_2C_6F_{13}$	OMe	*p*-dioxane	347	7.8	4.8	14	93
$COCF_3$	OMe	*p*-dioxane	368	4.2	3.9	16.4	83
CN	OH	*p*-dioxane	344	4.5	3.2	13	52
CN	OMe	$CHCl_3$	(340)	3.8	3.4	19	54
CN	$N(Me)_2$	$CHCl_3$	382	5.7	3.9	36	125
NO_2	H	*p*-dioxane	345	4.2	2.9	11	61
NO_2	Me	*p*-dioxane	351	4.7	3.5	15	77
NO_2	Br	*p*-dioxane	344	3.2	3.8	14	98
		$CHCl_3$	(356)	3.4	3.3	18	45
NO_2	OH	*p*-dioxane	370	5.5	3.3	17	104
NO_2	OPh	*p*-dioxane	350	4.6	4.2	18	80
NO_2	OMe	*p*-dioxane	364	4.5	3.4	28	79
		$CHCl_3$	(370)	4.5	3.4	34	93
NO_2	SMe	*p*-dioxane	374	4.3	3.9	26	113
		$CHCl_3$	(380)	4.3	3.8	34	100
NO_2	NH_2	$CHCl_3$	402	5.1	3.2	40	147
NO_2	$N(Me)_2$	$CHCl_3$	427	6.6	3.4	73	225
		NMP		7.2	3.1	70	270
NO_2	julolidinamine	$CHCl_3$	438	7	4.5	96	
NO_2	COOMe	CH_2Cl_2	350	4.0	3.8	4.0	46
NO_2	CHO	*p*-dioxane	352	4.1	3.5	6.0	57
Br	OMe	*p*-dioxane	325	4.0	3.4	2.5	54

less nonlinear than the para compounds and in most cases their β values are even less than the vector sums of their monosubstituted derivatives. In addition, ortho-substituted derivatives are not always superior to the meta derivatives, contrary to expectations based on resonance structures. For the nitroanilines, whose amino nitrogens are favorably hybridized, one finds para ≫ ortho > meta, which agrees well with previous findings.[24a] However, for the other donors, as a result of their sp^3 centers, their electron-donating mechanisms are less clear. In the case of weak donors such as the bromo and methyl groups, the β values for the different

TABLE IV: Results on Ortho- and Meta-Disubstituted Benzenes (Units in esu)

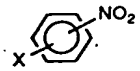

X	solvent	λ_{max}, nm	$\mu \times 10^{-18}$	$\alpha^\circ \times 10^{-23}$	$\beta \times 10^{-30}$	$\gamma \times 10^{-36}$
ortho						
Me	neat		3.9	1.6	1.0	6
Br	*p*-dioxane		4.0	1.8	0.4	7
OH	*p*-dioxane	348	3.4	1.5	1.2	3
OMe	neat	318	3.8	1.7	1.4	6
NH_2	*p*-dioxane		4.1	1.6	2.5	8
CN	*p*-dioxane		5.5	1.7	1.2	7
CHO	*p*-dioxane		4.0	1.6	0.8	6
meta						
Me	neat		3.9	1.6	1.5	6
Br	*p*-dioxane		3.4	1.7	1.0	5
OH	*p*-dioxane		3.6	1.3	0.8	6
OMe	*p*-dioxane	326	3.9	1.7	1.6	5
NH_2	*p*-dioxane	396	4.7	1.5	1.9	7
CN	*p*-dioxane		3.7	1.7	0.8	7
CHO	*p*-dioxane		2.8	1.6	1.7	6

TABLE V: Results on Methoxy- and Nitro-Disubstituted Stilbenes (Units in esu)

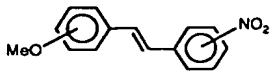

MeO	NO_2	solvent	λ_{max}, nm	$\mu \times 10^{-18}$	$\alpha^\circ \times 10^{-23}$	$\beta \times 10^{-30}$	$\gamma \times 10^{-36}$
2	2′	$CHCl_3$	360 s	3.8	3.3	4.4	29
3	2′	$CHCl_3$	370 s	3.7	3.3	1.6	29
4	2′	$CHCl_3$	390 s	3.5	3.3	3.8	35
2	3′	$CHCl_3$	320	4.4	3.3	5.5	25
3	3′	$CHCl_3$	292	3.9	3.3	4.5	28
4	3′	*p*-dioxane	318	3.9	3.3	5.3	26
2	4′	$CHCl_3$	362	5.0	3.3	22	61
3	4′	$CHCl_3$	352	4.0	3.4	21	56
4	4′	$CHCl_3$	370	4.5	3.4	34	93

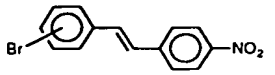

Br	NO_2	solvent	λ_{max}, nm	$\mu \times 10^{-18}$	$\alpha^\circ \times 10^{-23}$	$\beta \times 10^{-30}$	$\gamma \times 10^{-36}$
2	4′	$CHCl_3$	(346)	4.6	3.3	12	50
3	4′	$CHCl_3$	(346)	3.4	3.4	14	74
4	4′	$CHCl_3$	(356)	3.4	3.3	18	45

substitution patterns are found to be quite comparable with para > meta > ortho. Ortho-substituted isomers can also have significant H-bonding interaction between the substituents, which cannot occur in the other isomers and may strongly influence their optical nonlinearities.

The importance of factors other than resonance structures in determining β values is further illustrated by results obtained for the nitrostilbene derivatives (Table V). Most unexpected are the relatively large β values found for the 3–4′ and the very low value for the 2–2′ derivatives. Clearly conjugated resonance structures, which connect the donor and acceptor for the 2–2′ but not the 3–4′ substitution patterns, do not predict this result. A second unexpected result is found in the nonreciprocity of β values upon interchanging the donor and acceptor positions. Intuitively, CT interactions, if effective for 2–4′ and 3–4′, should also be effective for 4–2′ and 4–3′ substitution patterns.

In order to understand these observations, two factors which are undoubtedly important must be considered. First, the dominant portion of the molecular dipole moment of nitrostilbene derivatives is due to the polar nature of the nitro group itself, apart from the relatively small mesomeric contribution due to donor–acceptor interaction between the substituents. Therefore, the molecular dipole direction is principally determined by the orientation of the nitro group. Second, since the EFISH determined β is a vectorial projection of the hyperpolarizability tensor along the molecular dipole direction, it samples the dominant tensor components only if the dipole direction is coincident with the molecular charge-transfer axis. For *m*- and *o*-nitrobenzene derivatives and -3′- and -2′-nitrostilbene derivatives, whose CT and dipole directions are angularly displaced, their β values are expected to decrease according to the cosine of this angular deviation. With these simple geometric considerations, one can easily rationalize the low β values for these compounds which exhibit angular displacements greater than 60°. The comparable values for all stilbenes with 4′-nitro substitution are also partly explained by the good alignment of molecular dipoles with CT axes. Since the group moment of the methoxy donor is much smaller than that of the nitro acceptor, their substitution patterns have only minor effect on the molecular dipole directions. The effectiveness of 3-donor substitutions indicates that instead of a description base on resonance structures, charge transfer is more appropriately viewed as a less route-specific interaction between electron-rich and electron-deficient regions of a molecule. Adopting such a view, excluding any steric considerations, CT interaction is expected to be reciprocal upon interchanging donor and acceptor positions. Large tensor components, which are not fully accessed by EFISH because of geometric considerations, should also be present in all the 2′- and 3′-nitrostilbene derivatives.

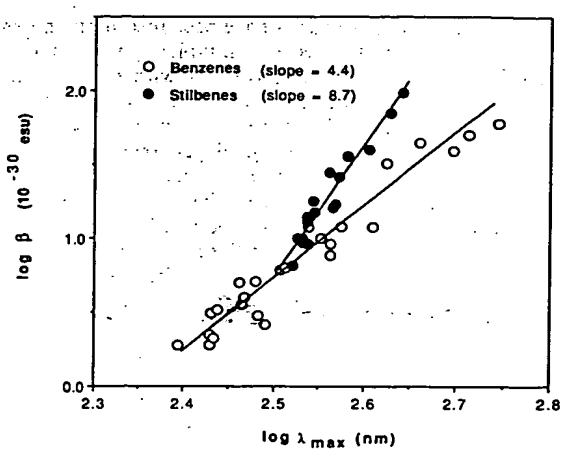

Figure 5. Logarithmic plot of β vs λ_{max} for para-substituted benzenes and 4-4′-disubstituted stilbenes.

3. Nonlinearity and Transparency Trade-Off. If low-lying CT excitations are responsible for the large nonlinearities, there should be a trade-off between nonlinearity and transparency. To explore this question, we have characterized a wide range of donor–acceptor para-disubstituted benzenes and 4,4′-disubstituted stilbenes, including the highly colored dicyanovinyl and tricyanovinyl derivatives and the transparent cyano and aldehyde derivatives. Measurement results for β and the wavelength of the lowest energy prominent transition are shown in a logarithmic plot in Figure 5. The good correlation between β and λ_{max} confirms that such a trade-off exists. Since measurements are made with 1.91-μm radiation, the increase is not a result of dispersive enhancement above the hypothetical zero-frequency electronic β due to the finite frequency of the experimental fundamental. A natural question then is whether the widely quoted two-state model, which is a single-term approximation of the full expression given by eq 2, can account for this clearly observed correlation.

At very low frequency, the two-state model[24b] states that, for long-axis polarizations, $\beta \propto (\lambda_{max})^3 f \Delta\mu$, the product of cubed wavelength with the oscillator strength and difference of Franck–Condon-state dipole moments. There is no known systematic dependence of f and $\Delta\mu$ on λ_{max}; therefore, critical assessment of the two-level model awaits further spectroscopic and solvatochromic measurements. One might expect f and $\Delta\mu$ within this class of weakly polarized molecules to be correlated with the combined donor–acceptor strength, which factor might also increase λ_{max}. Allowing for some unidentified positive correlation which is here approximated as $f\Delta\mu \propto (\lambda_{max})^m$ with $m \geq 1$ (since $f \propto \mu_{ge}^{2/\lambda}$) the two-state model predicts $\beta \propto (\lambda_{max})^n$, $n = 3 + m$.

Oscillator strengths of these bands have been measured and exhibit no direct correlation with wavelength, typically varying between 0.3 and 0.7. If λ_{max} correlates positively with $f\Delta\mu$ or $\Delta\mu$, $m \geq 0$ and $n \geq 3$ are to be expected. This prediction is in agreement with the data of Figure 5 for benzene derivatives which shows that, within the uncertainty of some dispersion enhancement for the high λ_{max} data, a near-quartic variation of β with λ_{max} occurs. It appears that the simple two-state model is not inconsistent when applied to a restricted class of compounds, benzene derivatives in this case, where structural modifications are directed at the charge-transfer bands and the hyperpolarizabilities.

Analogous trade-off between nonlinearity and transparency is also observed for the stilbene derivatives. For a given λ_{max}, however, substantially higher nonlinearity is offered by the stilbene derivatives. From the logarithmic plot, it is evident that the hyperpolarizability of the stilbene system shows a much stronger dependence on the wavelength of the CT band than that of the benzene system. Again this observation on the stilbene derivatives can be used to qualitatively assess the validity of the two-state model, and the reliability of using linear optical measurements, such as absorption spectroscopy and solvatochromic effect, to calculate the hyperpolarizabilities of compounds with different structures. According to the two-state model, since the oscillator strengths of the benzene and stilbene derivatives do not vary by more than a factor of 2 and do not correlate with λ_{max}, the larger values of β and its strong dependence on λ_{max} for the stilbene derivatives would have to be attributed to a much larger and strongly varying $\Delta\mu$. Our solvatochromic measurement, which is based on absorption spectral shift found in a series of solvents with similar refractive indexes but differing dielectric constants (using a spherical molecular radius of 7 Å for stilbenes and 5 Å for benzenes), however, revealed only a weakly varying excited-state dipole moment, μ_e, for the stilbene system, ranging from 20 to 28 D. Therefore, for the stilbene system, the two-state model cannot account for the sharp increase of β with increasing donor–acceptor strengths. When used to account for the difference between benzene and stilbene derivatives, the two-state model is also found to be inadequate. For instance, our solvatochromic measurements yield comparable values of oscillator strength and a factor of 2 increase in $\Delta\mu$ for the equally colored *p*-nitroaniline (λ_{max} = 365 nm, f = 0.3, and $\Delta\mu$ = 6 D) and 4-methoxy-4′-nitrostilbene (λ_{max} = 364 nm, f = 0.26, and $\Delta\mu$ = 13 D), leading to a two-state β ratio of 1.7. Their measured hyperpolarizabilities differ by a factor of 3.2 instead. Clearly, the higher excited states' contributions to the molecular nonlinearities must considered here and they are undoubtedly important for extended molecular structure such as stilbene derivatives.

4. Correlation and Subsequent Constants. Substituent constants are commonly used in color chemistry to predict the position of the CT band.[25] The good correlation we observed between β and λ_{max} implies that these substituent constants might also be useful as a semiempirical tool to predict β values in these compounds. This approach has been taken by others, with varying degrees of success.[26] Recent studies of correlations between substitution constants and computed gas-phase β_{zzz} values for 4-donor-4′-acceptor stilbenes found good linear correlation.[3i] The major contribution to the hyperpolarizability in the 4-donor-4′-acceptor stilbenes comes from the charge transfer. To a lesser extent, this also holds for the *p*-donor–acceptor benzenes. Therefore, one should look for correlation with the "through resonance" substituent constants, $\sigma_p^{+/-}$, which accounts for the donor–acceptor interactions.

In the case of the *p*-nitrobenzenes, an appropriate substituent constant would be σ_p^+, whereas for the *p*-methoxybenzenes it would be σ_p^- (for tabulations of these parameters, see Leo and Hansch[27]). Figure 6 shows that, for the first group, linear relation

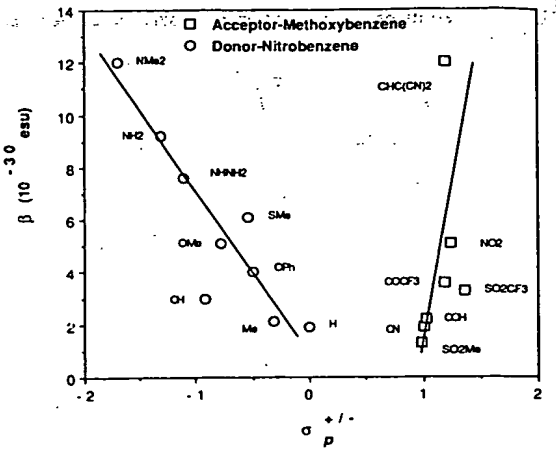

Figure 6. β vs $\sigma_p^{+/-}$ for para-disubstituted benzenes.

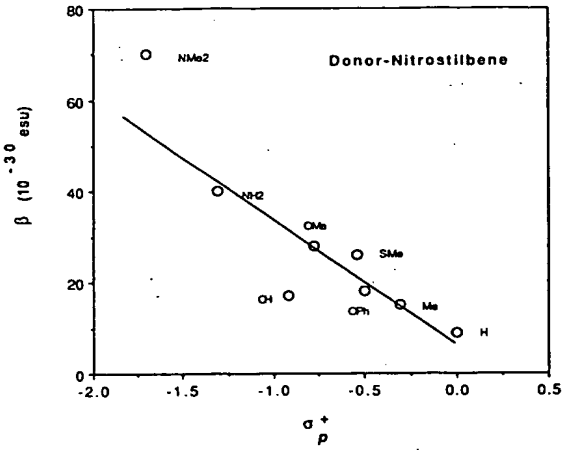

Figure 7. β vs σ_p^+ for 4′-donor-4-nitrostilbenes.

of β versus σ_p^+ is obtained. For the *p*-methoxybenzenes, an analogous statement can be made. In Figure 7, β versus σ_p^+ for the 4-donor–4′-nitrostilbenes is shown and good correlation is also obtained. However, a linear relationship fits β vs σ_p^+ less well for the stilbene derivatives. Dispersive enhancement as a result of the red shift of the high β compounds should be considered.

There is no a priori reason to expect a linear relationship between hyperpolarizability and substituent constants. For a given substituent, $\sigma_p^{+/-}$ are determined by its influence on the chemical reactivity of a parent compound. This property, which is largely determined by the ground-state charge density at a reaction center, seems quite remote from the substituent's influence on the hyperpolarizability which is the polarization property of the entire molecule involving excited states. The observed linear relation may be rationalized by considering β as the product of an anharmonicity factor, determined largely by the end groups, and a polarizability factor, determined by the conjugated structure. While the polarizability remains relatively constant within a particular structural class, the anharmonicity is strongly influenced by the substituents in similar manner as the reactivity of a reaction center.

5. Substitution Effects. There is very little information available on how molecular substitutions, intended to influence other material properties such as transparency, solubility, crystal packing, and chemically convenient functionality for incorporation into polymeric structures, will affect the hyperpolarizability. We address this issue by examining the effects of heteroatom and electron-donating or -withdrawing side-group substitutions in the benzene and stilbene systems. Our measurement results are tabulated in Table VI. Our observations can be summarized as follows: although the substitution effects on the absorption band largely obey Dewar's rules (there are notable exceptions such as

(25) See for example: Griffiths, J. *Colour and Constitution of Organic Molecules*; Academic Press: New York, 1976.
(26) Katz, H. E.; Dirk, C. W.; Singer, K. D.; Sohn, J. E. *SPIE Proc.* 1987, *824*, 86–92.
(27) Hansch, C.; Leo, A. *Substituent Constants For Correlation Analysis in Chemistry and Biology*; Wiley: New York, 1979.

TABLE VI: Results on Heteroatom and Side-Group-Substituted Benzenes and Stilbenes (Units in esu)

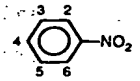

substitution	solvent	λ_{max}, nm	$\mu \times 10^{-18}$	$\alpha^\circ \times 10^{-23}$	$\beta \times 10^{-30}$	$\gamma \times 10^{-36}$
3-aza; 4-NH_2	acetone		6.5	1.7	3.7	11
2-aza; 4-OMe	*p*-dioxane		3.5	1.5	2.2	10
3-Me; 4-NH_2	*p*-dioxane		6.2	1.9	8.7	17
2-Cl; 4-NH_2	*p*-dioxane	350	5.9	1.8	6.8	12
3-OMe; 4-NH_2	*p*-dioxane		6.0	1.8	8.7	19
2-F; 4-OMe	*p*-dioxane	304	4.4	1.8	2.5	10
2,5-F; 4-OMe	*p*-dioxane	304	4.9	1.8	2.6	12
2,3,5,6-F; 4-OMe	*p*-dioxane	270	4.2	1.8	1.7	7

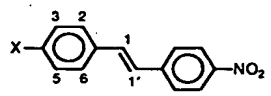

X	substitution	solvent	λ_{max}, nm	$\mu \times 10^{-18}$	$\alpha^\circ \times 10^{-23}$	$\beta \times 10^{-30}$	$\gamma \times 10^{-36}$
H	1-aza	*p*-dioxane	346	4.4	2.7	4.9	26
Me	1-aza	*p*-dioxane	351	4.7	3.5	15	77
OMe	1-aza	*p*-dioxane	376	4.4	3.3	14	76
OMe	1′-aza	*p*-dioxane	349	5.4	2.5	6.6	30
NH_2	1,1′-azo	*p*-dioxane	420	5.8	3.5	29	170
NEtEtOH	1,1′-azo	*p*-dioxane	455	7.0	3.8	49	190
OMe	3-Me	*p*-dioxane	366	5.2	3.7	26	96
OMe	3-OMe	*p*-dioxane	380	4.7	3.7	23	117
OMe	3-F	*p*-dioxane	363	4.1	3.4	18	92
OMe	2-OMe	*p*-dioxane	395	4.8	3.9	32	110
OMe	1′-CN	*p*-dioxane	361	5.3	3.8	21	86
Br	1′-CN	*p*-dioxane	340	4.6	2.9	8.0	30
Br	1-aza; 1′-CN	*p*-dioxane	382	4.1	3.6	2.1	59
OMe	2′-NO_2	*p*-dioxane	390	4.7	3.7	22	110

the dinitrostilbene derivatives), their effects on β are mostly detrimental and cannot be accounted for by dispersive considerations due to the substitution-induced shift of the absorption bands. In particular, aza substitutions on the 2- or 3-position of para-disubstituted benzene derivatives and azo or azomethine substitutions on 4,4′-disubstituted stilbene derivatives are very damaging, reducing the β value by as much as 80%. The effects of side-group substitutions with weak electron acceptors such as fluorine and cyano are also quite severe while only minor effects are observed with electron donors such as methyl and methoxy groups. Therefore, heteroatom and side-group-substituted derivatives are found to give no advantage over their parent compounds in the trade-off between nonlinearity and transparency.

The only exception to this decreasing trend is provided by 2′,4′-dimethoxy-4-nitrostilbene which shows a 20% increase in $\mu\beta$ product over the 4-4′-disubstituted derivative. This increase may be a result of the combined contributions from two donating groups whose substitution positions allow transfer of electron densities from both donors to the accepting group through charge-separated resonance structures. Such arguments will predict an enhancement of nonlinearity for 4′-methoxy-2,4-dinitrostilbene where two strong accepting groups act to polarize the charge distribution. Instead, a substantial (25%) reduction in β is observed with only slight increase in dipole moment. Since only one ortho substituent is present in either compound, steric hindrance, which may lead to nonplanarity and reduced nonlinearity, should be minimal. The observed spectral red shift supports such a contention. The reduction in nonlinearity for the dinitro compound again illustrates the importance of geometric considerations discussed earlier. Due to the large group dipole moments of most accepting groups, multiple acceptor substituents often lead to a large angular deviation between the molecular dipole axis and the molecular long axis containing dominant hyperpolarizability components, resulting in lower nonlinearity that is amenable to electrical poling. The reduced values for the dinitrostilbene and ethylenic cyanonitrostilbene derivatives demonstrate this point. Conversely, due to their low group dipole moments, multiple donors can be advantageously exploited to enhance nonlinearity.

Substituents which lower molecular symmetry can clearly have an effect on the hyperpolarizability, which depends ultimately on

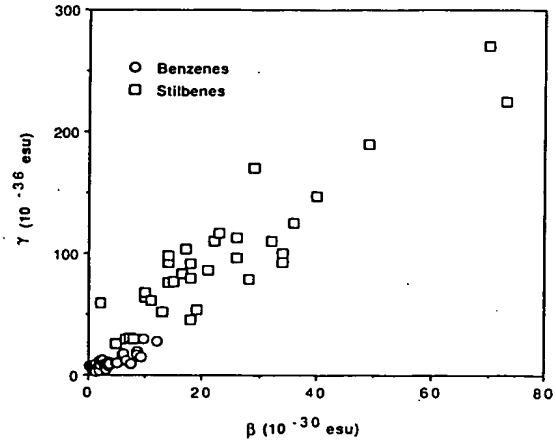

Figure 8. Correlation between β and γ of donor–acceptor-substituted benzene and stilbene derivatives. Data taken from Tables I, II, and III.

the molecular electronic structure. Such an effect is expected to be small for a substituent which does not greatly alter the effective symmetry of the π system. 2-Methyl substitution of *p*-nitroaniline may be such an example. The effect of 3-methyl, 3-methoxy, or ethylenic cyano substitutions on 4-methoxy-4′-nitrostilbene cannot be a result of symmetry changes since the parent molecule does not possess a symmetry axis. The substitution effects on the conjugation must be considered. Perhaps, our observation of a rather general reduction of hyperpolarizability resulting from heteroatom as well as side-group substitutions can be rationalized by realizing that the effectiveness of the benzene and stilbene conjugations arise from the delocalization of their π electrons, which offer properties such as planarity and bond equivalence. Any substituent which reduces bond equivalence, by altering the bond length, electronegativity, or hybridization of the substituted site, will lead to less effective delocalization hence reduced nonlinearity. Thus, drastic perturbations of the conjugation such as aza and perfluoro substitutions on benzene derivatives and azo and azomethine substitution for stilbene derivatives result in

significantly lower β values. This view is supported by measurement results on diphenylacetylene derivatives (see accompanying paper). The differences in bond length and hybridization between the acetylenic carbons and the phenyl carbons lead to a substantial reduction of hyperpolarizability in comparison to the stilbene derivatives.

6. Second Hyperpolarizability. Structure–property relationships for the second hyperpolarizability, beyond the general recognition of the importance of extended π conjugation, are much less well established.[28] A simple two-state approximation, in which γ is given by the field-dependent polarizability, $\alpha(E)$, according to perturbation theory with static external field, gives the following simple expression

$$\alpha(E) = \alpha(E=0) + \beta E + \gamma EE \propto \frac{|\mu'_{ge}(E)|^2}{\omega_{ge}} \qquad (16)$$

where

$$\mu'_{ge}(E) = \mu_{ge} - \frac{|\mu_{ge}|^2 \mu_{ge}}{\omega_{ge}^{\ 2}} E + \frac{\mu_{ge}(\mu_{ee} - \mu_{gg})}{\omega_{ge}} EE \qquad (17)$$

Collecting $(1/\omega_{ge})^3$ terms in eq 16 gives an expression for γ in which two contributions with opposing signs are evident:

$$\gamma \propto \frac{-\mu_{ge}^{\ 4}}{\omega_{ge}^{\ 3}} + \frac{\mu_{ge}^{\ 2}(\mu_{ee} - \mu_{gg})^2}{\omega_{ge}^{\ 3}} \qquad (18)$$

For centrosymmetric molecules, since the ground- and excited-state dipoles vanish, i.e., $\mu_{gg} = \mu_{ee} = 0$, the two-state model predicts a negative γ.

Several observations are evident from our cubic polarizability (γ) data. First, all values of γ are found to have positive signs. For centrosymmetric molecules, this is contrary to the prediction of the two-state model and clearly indicates that multiple states must be considered. Second, γ values show a strong dependence on conjugation length with about an order of magnitude increase between benzene and stilbene derivatives (see Tables I–III). Note also a factor of 2 difference between *trans*- and *cis*-stilbene. This is in agreement with the established guideline which identifies electron delocalization as a key factor for third-order optical response. Third, a strong correlation is found between γ and β, thus also λ_{max}, for both molecular classes. Figure 8 plots γ and β data given in Tables II, III, and VI for donor–acceptor-substituted species. The high β molecules have γ values up to 10 times of those found for the centrosymmetric species. Interpretation of this result is complicated by the presence of dispersive enhancement (3ω = 636 nm, close to absorption edge of the high-β compounds) and local field cascading process,[17] which can lead to a factor of 2 enhancement in moderately polarizable solvents for compounds with β values comparable to *p*-nitroaniline. Given the above reservations, our results nevertheless suggest a significant contribution from the CT nature of the molecular structure and are in qualitative agreement with the two-state prediction. This interpretation is quite reasonable in view of the substantial difference between typical transition moments of 3–7 D and the typical $\Delta\mu$ of 10–20 D for donor–acceptor-substituted benzene and stilbene derivatives.

Conclusion

We have systematically investigated the hyperpolarizabilities of benzene and stilbene derivatives using EFISH and THG measurements at 1.91 μm. An efficient, relatively precise, and novel methodology is described in detail. A wide range of donor and acceptor groups were studied and their relative effectiveness in inducing asymmetric polarizabilities established. Questions concerning donor–acceptor interactions and their dependence on substitution patterns are addressed. It was found that geometric factors are more important that resonance structure argument in understanding the structural dependence. The trade-off of nonlinearity vs transparency was examined and an empirical quartic dependence established for the benzene derivatives. Such a dependence is compatible with the widely used two-state model. For the stilbene derivatives, a much stronger variation of hyperpolarizability with CT band λ_{max} is revealed. Solvatochromic and absorption measurements establish the inadequacy of the two-state model for the stilbene system. Correlation with substituent constants was discussed. Measurements on heteroatom, side-group, and multiple donor–acceptor-substituted benzene and stilbene derivatives revealed a general reduction of the β values as a result of steric, dipole redirection, and localization of the conjugated electrons. The cubic hyperpolarizability was shown to have strong conjugation dependence. A large contribution resulting from acentric structure was revealed. Due to potential dispersive and cascading processes, its origin is inconclusive. Although some of the molecules included in this and the accompanying studies have been characterized before, the merit of the current study rests in its breadth and internal consistency.

Acknowledgment. We thank H. Jones (Du Pont), T. Hunt (Du Pont), and B. G. Tiemann (JPL) for expert technical assistance. The research described in this paper was performed, in part, by the Jet Propulsion Laboratory, California Institute of Technology, as part of its Center for Space Microelectronics Technology which is supported by the Strategic Defense Initiative Organization, Innovative Science and Technology Office, through an agreement with the National Aeronautics and Space Administration (NASA).

Registry No. HOC_6H_4-*p*-SO_2Me, 14763-60-1; CNC_6H_4-*p*-Me, 104-85-8; CNC_6H_4-*p*-Cl, 623-03-0; CNC_6H_4-*p*-Br, 623-00-7; CNC_6H_4-*p*-OPh, 3096-81-9; CNC_6H_4-*p*-OMe, 874-90-8; CNC_6H_4-*p*-SMe, 21382-98-9; CNC_6H_4-*p*-NH_2, 873-74-5; CNC_6H_4-*p*-NMe_2, 1197-19-9; $CHOC_6H_4$-*p*-Me, 104-87-0; $CHOC_6H_4$-*p*-OPh, 67-36-7; $CHOC_6H_4$-*p*-OMe, 123-11-5; $CHOC_6H_4$-*p*-SMe, 3446-89-7; $CHOC_6H_4$-*p*-NMe_2, 100-10-7; *i*-$SO_2C_3F_7C_6H_4$-*p*-OMe, 136827-54-8; $COCF_3C_6H_4$-*p*-OMe, 711-38-6; $COCF_3C_6H_4$-*p*-OPh, 70783-32-3; $COCF_3C_6H_4$-*p*-NMe_2, 2396-05-6; NOC_6H_4-*p*-NMe_2, 138-89-6; $NO_2C_6H_4$-*p*-Me, 99-99-0; $NO_2C_6H_4$-*p*-Br, 586-78-7; $NO_2C_6H_4$-*p*-OH, 100-02-7; $NO_2C_6H_4$-*p*-OPh, 620-88-2; $NO_2C_6H_4$-*p*-OMe, 100-17-4; $NO_2C_6H_4$-*p*-SMe, 701-57-5; $NO_2C_6H_4$-*p*-N_2H_3, 100-16-3; $NO_2C_6H_4$-*p*-NH_2, 100-01-6; $NO_2C_6H_4$-*p*-NMe_2, 100-23-2; $NO_2C_6H_4$-*p*-CN, 619-72-7; $NO_2C_6H_4$-*p*-CHO, 555-16-8; $CHC(CN)_2C_6H_4$-*p*-CHO, 2826-26-8; $CHC(CN)_2C_6H_4$-*p*-NMe_2, 2826-28-0; $C_2(CN)_3C_6H_4$-*p*-NH_2, 17082-33-6; $C_2(CN)_3C_6H_4$-*p*-NMe_2, 6673-15-0; (*E*)-HOHEXOC_6H_4-*p*-CH=CHC_6H_4-*p*-$SO_2C_5H_{11}$, 136827-55-9; (*E*)-$MeOC_6H_4$-*p*-CH=CHC_6H_4-*p*-$SO_2C_6F_{13}$, 135448-28-1; (*E*)-$MeOC_6H_4$-*p*-CH=CHC_6H_4-*p*-$COCF_3$, 136827-56-0; (*E*)-HOC_6H_4-*p*-CH=CHC_6H_4-*p*-CN, 136827-57-1; (*E*)-$MeOC_6H_4$-*p*-CH=CHC_6H_4-*p*-CN, 57193-97-2; (*E*)-$Me_2NC_6H_4$-*p*-CH=CHC_6H_4-*p*-CN, 2844-17-9; (*E*)-PhCH=CHC_6H_4-*p*-NO_2, 1694-20-8; (*E*)-MeC_6H_4-*p*-CH=CHC_6H_4-*p*-NO_2, 24325-70-0; (*E*)-BrC_6H_4-*p*-CH=CHC_6H_4-*p*-NO_2, 24325-71-1; (*E*)-HOC_6H_4-*p*-CH=CHC_6H_4-*p*-NO_2, 14064-83-6; (*E*)-PhOC_6H_4-*p*-CH=CHC_6H_4-*p*-NO_2, 136827-58-2; (*E*)-$MeOC_6H_4$-*p*-CH=CHC_6H_4-*p*-NO_2, 4648-33-3; (*E*)-$MeSC_6H_4$-*p*-CH=CHC_6H_4-*p*-NO_2, 20101-50-2; (*E*)-$NH_2C_6H_4$-*p*-CH=CHC_6H_4-*p*-NO_2, 7297-52-1; (*E*)-$Me_2NC_6H_4$-*p*-CH=CHC_6H_4-*p*-NO_2, 2844-15-7; (*E*)-$MeO_2CC_6H_4$-*p*-CH=CHC_6H_4-*p*-NO_2, 136827-59-3; (*E*)-$CHOC_6H_4$-*p*-CH=CHC_6H_4-*p*-NO_2, 84645-79-4; (*E*)-$MeOC_6H_4$-*p*-CH=CHC_6H_4-*p*-Br, 58358-51-3; MeC_6H_4-*o*-NO_2, 88-72-2; BrC_6H_4-*o*-NO_2, 577-19-5; HOC_6H_4-*o*-NO_2, 88-75-5; $MeOC_6H_4$-*o*-NO_2, 91-23-6; $H_2NC_6H_4$-*o*-NO_2, 88-74-4; CNC_6H_4-*o*-NO_2, 612-24-8; $CHOC_6H_4$-*o*-NO_2, 552-89-6; MeC_6H_4-*m*-NO_2, 99-08-1; BrC_6H_4-*m*-NO_2, 585-79-5; HOC_6H_4-*m*-NO_2, 554-84-7; $MeOC_6H_4$-*m*-NO_2, 555-03-3; $H_2NC_6H_4$-*m*-NO_2, 99-09-2;

(28) See for example: (a) Herman, J. P.; Ricard, D.; Ducuing, J. *Appl. Phys. Lett.* **1973**, *23*, 178. Herman, J. P.; Ducuing, J. *Appl. Phys. Lett.* **1973**, *45*, 5100. (b) Mehendale, S. C.; Rustagi, K. C. *Opt. Commun.* **1979**, *28*, 359. (c) MaIntyre, E. F. *J. Chem. Phys.* **1979**, *70*, 2215. (d) Dewer, M. J. S.; Thiel, W. *J. Am. Chem. Soc.* **1977**, *99*, 4899. Dewer, M. J. S.; Yamagughi, Y. *Chem. Phys. Lett.* **1978**, *59*, 541. (e) Zyss, J. *J. Chem. Phys.* **1979**, *70*, 3333–3340. (f) Waite, J.; Papadopoulos, M. G. *J. Chem. Phys.* **1985**, *82*, 1427–1434; *J. Am. Chem. Soc.* **1989**, *93*, 43; *J. Mol. Struct.* **1989**, *202*, 212; *J. Phys. Chem.* **1990**, *94*, 1755. (g) Williams, G. R. J. *J. Mol. Struct.* **1987**, *151*, 215–222. (h) de Melo, C. P.; Silbey, S. *J. Chem. Phys.* **1988**, *88*, 2567. (i) Prasad, P. N., et al. *J. Chem. Phys.* **1988**, *89*, 5535; **1989**, *93*, 7120, 7916. (j) Helfin, J. R.; Wong, K. Y.; Zamani-Khamiri, O.; Garito, A. F. *Phys. Rev. A* **1988**, *38*, 1573. Wu, J. W.; Heflin, J. R.; Norwood, R. A.; Wong, K. Y.; Zamani-Khamiri, O.; Garito, A. F.; Kalyanaraman, P.; Sounik, J. *J. Opt. Soc. Am. B* **1989**, *6*, 707–720. (k) Meredith, G. R.; Stevenson, S. H. *Nonlinear Optical Effects in Organic Polymers*; Messier et al., Eds.; Kluwer-Academic: New York, 1989; pp 105–122. (l) Pierce, B. M. *J. Chem. Phys.* **1989**, *91*, 791. (m) Hurtz, Henry, A.; Stewart, J. J. P.; Dieter, K. M. *J. Comput. Chem.* **1990**, *11*, 82.

CNC_6H_4-*m*-NO_2, 619-24-9; $CHOC_6H_4$-*m*-NO_2, 99-61-6; (*E*)-$MeOC_6H_4$-*o*-$CH{=}CHC_6H_4$-*o*-NO_2, 55801-78-0; (*E*)-$MeOC_6H_4$-*m*-$CH{=}CHC_6H_4$-*o*-NO_2, 136827-60-6; (*E*)-$MeOC_6H_4$-*p*-$CH{=}CHC_6H_4$-*o*-NO_2, 112768-16-8; (*E*)-$MeOC_6H_4$-*o*-$CH{=}CHC_6H_4$-*m*-NO_2, 136827-61-7; (*E*)-$MeOC_6H_4$-*m*-$CH{=}CHC_6H_4$-*m*-NO_2, 14064-59-6; (*E*)-$MeOC_6H_4$-*p*-$CH{=}CHC_6H_4$-*m*-NO_2, 55532-22-4; (*E*)-$MeOC_6H_4$-*o*-$CH{=}CHC_6H_4$-*p*-NO_2, 28915-66-4; (*E*)-$MeOC_6H_4$-*m*-$CH{=}CHC_6H_4$-*p*-NO_2, 14064-58-5; (*E*)-$MeOC_6H_4$-*p*-$CH{=}CHC_6H_4$-*p*-NO_2, 4648-33-3; (*E*)-BrC_6H_4-*o*-$CH{=}CHC_6H_4$-*p*-NO_2, 136827-62-8; (*E*)-BrC_6H_4-*m*-$CH{=}CHC_6H_4$-*p*-NO_2, 7297-54-3; (*E*)-BrC_6H_4-*p*-$CH{=}CHC_6H_4$-*p*-NO_2, 24325-71-1; (*E*)-$PhN{=}CHC_6H_4$-*p*-NO_2, 1614-00-2; (*E*)-MeC_6H_4-*p*-$N{=}CHC_6H_4$-*p*-NO_2, 33442-37-4; (*E*)-$MeOC_6H_4$-*p*-$N{=}CHC_6H_4$-*p*-NO_2, 39963-93-4; (*E*)-$MeOC_6H_4$-*p*-$CH{=}NC_6H_4$-*p*-NO_2, 97221-15-3; (*E*)-NHC_6H_4-*p*-$N{=}NC_6H_4$-*p*-NO_2, 70734-98-4; (*E*)-$N(Et)_2OHC_6H_4$-*p*-$N{=}NC_6H_4$-*p*-NO_2, 136827-63-9; (*Z*)-$MeOC_6H_4$-*p*-$CH{=}C(CN)C_6H_4$-*p*-NO_2, 42172-62-3; (*Z*)-BrC_6H_4-*p*-$CH{=}C(CN)C_6H_4$-*p*-NO_2, 50632-41-2; (*Z*)-BrC_6H_4-*p*-$N{=}C(CN)C_6H_4$-*p*-NO_2, 136827-66-2; PhH, 71-43-2; PhMe, 108-88-3; PhOH, 108-95-2; PhSH, 108-98-5; PhOMe, 100-66-3; PhSMe, 100-68-5; $PhNH_2$, 62-53-3; $PhNMe_2$, 121-69-7; PhF, 462-06-6; PhCl, 108-90-7; PhBr, 108-86-1; PhI, 591-50-4; $PhSO_2Me$, 3112-85-4; $PhSO_2F$, 368-43-4; PhCN, 100-47-0; PhCHO, 100-52-7; $PhCOCF_3$, 434-45-7; PhNO, 586-96-9; $PhNO_2$, 98-95-3; $PhC_2H(CN)_2$, 2700-22-3; (*E*)-PhCH=CHPh, 103-30-0; (*Z*)-PhCH=CHPh, 645-49-8; (*E*)-$PhCH{=}CHNH_2$, 4309-66-4; (*E*)-$PhCH{=}CHNMe_2$, 838-95-9; (*E*)-$PhCH{=}CHNO_2$, 1694-20-8; (*E*)-2-(4-julolidinephenyl)-1-cyanoethenenitrile, 126691-59-6; (*E*)-2-(4-julolidinephenyl)-1,2-dicyanoethenenitrile, 126691-60-9; (*E*)-1-(3-methyl-4-methoxyphenyl)-2-(4-nitrophenyl)ethene, 120191-48-2; (*E*)-1-(3,4-dimethoxyphenyl)-2-(4-nitrophenyl)ethene, 51042-54-7; (*E*)-1-(3-fluoro-4-methoxyphenyl)-2-(4-nitrophenyl)ethene, 136827-64-0; (*E*)-1-(2,4-dim[illegible] (*E*)-1-(2,4-din[illegible] phenyl-1,4-dio[illegible] 85-2; (*E*)-2,3[illegible] 1*H*,5*H*-benzo[i[illegible] phenyl-1*H*,5*H*-[illegible]

Experimental Investigations of Organic Molecular Nonlinear Optical Polarizabilities. 2. A Study of Conjugation Dependences

Lap-Tak Cheng,* Wilson Tam,

Central Research and Development Department, E. I. Du Pont de Nemours & Co. (Inc.), Experimental Station, P.O. Box 80356, Wilmington, Delaware 19880-0356

Seth R. Marder, Albert E. Stiegman,

Jet Propulsion Laboratory, California Institute of Technology, 4800 Oak Grove Drive, Pasadena, California 91109

Geert Rikken,

Philips Research Laboratories, P.O. Box 80000, 5600JA, Eindhoven, The Netherlands

and Charles W. Spangler

Department of Chemistry, Northern Illinois University, Dekalb, Illinois 60115 *(Received: May 13, 1991; In Final Form: August 5, 1991)*

In the present contribution, we broaden our investigations to include the conjugation dependences of molecular optical hyperpolarizabilities. In addition to the benzene and stilbene derivatives reported earlier, dc electric field induced second-harmonic generation (EFISH) and third-harmonic generation (THG) measurement results on the hyperpolarizabilities of a wide range of donor–acceptor-substituted π systems are presented. These include results for styrene, biphenyl, fluorene, diphenylacetylene, various phenylvinyl heterocyclics, oligomeric polyphenyl, α,ω-diphenylpolyyne, α-phenylpolyene, and α,ω-diphenylpolyene, as well as other extended phenylvinyl derivatives. Drawing from the experimental phenomenology illustrated by a large set of internally consistent data, issues concerning the efficacies of various conjugation units, conjugation planarity, aromaticity and bond alternation, and electron localization and delocalization effects, as well as the conjugation length and end-group dependences, are examined.

Introduction

In the preceding paper,[1] structure–property relations for donor–acceptor-substituted organics and their molecular nonlinear optical polarizabilities were examined with dc electric field induced second-harmonic generation (EFISH) and third-harmonic generation (THG) experiments. We detailed a novel experimental methodology which is relatively accurate and experimentally efficient. Using benzene and stilbene derivatives as model compounds, we focused our attention on the electronic biasing strengths, charge-transfer couplings, substitution patterns, and linear property trade-offs of various substituents. Although steady enhancement of hyperpolarizabilities were realized with increasing donor–acceptor strengths and appropriate substitution patterns, the most significant enhancement of both β and γ resulted from the extension of conjugation with the stilbene derivatives. This is a well-known result since the early work of Oudar and others.[2] Further investigations with computations predicted strong enhancements of hyperpolarizabilities through conjugation extension in polyene systems,[3] and such enhancement was subsequently confirmed in α,ω-diphenylpolyene,[4] α-phenylpolyene,[5] and polyene[5] derivatives by experiments.

(1) Cheng, L.-T.; Tam, W.; Stevenson, S. H.; Meredith, G. R.; Rikken, Geert; Marder, S. R. *J. Phys. Chem.*, preceding paper in this issue.

(2) (a) Oudar, J. L. *J. Chem. Phys.* **1977**, *67*, 446–457. At 1.9 μm: (b) Dulcic, A.; Flytzanis, C.; Tang, C. L.; Pepin, D.; Fetizon, M.; Hoppilliard, Y. *J. Chem. Phys.* **1981**, *74*, 1559–1563.

(3) Morley, J. O.; Docherty, V. J.; Pugh, D. *J. Chem. Soc., Perkin Trans. 2* **1987**, 1351–1355.

(4) Huijts, R. A.; Hesselink, G. L. J. *Chem. Phys. Lett.* **1989**, *156*, 209–212.

(5) Barzoukas, M.; Blanchard-Desce, M.; Josse, D.; Lehn, J.-M.; Zyss, J. *Chem. Phys.* **1989**, *133*, 323–329.

TABLE I: Results on 4- and β-Substituted Styrenes (Units in esu)

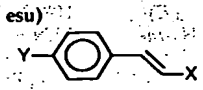

X	Y	solvent	λ_{max}, nm	$\mu \times 10^{-18}$	$\alpha^\circ \times 10^{-23}$	$\beta \times 10^{-30}$	$\gamma \times 10^{-36}$
CN	OMe	$CHCl_3$	(304)	4.2	2.3	7.0	11 ± 5
CN	NMe_2	$CHCl_3$	(364)	6.0	2.8	23	29
CHO	Br	$CHCl_3$	(298)	2.0	2.3	6.5	36
CHO	OMe	$CHCl_3$	(318)	4.2	2.5	11	28
CHO	NMe_2	$CHCl_3$	(384)	5.6	2.6	30	63 ± 5
COMe	OMe	$CHCl_3$	(316)	4.0	2.7	8.9	29
NO_2	H	$CHCl_3$	(312)	3.8	2.0	8.0	29
NO_2	OH	$CHCl_3$	(352)	5.1	2.4	18	52 ± 10
NO_2	OMe	$CHCl_3$	(352)	4.6	2.6	17	35 ± 10
NO_2	NMe_2	$CHCl_3$	(438)	6.5	3.2	50	
NMe_2	NO_2	$CHCl_3$	(438)	5.9	2.6	35	

While the expectation of enhanced hyperpolarizabilities for extended π systems is quite reasonable considering the increased numbers of polarizable and hyperpolarizable electrons and the reduced energy gaps of the charge-transfer (CT) states in such structures, subtleties concerning the structural features of a π system, such as bond alternation and aromaticity, are also expected to play important roles. Such structure–property relationships have thus far received only peripheral attention. In the present study, we broaden our investigations to include the detailed conjugation dependences of hyperpolarizabilities. In addition to the benzene and stilbene derivatives reported earlier, measurement results on the hyperpolarizabilities of a wide range of donor–acceptor-substituted π systems are presented. These include results for styrene, biphenyl, fluorene, diphenylacetylene, various phenylvinyl heterocyclics, oligomeric polyphenyl, α,ω-diphenylpolyyne, α-phenylpolyene, and α,ω-diphenylpolyene, as well as other extended phenylvinyl derivatives. Emphasis is placed on the detailed dependences between molecular quadratic hyperpolarizability and conjugation characteristics. In the remainder of this paper, the nonlinear optical experiments and data analysis scheme will be summarized. Measurement results on various classes of materials will be presented in a manner which facilitates discussions. Systematics in the measurement results as they relate to the planarity, aromaticity, bond alternation, and length of various π systems will be discussed.

Experimental Section

To obtain various relevant molecular parameters, a lengthy set of physical and optical measurements are needed. These include, on a series of solutions with graded concentrations, measurements of density, refractive index at several wavelengths, solution dielectric constant, THG, and EFISH amplitudes as well as their coherence lengths for harmonic generations. These measurements respectively determine the specific volume of a solute molecule in solution, solution dispersion, dielectric properties, and the THG and EFISH nonlinear susceptibilities for each solution. The details of our experimental methodology were given in the preceding paper[1] and are summarized below.

The experimental setup for EFISH and THG consists of a 20-Hz Nd:YAG laser with 10-ns pulses of 0.4 J in energy. The 1.06-μm output pumps a hydrogen Raman shifter, providing up to 120 mW of Stokes-shifted radiation at 1.91 μm. This radiation serves as the fundamental for both the EFISH and THG experiments. The output harmonic wavelengths are at 954 and 636 nm, respectively. For most lightly colored compounds with absorption edge at wavelengths below 500 nm, the measurement can be considered as minimally influenced by dispersive enhancement. THG and EFISH experiments are carried out with an unconventional technique in which the harmonic amplitudes and coherence lengths are measured separately. For the determination of harmonic amplitudes, we adopted a tight-focusing geometry in which the focal region of the laser beam is placed at the window–liquid interface of a "single interface" sample cell. The sample cell is equipped with a thick (2 cm) front optical window and two adjacent liquid chambers (3 cm path length) holding a reference liquid and a sample solution for comparative measurement. Electrodes are fabricated at the front window–liquid interface so that both THG and EFISH measurements can be carried out concurrently. The coherence lengths for the harmonic generations are determined with a wedged liquid cell consisting of two crystalline quartz windows, which generate sufficient second- and third-harmonic radiations for easy measurement.

With the known THG and EFISH nonlinearities and coherence lengths of the window material and the reference liquid at 1.91 μm (BK7-grade A glass: $\chi^{(3)}_{THG} = 4.7 \times 10^{-14}$ esu, $l_{THG} = 16.7$ μm, $\chi^{(3)}_{EFISH} = 3.5 \times 10^{-14}$ esu, and $l_{EFISH} = 38.8$ μm; toluene: $\chi^{(3)}_{THG} = 9.9 \times 10^{-14}$ esu, $l_{THG} = 18.3$ μm, $\chi^{(3)}_{EFISH} = 9.1 \times 10^{-14}$ esu, and $l_{EFISH} = 73.5$ μm), as well as the coherence lengths of the sample solution, the solution nonlinear susceptibilities can be computed from the ratios of the harmonic intensities measured at the sample and reference liquid chambers. From the measured solution properties, following a full Onsager local field treatment for both static and optical fields and taking the infinite dilution limits for all concentration-dependent quantities, the relevant molecular properties including the dipole moment, μ; the static linear polarizability, α°; the vectorial projection of the quadratic hyperpolarizability tensor along μ, β; and the scalar part of the cubic hyperpolarizability, γ, are calculated.

Results and Discussion

1. Styrene Derivatives: The Efficacy of Vinyl Extension. We first extend our investigations to the styrene derivatives. The relevant molecular parameters (μ, α°, β, and γ) have been determined for 10 4-donor, β-acceptor substituted and one 4-acceptor, β-donor substituted styrene derivatives at infinite dilution in chloroform solutions. Combinations of donors and acceptors with varying strengths are used to obtain a wide range of β values. Results are tabulated in Table I (see ref 1 for details concerning experimental conditions and uncertainties).

The extent of charge transfer and thus the β values are expected to be sensitive to the molecular geometry of the styrene derivatives. While the geometry is not known for the asymmetrically substituted charge-transfer (CT) derivatives, all available experimental and theoretical evidence indicates that the parent unsubstituted styrene has a planar geometry.[6] Since the CT interaction is favored by a planar geometry, CT derivatives are expected to have planar structures. In addition, since all carbon atoms in styrene are sp^2 hybridized, there is little variation in the π-electron distribution among the ring and vinyl carbons, giving an essentially zero dipole moment (<0.3 D[7]). Any polarization of the structure can be largely attributed to interactions between styrene and substituents. Therefore, results obtained for CT styrene derivatives can be reasonably compared to those for the benzene and stilbene derivatives studied earlier.[1]

(6) (a) Britton, P. L.; Cheng, C. L.; LeFevre, R. J. W.; Radom, L.; Ritchie, G. L. *J. Chem. Soc. B* 1971, 2100. (b) Suzuki, H. *Electronic Absorption Spectra and Geometry of Organic Molecules*, Academic Press: New York, 1967; Chapter 13. (c) Barfield, M.; MacDonald, C. J.; Peat, I. R.; Reynolds, W. F. *J. Am. Chem. Soc.* 1971, *93*, 4195. (d) Hehre, W. J.; Radom, L.; Pople, J. A. *J. Am. Chem. Soc.* 1972, *94*, 1496.

(7) McClellan, A. L. *Tables of Experimental Dipole Moments*; Rahara Enterprises: 1974; Vol II.

TABLE II: Results on 4-4'-Disubstituted Biphenyls and Fluorenes (Units in esu)

X	Y	solvent	λ_{max}, nm	$\mu \times 10^{-18}$	$\alpha^\circ \times 10^{-23}$	$\beta \times 10^{-30}$	$\gamma \times 10^{-36}$
			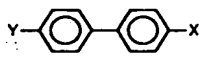				
H	H	*p*-dioxane	252	0.0	2.2	0.0	10
CN	H	*p*-dioxane	272	4.0	2.4	1.9	17
$COCH_3$	H	*p*-dioxane	280	3.1	2.7	2.0	8
NO_2	H	*p*-dioxane	304	3.8	2.5	4.1	15
$SO_2C_6H_{12}OH$	NMe_2	$CHCl_3$	340	6.0	4.6	13	38
CN	OH	*p*-dioxane	292	4.8	2.5	6.3	10
$COCH_3$	OMe	*p*-dioxane	304	3.4	2.9	4.9	23
NO_2	Br	*p*-dioxane	306	2.7	2.9	4.4	32
NO_2	OH	*p*-dioxane	334	4.9	2.6	7.7	37
NO_2	OMe	*p*-dioxane	332	4.5	2.8	9.2	39
NO_2	NH_2	$CHCl_3$	372	5.0	2.8	24	70
		NMP		7.8	2.6	24	96
NO_2	NMe_2	$CHCl_3$	390	5.5	3.4	50	130
							
H	H	*p*-dioxane	262	0.0		0.0	
CN	H	*p*-dioxane	284	3.9	2.6	3.0	8
NO_2	H	*p*-dioxane	328	4.1	2.6	5.1	29
NO_2	Br	*p*-dioxane	330	2.8	2.6	6.0	30
NO_2	OMe	*p*-dioxane	356	4.7	2.7	11	28
NO_2	NMe_2	*p*-dioxane	410	5.6	3.6	40	95
		$CHCl_3$	417	6.0	3.6	55	

Since styrene has a conjugation length intermediate to those of benzene and stilbene, the β values of its derivatives are expected to fall between those of benzene and stilbene derivatives. Comparison of entries in Table I and those of Tables II and III of ref 1 confirms this expectation for all donor–acceptor pairs. For the case of NMe_2 and NO_2 substituents, the β values are 12×10^{-30}, 50×10^{-30}, and 73×10^{-30} esu for benzene, styrene, and stilbene derivatives, respectively. Clearly, β increases nonlinearly with conjugation length. The vinyl addition going from the benzene to the styrene structures appears to have a much greater enhancement on β than the phenyl addition going from the styrene to the stilbene structures. This observation has been noted before.[2a,8] Comparison with properties of the planar fluorene derivatives (see Table II) discussed below also leads to such a conclusion. We will return to the detailed conjugative length dependence of hyperpolarizability in a later section where derivatives with extended conjugations are examined. However, the efficacy of the vinyl unit over that of the phenyl unit is noteworthy since it offers greater efficiency per unit molecular volume. It is also interesting to note that the superior accepting strengths of the dicyanovinyl and tricyanovinyl groups[9] arise largely from the vinyl extension of conjugation length. This can be seen by comparing the β values of 5.0×10^{-30}, 23×10^{-30}, 32×10^{-30}, and 50×10^{-30} esu for 1-(*N*,*N*-dimethylamino)-4-X-benzene where X = CN, CHCHCN, $CHC(CN)_2$, and $CCNC(CN)_2$, respectively. Accounting for dispersive enhancement according to a two-state approximation,[10] $\beta(\omega=0)$ are 4.4×10^{-30}, 19×10^{-30}, 24×10^{-30} and 33×10^{-30} esu. Clearly the vinyl extension results in more than a factor of 4 enhancement while each additional cyano group leads to about a 30% increase only.

When the donor and acceptor positions are interchanged as illustrated with derivatives of NMe_2 and NO_2, significant differences are found in their properties. While the CT band position and bandwidth are very similar, the oscillator strength of 4-(*N*,*N*-dimethylamino)phenyl-β-nitrostyrene is found to be 1.6 times higher than that of 4-nitrophenyl-β-(*N*,*N*-dimethylamino)styrene. This is consistent, within the two-state approximation, with the lower β value found for the later derivative, which also has a lower dipole moment. Since the styrene parent compound possesses a small dipole moment with excess charge on the vinyl fragment, the dipole moment and β value of the former derivatives, where the substituent-induced electronic asymmetry is in the same direction as that of the conjugation, are expected to be higher than those found for the later. Therefore, it is generally advantageous to have the acceptor substituted at the vinyl position when $\mu\beta$ is to be optimized.

2. Biphenyl, Fluorene, and Oligophenylene Derivatives: Conjugation Planarity. An interesting structure–property relationship concerns the dependence of the hyperpolarizability on conjugation planarity. Clearly, such a dependence is expected because of the diminution of π-electron overlap in a nonplanar geometry, which will certainly hamper donor–acceptor interactions and reduce quadratic nonlinearities. An estimate of the torsional effect on optical nonlinearity can be obtained from spectroscopic evidences. It is well-known that a nonzero torsional angle, θ, between two π systems will lead to an increase of the transition energy and a reduction of the extinction coefficient of the π–π^* transition.[11] For small θ, the former effect is relatively minor, while the extinction coefficient $\epsilon(\theta)$ is found to decrease as $\cos^2(\theta)$.[12] Within the two-state approximation, in which the long axis hyperpolarizability β_{xxx} is proportional to ϵ, the torsional effect on β is expected to be weak since $\cos^2(\theta)$ is a slowly varying function for small θ. Theoretical studies of the torsional effect between donor orbital and the π system in CT phenyl derivatives have led to similar conclusions.[13] In addition, for donor- and acceptor-substituted derivatives, one may expect the torsion itself to be dependent on the charge-transfer strength of the substituents. To further explore these topics, we have investigated the linear and nonlinear optical properties of 4-donor,4'-acceptor-substituted biphenyls with nonzero torsions and the corresponding fluorene derivatives with planar structures. Measurement results are given in Table II.[14]

The torsional angle in biphenyl is well-known and the gas-phase and solution-phase values are at about $\theta_m = 40°$ and 30°, respectively.[15,16] These values are determined by potential barriers

(8) Zyss, J. *J. Chem. Phys.* **1979**, *71*, 909–916.
(9) (a) Katz, H. E.; Singer, K. D.; Sohn, J. E.; Dirk, C. W.; King, L. A.; Gordon, H. M. *J. Am. Chem. Soc.* **1987**, *109*, 6561–6563. (b) Katz, H. E.; Dirk, C. W.; Singer, K. D.; Sohn, J. E. *SPIE Proc.* **1987**, *824*, 86–92.
(10) (a) Oudar, J. L.; Chemla, D. S. *J. Chem. Phys.* **1977**, *66*, 2664–2668. (d) Singer, K. D.; Sohn, J. E.; King, L. A.; Gordon, H. M.; Katz, H. E.; Dirk, C. W. *J. Opt. Soc. Am. B* **1989**, *6*, 1339–1350.
(11) Jaffé, H. H.; Orchin, M. *J. Am. Chem. Soc.* **1960**, *82*, 1078.
(12) Braude, E. A.; Sondheimer, F. *J. Chem. Soc.* **1955**, 3754.
(13) Leung, P. C.; Stevens, J.; Harelstad, R. E.; Spiering, M. S.; Gerbi, D. J.; Francis, C. V.; Trend, J. E.; Tiers, G. V. D.; Boyd, G. T.; Ender, D. A.; Williams, R. C. *SPIE Proc.* **1989**, 1147.
(14) Previous measurements of several cyano derivatives performed at 1.06 μm were reported in Combellas, C.; Gautier, H.; Simon, J.; Thiebault, A.; Tournilhac, F.; Barzoukas, M.; Josse, D.; Ledoux, I.; Amatore, C.; Verpeaux, J.-N. *J. Chem. Soc., Chem. Commun.* **1988**, 203.

TABLE III: End-Group-Dependent Torsional Angle As Deduced from Spectroscopic and Hyperpolarizability Data

D, A	R_λ	θ_λ, deg	R_β	θ_β, deg
H, NO_2	0.78	28	0.80	27
Br, NO_2	0.79	27	0.73	31
OMe, NO_2	0.85	23	0.83	24
NMe_2, NO_2	0.89	19	0.91	18

arising from the steric hindrance of the ortho hydrogens near $\theta = 0°$ and the loss of resonance energy near $\theta = 90°$. From perturbative arguments, the decrease of resonance energy is well approximated by $\cos^2(\theta)$.[17] For CT derivatives, it is reasonable to expect lower θ values since CT interaction should introduce additional resonance energy and certain double bond character to the biphenyl linkage according familiar arguments based on resonance structures. For fluorene, the two phenyl fragments are near planar due to the *o,o'*-methylene bridge. Assuming minimum perturbation of the π system as a result of the strained five-member ring (which is a reasonable assumption considering the similarity of their spectra), CT fluorene derivatives can be taken as planar analogues to biphenyl derivatives in our study of the torsional effects on hyperpolarizability.

Measurement results on biphenyl and fluorene derivatives are characterized by their similarities and can be summarized as follow. The low-energy feature in the absorption spectrum of unsubstituted fluorene is found to be 10 nm red-shifted from that of biphenyl. For both donor–acceptor-substituted biphenyl and fluorene derivatives, this low-energy band acquires CT character and its λ_{max} shifts to higher value (up to 155 nm) with increasing electronic biasing strength of the substituents. For a given donor–nitro pair, fluorene derivatives consistently show similar μ, higher λ_{max}, and higher β values in comparison with biphenyls. Denoted as $\Delta\lambda_{CT}^F = \lambda_{max}$(CT fluorene derivatives) $- \lambda_{max}$(fluorene) and $\Delta\lambda_{CT}^B = \lambda_{max}$(CT biphenyl derivatives) $- \lambda_{max}$(biphenyl), these spectral shifts are good indicators of the charge-transfer nature of the excitations and the ratio $R_\lambda = \Delta\lambda_{CT}^B/\Delta\lambda_{CT}^F$ reflects the influence of torsion on CT. Although the β values of the fluorene derivatives are higher than those of the biphenyl analogues, the differences are small and the ratio $R_\beta = \beta^B/\beta^F$ approaches unity with increasing donor–acceptor strength.

Qualitatively, if one assumes that the observed differences in spectroscopic and nonlinear optical data between fluorene and biphenyl derivatives are due to torsional hindrance of the CT interaction, the torsion angle of biphenyl derivatives can be crudely estimated according to the expected $\cos^2(\theta)$ dependences of resonance stabilization and hyperpolarizability discussed earlier. Using $\theta_\lambda = \arccos(R_\lambda)^{1/2}$ and $\theta_\beta = \arccos(R_\beta)^{1/2}$, the deduced θ values from spectroscopic and nonlinear optical measurements are in good agreement (see Table III). While the θ values fall within the expected range of 20°–30°, the torsional angle shows a decreasing trend with increasing donor–acceptor strength. X-ray data[23] on single crystal of *p*-amino-*p*-nitrobiphenyl revealed a near-planar geometry with a torsion about the phenyl–phenyl bond of about 3°. This geometry is probably quite different from the solution geometry since crystal-packing effects are known to strongly influence torsion (biphenyl has a planar geometry in its crystalline state). However, X-ray data also show that the phenyl–phenyl distance in *p*-amino-*p*-nitrobiphenyl gives no evidence of quinonoid character, suggesting that CT is limited in the ground state and the polarization is confined to region immediately connected to the donor and acceptor. This may help explain the similar dipole moments of fluorene and biphenyl derivatives and their relatively low values when compared to phenyl derivatives.

Although the torsional dependence of hyperpolarizability appears to be weak for small torsional angle, this effect is expected to be cumulative and become quite important for conjugated structures with two or more torsional angles. The arguments used in the biphenyl case can be extended to that of the ter- and quaterphenyl derivatives by associating a $\cos^2(\theta)$ factor with each torsional angle, such that $\beta(\theta_1,\theta_2,\theta_3) \propto \cos^2(\theta_1)\cos^2(\theta_2)\cos^2(\theta_3)$. For small θ's, the torsional effect leads to an asymptotic reduction of β. A competing effect is the general enhancement of β due to the extension of conjugation. To further explore the balance of these two effects in oligomeric polyphenyl derivatives, we compare the experimental results on 4'-amino- and 4'-methoxy-4-nitropolyphenyl derivatives up to four phenyl units with the computational results on the β values of polyphenyls with planar geometries published by Morley et al.[3] Measurement results are given in Table IV.

For the 4'-(*N*,*N*-dimethylamino)-4-nitropolyphenyls, Morley's calculation revealed an unexpected rapid saturation of the hyperpolarizability with the conjugation length even for planar geometries, predicting an increasing β up to a saturating value at six phenyl units, and a volume-normalized hyperpolarizability, ρ_β, peaking at the terphenyl derivatives. Contrary to this prediction, measurement results in Table IV show a maximum β for the biphenyl derivative for the amino series and a virtual equality between bi- and terphenyl derivatives for the methoxy series. Clearly, ρ_β maximizes at the biphenyl derivatives for both series. The experimental trend in β is also found to correlate with trends in λ_{max}, which shifts to higher values with increasing β. Since the donor group of the phenylene series studied by Morley differs from those we have measured, a direct comparison of the β values cannot be made. However, the ratio of β_n/β_{n+1}, where n is the number of phenyl units, can be compared to reveal the effects of nonplanar geometries.

The theoretical $\beta_n(\omega=0)$ for n = 1–4 phenyl units are 12.3×10^{-30}, 31.4×10^{-30}, 42.2×10^{-30}, and 47.7×10^{-30} esu, with ratios of β_n/β_{n+1} = 0.39, 0.74, and 0.89 for n = 1, 2, and 3, respectively. For the 4'-amino series, the experimental $\beta_n(\omega=0)$ values, deduced from 1.91-μm measurements according to the two-state model, are 8×10^{-30}, 19×10^{-30}, 13×10^{-30}, and 9×10^{-30} esu with β_n/β_{n+1} = 0.4, 1.5, and 1.4, where n = 1, 2, and 3, respectively. To see if this difference between experimental and theoretical results can be accounted for by the torsional effect, the theoretical β_n values are corrected according to the $[\cos^2(\theta)]^n$ dependence discussed previously. Using a θ value of 30°, such an exercise yields corrected β_n/β_{n+1} ratios of 0.52, 1.0, and 1.2 for n = 1, 2, and 3, respectively. This is in reasonable agreement with the experimental results, and the down turn of β values at n = 3 can readily be accounted for with reasonable θ values and the $[\cos^2(\theta)]^n$ dependence.

Our findings on the oligophenylene derivatives can be summarized as follow: (1) Donor–acceptor biphenyls have lower β values relative their fluorene analogous due to torsion along the phenyl–phenyl bond. (2) The differences in β are, however, small presumably due to a weak dependence on torsion for small angles. (3) As the donor and acceptor strength increases, the β values for the biphenyl and the fluorene derivatives converge. (4) This appears to be a result of an end group effect on the torsional angle resulting in more planar biphenyl derivatives with strong donor–acceptor substituents. (5) The β values maximize at biphenyl for the oligophenylene series. (6) The rapid saturation and decrease of β with length can be explained by the combined effect of the intrinsic ineffectiveness of the phenyl extension which leads to rapid saturation of β and the geometric constrains on π overlap due to the torsional angles between phenyl units.

3. Diphenylacetylene and Oligomeric α,ω-Diphenylpolyyne Derivatives: Extreme Bond Alternation. In order to study the effect of orbital hybridization and bond alternation on hyperpolarizability, we have examined a series of α,ω-diphenylpolyyne CT derivatives containing-up-to-three-triple-bonds. Theoretical investigations of the longitudinal polarizabilities, α_{zz}, and the second hyperpolarizabilities, γ_{zzzz} of $(-\equiv-)_n$ and $(-\equiv-)_n$ have been reported. For n = 1–3, an ab initio study[18] found lower α_{zz} while

(15) Bastiansen, O.; Samdal, S. *J. Mol. Struct.* **1985**, *128*, 115–125.
(16) (a) Eaton, V. J.; Steele, D. *J. Chem. Soc., Perkin Trans. 2* **1973**, 1601–1608. (b) Suzuki, H. *Bull. Chem. Soc. Jpn.* **1959**, *32*, 1350.
(17) (a) Dewar, M. J. S. *J. Am. Chem. Soc.* **1952**, *74*, 3345. (b) Klevens, H. B.; Platt, J. R. *J. Am. Chem. Soc.* **1949**, *71*, 1714.
(18) Bodart, V. P.; Delhalle, J.; Andre, J. M.; Zyss, J. *Can. J. Chem.* **1985**, *63*, 1631–1634.

TABLE IV: Results on 4-4′-Nitropolyphenyl Oligomers (Units in esu)

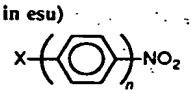

n	X	solvent	λ_{max}, nm	$\mu \times 10^{-18}$	$\alpha^\circ \times 10^{-23}$	$\beta \times 10^{-30}$	$\gamma \times 10^{-36}$
1	NH_2	NMP	370 (384)	7.8	1.6	10	21
2	NH_2	NMP	372 (386)	7.8	2.6	24	96
3	NH_2	NMP	360 (388)	7.6	3.5	16	124
4	NH_2	NMP	344 (354)	10	3.3	11	133
1	OMe	*p*-dioxane	302	4.6	1.5	5.1	10
2	OMe	*p*-dioxane	332	4.5	2.8	9.2	39
3	OMe	*p*-dioxane	340	5.0	3.8	11	

TABLE V: Results on 4-4′-Disubstituted Diphenylacetylenes (Units in esu)

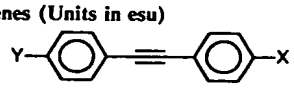

X	Y	solvent	λ_{max}, nm	$\mu \times 10^{-18}$	$\alpha^\circ \times 10^{-23}$	$\beta \times 10^{-30}$	$\gamma \times 10^{-36}$
SO_2Me	NH_2	$CHCl_3$	(338)	6.5	3.4	13	59
CO_2Me	SMe	$CHCl_3$	(328)	2.9	3.5	8	14
CO_2Me	NH_2	$CHCl_3$	(332)	3.8	3.7	15	62
COMe	SMe	$CHCl_3$	(336)	3.7	3.6	9.8 ± 2	19 ± 10
COMe	NH_2	$CHCl_3$	(334)	3.3	3.2	12	29
COPh	NH_2	$CHCl_3$	(352)	3.7	3.7	19	57
CN	SMe	$CHCl_3$	(333)	4.0	3.5	15	35
CN	NH_2	$CHCl_3$	(342)	5.2	3.2	20	55
CN	NHMe	$CHCl_3$	(358)	5.7	3.4	27	90
CN	NMe_2	$CHCl_3$	(372)	6.1	3.7	29	99
NO_2	Br	$CHCl_3$	(335)	3.0	3.5	10	50
NO_2	OMe	*p*-dioxane	(356)	4.4	3.9	14	52
NO_2	SMe	$CHCl_3$	(362)	4.0	3.8	20	95
NO_2	NH_2	$CHCl_3$	(380)	5.5	3.2	24	120
NO_2	NH_2	NMP	(410)	5.5	3.6	40	140
NO_2	NHMe	$CHCl_3$	(400)	5.7	4.0	46	130
NO_2	NMe_2	$CHCl_3$	(415)	6.1	4.1	46	151

TABLE VI: Results on 4-4′-Disubstituted α,ω-Diphenylpolyyne Oligomers (Units in esu)

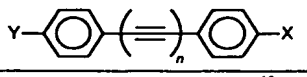

n	X	Y	solvent	λ_{max}, nm	$\mu \times 10^{-18}$	$\alpha^\circ \times 10^{-23}$	$\beta \times 10^{-30}$	$\gamma \times 10^{-36}$
1	CN	SMe	$CHCl_3$	(333)	4.0	3.5	15	35
2	CN	SMe	$CHCl_3$	(330 ± 40)	3.7	3.8	17 ± 2	42 ± 10
1	CN	NH_2	$CHCl_3$	(342)	5.2	3.2	20	55
2	CN	NH_2	NMP	(388)	$\alpha = 3.4$, $\mu\beta = 11 \times 10^{-47}$ esu			
1	NO_2	SMe	$CHCl_3$	(362)	4.0	3.8	20	95
2	NO_2	SMe	$CHCl_3$	(338 ± 40)	3.9	4.0	17 ± 2	61 ± 10
1	NO_2	NH_2	NMP	(410)	$\alpha = 3.6$, $\mu\beta = 22 \times 10^{-47}$ esu			140
2	NO_2	NH_2	$CHCl_3$	(334 ± 50)	6.3	4.4	28 ± 2	81 ± 10
			NMP	(416)	$\alpha = 4.0$, $\mu\beta = 24 \times 10^{-47}$ esu			
3	NO_2	NH_2	NMP	(440 shoulder)	$\alpha = 4.0$, $\mu\beta = 41 \times 10^{-47}$ esu			

a tight-binding calculation[19] using Hückel wave functions reported higher γ_{zzzz} for the acetylenic structures. Both studies found rapid increases in their respective properties with *n*. However, the experimental γ^{THG} for α,ω-diphenylpolyyne with one and two triple bonds were found to be significantly lower than that of α,ω-diphenylpolyene analogues.[20] Therefore, from a perturbative picture in which β arises from the polarization of γ by an internal field created by donor–acceptor substituents,[21] the acetylenic linkages are anticipated to be less effective than the ethylenic ones for asymmetric polarizability. This conjecture is borne out by experiments. Measurement results on 17 4-donor,4′-acceptor-disubstituted diphenylacetylenes are given in Table V.

Despite the extended and planar structure of diphenylacetylene in comparison to that of biphenyl, only moderate increases of β values are observed. The disparity between diphenylacetylene and *trans*-stilbene derivatives (see Table III of ref 1) is even more striking considering the similarity of the two structures. For all combinations of donor and acceptor groups examined, the diphenylacetylenic derivatives are found to be much less nonlinear, with β values about 50% lower than that of the *trans*-stilbene analogues. Since β is a measure of the asymmetric long axis polarizability between the two ends of these elongated molecules, it is unlikely that the difference in axial symmetry is responsible for the lower values. The difference in orbital hybridizations between the acetylenic and ethylenic linkages is, however, more significant. Although the π orbitals of both linkages are coplanar with the phenyl rings, the p orbitals of the sp-hybridized acetylenic carbons, which are electron rich due to the low energy of the σ orbitals, may lead to less effective π delocalization due to the orbital energy mismatch with the p orbitals of the sp^2-hybridized phenyl carbons. In addition, due to the short triple bond length, p-orbital overlap is maximized in the acetylenic resonance structure. These factors are likely to result in a localization of electron density at the phenyl rings. Such a difference of course does not exist in the *trans*-stilbene structure where all carbons are sp^2 hybridized, allowing effective delocalization of all the π electrons.

The consequences of extreme bond alternation are further illustrated with additional acetylenic units in the π system.

(19) Beratan, D. N.; Onuchic, J. N.; Perry, J. W. *J. Phys. Chem.* **1987**, *91*, 2696–2698.
(20) Perry, J. W.; Stiegman, A. E.; Marder, S. R.; Coulter, D. R. *Organic Materials for Non-linear Optics*; Proceedings of conference sponsored by Royal Society of Chemical Society; Applied Solid State Chemistry Division; Burlington House, London, 1989; pp 189–195.
(21) Oudar, J. L.; Chemla, D. S. *J. Chem. Phys.* **1977**, *66*, 2664–2668.

TABLE VII: Results on 4-Donor,β-Acceptor-Substituted α-Phenylpolyene Oligomers (Units in esu)

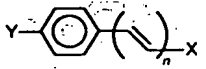

n	X	Y	solvent	λ_{max}, nm	$\mu \times 10^{-18}$	$\alpha^\circ \times 10^{-23}$	$\beta \times 10^{-30}$	$\gamma \times 10^{-36}$
0	CHO	MeO	neat	280	3.5	1.7	2.2	8
1	CHO	MeO	$CHCl_3$	(318)	4.0	2.5	12	28
2	CHO	MeO	$CHCl_3$	(350)	4.3	3.0	28	43
3	CHO	MeO	$CHCl_3$	(376)	4.6	3.5	42	120
0	CHO	NMe_2	*p*-dioxane	326	5.1	2.0	6.3	17
1	CHO	NMe_2	$CHCl_3$	(384)	5.6	2.6	30	63
2	CHO	NMe_2	$CHCl_3$	(412)	6.0	3.3	52	140
3	CHO	NMe_2	$CHCl_3$	(434)	6.3	4.0	88	257
0	$CHC(CN)_2$	MeO	$CHCl_3$	(350)	5.5	1.7	9.8	25
1	$CHC(CN)_2$	MeO	$CHCl_3$	(392)	5.8	2.5	32	83
0	$CHC(CN)_2$	NMe_2	$CHCl_3$	(420)	7.8	2.8	32	72
1	$CHC(CN)_2$	NMe_2	$CHCl_3$	(486)	8.4	3.2	82	
2	$CHC(CN)_2$	NMe_2	$CHCl_3$	(520)	9.0	3.6	163	

Measurement results of several α,ω-diphenyldiyne and one α,ω-diphenyltriyne derivatives are given in Table VI. The absorption spectra of the 4′-amino,4-nitro series have been reported before.[22] Strong intramolecular CT bands are observed together with low energy $\pi-\pi^*$ transitions which show considerable vibronic structures for the extended derivatives. To the extent that λ_{max} for the CT band can be determined, no clear red shift of λ_{max} and increase of ϵ are found when the acetylenic bridge is extended from one to three triple bonds. Furthermore, structural analysis[23] of the series have shown that quinoidal character is present only in the phenyl fragments and the acetylenic linkages remain largely unchanged in the ground state. A high degree of invariance of the quinoidal distortions across the series was also noted.

On the basis of the spectral and structural behaviors, it can be concluded that the π system is poorly delocalized in the ground state and the extent of charge transfer in the ground and excited states is relatively independent of the length of the acetylenic linkage. The acetylene linkage acts as a rather passive conduit to transfer charge into what are ultimately highly localized orbitals at the nitrophenyl and aniline fragments. Considerations based on resonance structures can be invoked to rationalize these observations. Delocalization of charge along the π system must be considered as effective mixing of not only the neutral acetylenic and the fully charge separated cumulenic resonance structures, but also the mixing of intermediate structures in which charges are localized at other positions along the carbon backbone. Due to the large difference in the single and triple bond lengths, all structures containing allene fragments are high in energy because of reduced p overlap, and their mixings are therefore energetically disfavored in the ground state. Therefore, charge is not effectively delocalized into the acetylenic linkage. Such conclusions are supported by the current molecular studies. The μβ values for all combinations of donor and acceptor groups are found to be essentially the same for the mono- and diyne derivatives, while moderate enhancement is realized for the triyne derivatives. Thus charge localization as a result of extreme bond alternation is seen to strongly constrain the hyperpolarizability. In particular, the strong length dependence is severely curtailed. This behavior is quite different from that of the α,ω-diphenylpolyene series.

4. Oligomeric α-Phenylpolyene and α,ω-Diphenylpolyene Derivatives: Conjugation Extension. While it is generally perceived that extension of the π system between donor and acceptor groups is an effective route to enhance hyperpolarizability, experimental confirmations[2b,4,5] have been reported only for polyene derivatives most of which contain phenyl end groups. Data presented above on oligomeric polyphenyl and α,ω-diphenylpolyyne derivatives clearly show that conjugation extension does not in general lead to higher hyperpolarizability. In this section, the structural details which influence the efficacy of a conjugated system will be explored from a chemical view point. Measurement results for α-phenylpolyene and α,ω-diphenylpolyene derivatives are presented. The power law dependence of β on conjugation length and the end-group effects on the exponent are discussed.

Morley's computation results predicted dramatically different length dependences for the planar polyphenyl and the polyenic derivatives.[3] The former is found to saturate rapidly at very modest value while the latter series of comparable length affords values up to 50 times higher without saturation. Polarization of the phenyl unit, whose aromatic character advocates an equal distribution of the π electrons among the carbon π orbitals, into a quinoidal form is energetically costly, and this energetic consideration may account for its relative ineffectiveness. In particular, for extended phenylenic or phenylvinyl conjugations, the charge separation resulting from donor–acceptor interactions may tend to localize at the end groups to allow the unpolarized central region to preserve aromatic stabilization. Therefore, the aromatic centroid represents a potential barrier of lower orbital energy and leads to poor delocalization of the π systems. In the α,ω-diphenyltriyne derivatives considered earlier, the extreme bond alternation of the acetylenic linkage, whose cumulenic charge-separated forms are energetically disfavored, clearly leads to charge localization at the phenyl end units. For polyene derivatives, since the neutral and other charge-separated states formally consist of similar π system of alternating single and double bonds and are equally favored based on energy considerations, effective delocalization is realized for derivatives with length up to the saturation limit, which is in turn determined by bond alternation. Due to their reduced aromaticity and polyene-like structures, similar arguments suggest auspicious predictions for the hyperpolarizabilities of oligomeric polyquinoid, polythiophene, and other heteropentacyclic derivatives.

The conjugation length dependence of β is investigated with oligomeric α-phenylpolyene and α,ω-diphenylpolyene derivatives with a range of donor and acceptor groups. Measurement results are given in Table VII and VIII. Together with results obtained for benzene, styrene, fluorene, and stilbene derivatives, the length dependence of planar structures consisting of ethylenic units with phenyl end caps from $n = 2$ up to 8 double bonds can be studied (if each phenyl unit is considered as contributing two double bonds). Structures capped at both ends by phenyl groups behave quite differently from those capped at just the donor end. Results for the two series are therefore presented and analyzed separately. Benzene derivatives are used as the short conjugation length limit for both series to insure consistency in our observations. Logarithmic plots of β vs n for the two series are given in Figure 1. Power law dependences with conjugation lengths are also found for the λ_{max} of CT bands and they are plotted in Figure 2. Except for the benzene derivatives, all results are obtained in chloroform solutions. The solvent dependence of the benzene results is not expected to be very large (≈10%) and should not lead to significantly different exponents. Least-squares fits give reasonably good linear fits for all data sets. Systematic deviations in both

(22) Stiegman, A. E.; Miskowski, V. M.; Perry, J. W.; Coulter, D. R. *J. Am. Chem. Soc.* **1987**, *109*, 5884–5886.

(23) Graham, E. M.; Miskowski, V. M.; Perry, J. W.; Coulter, D. R.; Stiegman, A. E.; Schaefer, W. P.; Marsh, R. E. *J. Am. Chem. Soc.* **1989**, *111*, 8771–8779.

TABLE VIII: Results on Disubstituted α,ω-Diphenylpolyene Oligomers (Units in esu)

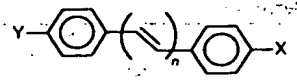

n	X	Y	solvent	λ_{max}, nm	$\mu \times 10^{-18}$	$\alpha^{\circ} \times 10^{-23}$	$\beta \times 10^{-30}$	$\gamma \times 10^{-36}$
1	CN	OMe	$CHCl_3$	(340)	3.8	3.4	19	54
2	CN	OMe	$CHCl_3$	(360)	4.5	3.8	27	122
3	CN	OMe	$CHCl_3$	(380)	4.4	4.4	40	234
1	NO_2	Br	$CHCl_3$	(356)	3.4	3.2	18	45
2	NO_2	Br	$CHCl_3$	(378)	3.5	3.9	21	146
3	NO_2	Br	$CHCl_3$	(400)	3.8	4.4	35	224
1	NO_2	MeO	$CHCl_3$	(376)	4.5	3.4	34	93
2	NO_2	MeO	$CHCl_3$	(397)	4.8	4.0	47	130
3	NO_2	MeO	$CHCl_3$	(414)	5.1	4.2	76	230
4	NO_2	MeO	$CHCl_3$	(430)	5.8	4.8	101	
1	NO_2	MeS	$CHCl_3$	(380)	4.3		34	
2	NO_2	MeS	$CHCl_3$	(398)	4.5	4.2	55	206
1	NO_2	NMe_2	$CHCl_3$	(430)	6.6	3.4	73	225
2	NO_2	NMe_2	$CHCl_3$	(442)	7.6	4.0	107	
3	NO_2	NMe_2	$CHCl_3$	(458)	8.2	4.2	131	
4	NO_2	NMe_2	$CHCl_3$	(464)	9 ± 1		190 ± 50	

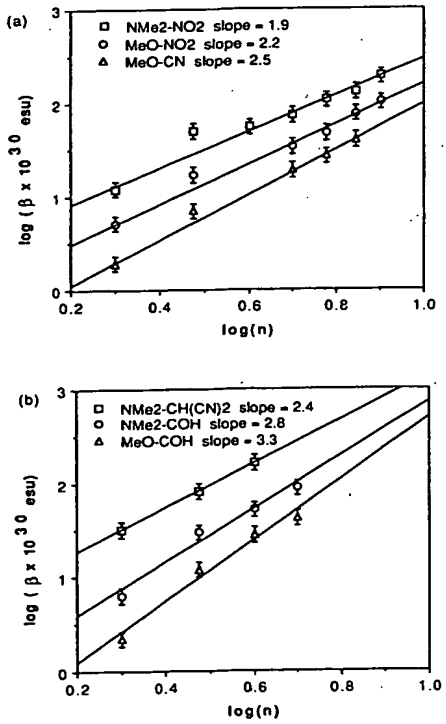

Figure 1. Conjugation length dependences, where $n = 2$, for each phenyl unit, for (a) α,ω-diphenylpolyene and (b) α-phenylpolyene CT oligomers.

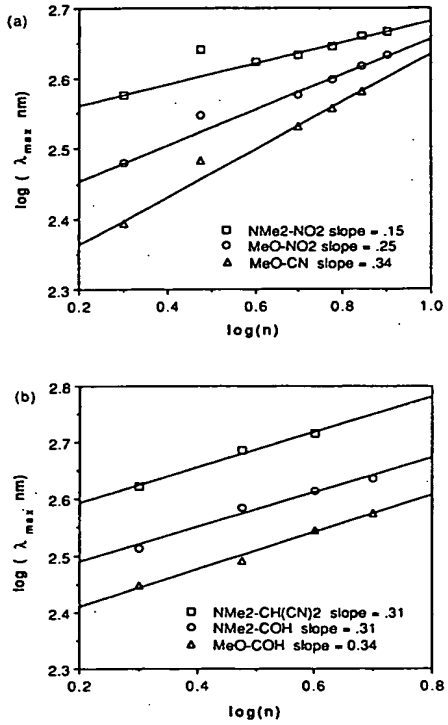

Figure 2. λ_{max} length dependences, where $n = 2$, for each phenyl unit, for (a) α,ω-diphenylpolyene and (b) α-phenylpolyene CT oligomers.

β and λ_{max} of the styrene derivatives if included in the α,ω-diphenylpolyene series, as in previous works,[2b,4] are, however, noted (see Figures 1a and 2a). Since the experimental accuracy in λ_{max} determinations are high (±2 nm) and the deviations for all donor–acceptor pairs are toward the long-wavelength side of the trend corroborating with the higher β values, the styrene structure is viewed as incompatible with the diphenyl capped series and results for styryl derivatives are not used to determine exponents.

Clearly, the magnitude of the exponent η which describes the power law dependence of $\beta \propto L^{\eta}$, where L is a length scale, depends strongly on the counting scheme used to determine L for a series of chemical structures studied. If η is to be compared with a physical model, such as results obtained from a free-electron theory[24] and an effective internal field model,[21] L, which is the delocalization length in the theories just mentioned, must be accurately determined. This is particularly important for the short-length structures in determining the power law dependence. However, it is difficult to rigorously account for the extent of delocalization into the acceptor and/or donor orbitals. For substituents such as amino, carbonyl, nitro, and di- and tricyanovinyl groups, conjugation extension is extensive due to the strong participation of their orbitals in the ground state. When such orbitals are accounted for, results on η can readily be increased by 1 or higher. These considerations have largely been ignored in the past.

A second consideration concerns the dispersive enhancement associated with measurement results obtained for the extended structures which have relatively low-lying CT transitions. Even with the longest convenient optical frequency such as 1.91 μm, dispersive enhancement is significant and is progressively more so as the CT transitions bathochromically shift with conjugation length. Corrections are often attempted by reporting β_0 values[9] which are deduced from the dispersion expression for the two-state model. As the π system is extended, the number of states con-

(24) (a) Davies, P. L. *Trans. Faraday Soc.* **1952**, *48*, 789. (b) Rustagi, K. Ducuing, J. *Opt. Commun.* **1972**, *10*, 258. (c) Agrawal, G. P.; Cojan, C.; Flytzanis, C. *Phys. Rev. B* **1978**, *17*, 776.

TABLE IX: Exponents Determined from Data in Literature and Those Obtained in the Current Study for the Conjugation Length (n As Defined in Text) Dependence of Phenyl-Capped Oligomeric Polyene Derivatives

source (ω)	structure	length (n)	η for $\beta(\omega)$	η for β_0	η for $\mu\beta(\omega)$	η for $\mu\beta_0$
ref 2b (1.9 μm)	Me_2N–Ph–(=)$_x$–Ph–CN	2, 5, 6			2.6	
ref 4 (1.06 μm)	MeO–Ph–(=)$_x$–Ph–NO_2	2, 3, 5, 6, 7, 8	3.1	2.6	3.3	2.8
ref 5 (1.34 μm)	Me_2N–Ph–(=)$_x$–COH	3, 6, 8,[a] 10			2.7	2.4
ref 5 (1.34 μm)	$C_6H_4S_2$(=)$_x$–COH	1, 4, 6,[a] 8			2.6	2.3
ref 3[b]	Me_2N–(=)$_x$–NO_2	2, 4, 6, 8, 10	2.5[c]			
ref 3[b]	Me_2N–(=)$_x$–COH	2, 3, 4, 5, 6	2.7[c]			
this work (1.9 μm)	Me_2N–Ph–(=)$_x$–Ph–NO_2	2, 3, 5, 6, 7, 8	1.9	1.9	2.2	2.1
this work (1.9 μm)	MeO–Ph–(=)$_x$–Ph–NO_2	2, 3, 5, 6, 7, 8	2.2	2.0	2.3	2.2
this work (1.9 μm)	MeO–Ph–(=)$_x$–Ph–CN	2, 3, 5, 6, 7, 8	2.5	2.3	2.4	2.3
this work (1.9 μm)	Me_2N–Ph–(=)$_x$–$CH(CN)_2$	2, 3, 5, 6, 7, 8	2.4	2.1	2.6	2.3
this work (1.9 μm)	Me_2N–Ph–(=)$_x$–COH	2, 3, 5, 6, 7, 8	2.8	2.7	3.1	2.9
this work (1.9 μm)	MeO–Ph–(=)$_x$–COH	2, 3, 5, 6, 7, 8	3.3	3.2	3.6	3.5

[a] Contains one acetylenic unit. [b] Computational results. [c] Calculated at $\omega = 0$.

tributing significantly to the hyperpolarizability increases rapidly.[25] Therefore, it is doubtful that such β_0 values are free from systematic errors. When short-wavelength lasers are used for the measurements, this problem is exacerbated. In addition, due to the low solubilities of the extended derivatives, their fractional experimental uncertainties are generally significantly larger than those of the shorter members of the series.[4] Since data are compressed at large n for a power law dependence, and the relatively high uncertainties for the extended derivatives procures lower statistical weights, the values of the exponents are often determined primarily by derivatives of short and moderate lengths. Therefore, experiments involving longer derivatives do not necessarily yield more reliable results.

A third critical issue concerns the deformational contribution, which is dominated by the electronic cubic polarizability, γ, to the EFISH signal.[26] As γ increases with both the conjugation length and β, this contribution becomes more significant for extended structures and must be taken into account prior to the determination of $\mu\beta$. Failure to do so will lead to overestimated exponents. Due to the presence of solvent cascading[27] and dispersive enhancement in THG, our procedure of making such a correction by relying on THG results is by no means rigorous.[1] However, it is probably better than ignoring such a effect. Again this uncertainty is less severe for the shorter derivatives.

Because of the reservations just discussed, we refrain from attaching great physical significance to the magnitude of the exponents. We have chosen a simple counting scheme in which donor and acceptor groups are excluded from the molecular length, and the length parameter n represents the number of double bonds with a count of 2 for each phenyl ring present in the conjugation. In order to make a numerical comparison with previous results, data given in refs 2b, 4, and 5 as well as computational results from ref 3 are analyzed according to the current scheme and the exponents, together with those obtained from our measurements, are tabulated in Table IX. All exponents fall within a range of about 2–3. Differences with previous results can be readily attributed to the differences in methodologies, counting schemes for L, as well as uncertainties discussed earlier, and will not be pursued further. We instead focus on the variations found within the current study. Two key features of the current findings are as follows: (1) the α-phenylpolyene and α,ω-diphenylpolyene series do not have the same exponents and the difference is about 0.6 with higher values for the former series; and (2) within each series, the exponents are end-group dependent and their values appear to be inversely related to the combined donor–acceptor strength or the magnitude of the hyperpolarizability.

The different exponents between the two series clearly point to the more efficient nature of the α-phenylpolyene series since, for a given extension from the benzene derivatives, significantly higher β value is realized. The only structural difference between the two series is the presence of one additional phenyl ring. Morley's calculation[3] and our discussions on styrene, fluorene, and stilbene derivatives suggest that the phenyl unit is much less effective than the olefinic unit for hyperpolarizability. A different counting scheme for L which better reflects this difference may eliminate the difference in the power law behaviors. By assigning one unit length for each phenyl unit, the difference between the two series as well as the deviation observed for the styryl derivatives is largely eliminated. All the exponents decrease from 1.9–3.3 to 1.5–2.2. Therefore, we can conclude that there is indeed a difference in effectiveness per unit physical length for the two series and the difference may be seen as further evidence that the olefinic unit is superior to the phenyl unit in engineering hyperpolarizability. This difference may be a result of the aromatic stabilization of the phenyl π system as discussed before. The two-dimensional nature of the phenyl ring should also be considered.[28] The magnitude of the new exponents are, however, considerably lower than those calculated by Morley for polyene systems with similar end groups (see Table IX).

The observed end-group dependence that gives lower exponents for the strong end groups may be partly rationalized by the extension of electron delocalization into the substituent orbitals, since it is reasonable to expect that stronger substituents will result in a longer delocalization length, which in turn results in a correction toward higher exponents. An alternative speculation may attribute the end-group dependence to bond alternation effects that are well-known for polyene systems. From simple valence bond considerations, the degree of bond alternation in CT polyene derivatives should be somewhat relieved as a result of the donor–acceptor stabilization of charge-separated resonance structures. However, such an effect appears to be insignificant judging from the moderate rate with which the CT bands bathochromically shift as a function of increasing chain length. As can be seen in Figure 2, the CT bands for both series red shift with n, but the exponents for λ_{max} are much less than unity, which is the familiar result from Hückel theory for systems free from bond alternation.[29] In any case, a reduction of bond alternation by strong donor–acceptor substituents will logically lead to a lower band gap and higher nonlinearity at saturation, which likely requires higher exponents for the length dependence. This is opposite to the observed end-group effects.

The most probable explanation for the end-group dependence is the recognition that the hyperpolarizabilities of extended CT structures are dominated by the participation of the π systems which become increasingly more polarizable. The end groups which dominate the asymmetric polarizability of the short structures play a reduced role in extended structures, resulting in a diminishing differential in properties of the extended structures

(25) (a) Docherty, V. J.; Pugh, D.; Morley, J. O. *J. Chem. Soc., Faraday Trans. 2* 1985, *81*, 1179–1192. (b) Li, D.-Q.; Ratner, M. A.; Marks, T. J. *J. Am. Chem. Soc.* 1988, *110*, 1707–1715. (c) Ulman, A. *J. Phys. Chem.* 1988, *92*, 2385–2390.
(26) Levine, B. F.; Bethea, C. G. *J. Chem. Phys.* 1975, *63*, 2666–2682.
(27) Meredith, G. R. *Chem. Phy. Lett.* 1982, *92*, 165–171.
(28) Wu, J. W.; Heflin, J. R.; Norwood, R. A.; Wong, K. Y.; Zamani-Khamiri, O.; Garito, A. F.; Kalyanaraman, P.; Sounik, J. *J. Opt. Soc. Am. B* 1989, *6*, 707–720.
(29) Jones, L. *Proc. R. Soc.* 1937, *A158*, 280.

TABLE X: Results on 2′-Acceptor,2- or 4-Donor-Substituted α,ω-Diphenylpolyene Oligomers (Units in esu)

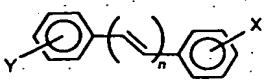

n	X	Y	solvent	λ_{max}, nm	$\mu \times 10^{-18}$	$\alpha^{o} \times 10^{-23}$	$\beta \times 10^{-30}$	$\gamma \times 10^{-36}$
2	2′-CN	2-OMe	$CHCl_3$	(354)	3.8	3.7	4.5	60
3	2′-CN	2-OMe	$CHCl_3$	(376)	3.8	4.4	7.1	147
2	2′-CN	4-OMe	$CHCl_3$	(356)	3.9	3.7	2.6	88
3	2′-CN	4-OMe	$CHCl_3$	(378)	3.9	4.3	4.3	165
2	4′-CN	2-OMe	$CHCl_3$	(358)	4.9	3.8	16	90
1	2′-NO_2	2-OMe	$CHCl_3$	360s	3.8	3.3	4.4	29
2	2′-NO_2	2-OMe	$CHCl_3$	(376s)	3.7	3.8	6.4	51
3	2′-NO_2	2-OMe	$CHCl_3$	(392s)	4.1	4.4	11	131
1	2′-NO_2	4-OMe	$CHCl_3$	390s	3.5	3.3	3.8	35
2	2′-NO_2	4-OMe	$CHCl_3$	(370s)	3.8	3.8	4.9	75
3	2′-NO_2	4-OMe	$CHCl_3$	(392s)	3.8	4.3	11	123
1	4′-NO_2	2-OMe	$CHCl_3$	362	5.0	3.3	22	61
2	4′-NO_2	2-OMe	$CHCl_3$	(380)	4.3	3.7	17	55
3	4′-NO_2	2-OMe	$CHCl_3$	(412)	4.8	4.5	56	149

with different substituents. Since the hyperpolarizability is expected to saturate at some length due to the presence of bond alternation and other localization effects, and it is likely that saturation occurs prior to the unphysical crossing of the lines for different end groups in Figure 1, a high saturation limit of about 35 double bonds can be deduced. This is not in disagreement with the computation results of Morley that predicted an onset of saturation at $n \approx 20$ for the α,ω-(*N*,*N*-dimethylamino)nitropolyenes.[3]

The properties of extended α,ω-diphenylpolyene derivatives with 2′- or 4′-acceptor, 2- or 4-donor substitution patterns are also examined. Measurement results are presented in Table X. The β values for these compounds are always considerably lower than the 4′-acceptor,4-donor-substituted derivatives despite comparable CT band positions. The lower values can be attributed to two reasons. Firstly, the effective length of the conjugation is reduced. Secondly, for compounds with 2′-acceptor substitution, the very low values are the result of an experimental artifact of the EFISH measurement, which projects only the vectorial component of the hyperpolarizability tensor onto the molecular dipole. Since the dipole moment direction is dominated by the large group dipole moment of the highly polar nitro and cyano groups, it deviates significantly from the long molecular axis along which β is expected to be the highest. Along that axis, considerably higher β components are expected. It is interesting to note that, in spite of a shorter effective conjugation length, the 2′-acceptor,2-donor derivatives are found to have consistently higher values than the 2′-acceptor,4-donor analogues. These geometric factors are not as important for 4′-acceptor,2-donor-substituted derivatives since the group dipole moments of the donors are much weaker. The relative importance of through-resonance structures and geometric considerations in the interpretation of EFISH results was discussed in more detail in ref 1 where different substitution patterns on stilbenes were considered. The β values of all substitution patterns are found to increase with the extension of conjugation and the fractional increases appear to be quite comparable to the 4′-4-substituted derivatives.

5. Heteropentacyclic Derivatives: Minimization of Aromaticity. The observations presented above suggest that the hyperpolarizabilities of conjugated structures containing phenyl units can be enhanced by replacing phenyl groups with groups that have reduced aromatic stabilization and more polyene-like structures. To explore this hypothesis further, we have investigated CT structures in which phenyl units in conventional arene derivatives such as stilbene, diphenylbutadiene, and terphenyl are replaced with five-member heterocyclics such as furan and thiophene functionalities with reduced aromatic characters. Measurement results of these compounds together with results from their arene analogues are given in Table XI. In each case, the CT band occurred at longer wavelength and the β value was significantly higher for the heteropentacyclic derivative. Spectroscopic and

TABLE XI: Results on Heteropentacyclic and Related Arene Derivatives

compd	λ_{max},[a] nm	$\mu \times 10^{-18}$, esu	$\beta \times 10^{-30}$, esu
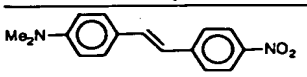	430*	6.6	73
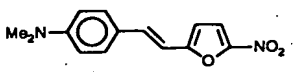	478**	6.9	83
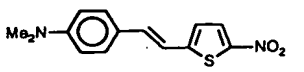	492***	7.4	98
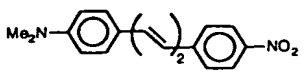	442	7.6	107
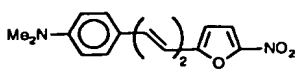	488	7.2	113
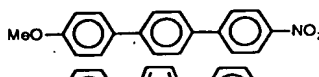	340	5.0	11
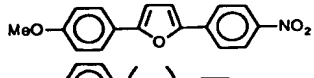	400	5.2	40
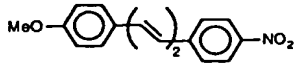	397	4.8	47

[a] Oscillator strength: 0.60 (*), 0.45 (**), and 0.42 (***). Δμ: 13 D (*), 13 D (**), and 13 D (***).

logues. $\Delta\mu = \mu_e - \mu_g$ is extracted from solvatochromic shifts ($\Delta\nu$) of absorption spectra in solvents with closely matching refractive indexes but quite different dielectric constants (D) according to the following equation[30]

$$hc(\Delta\nu) = \frac{2\mu_g(\mu_g - \mu_e)}{a^3}\Delta\left(\frac{D-1}{D+2}\right)$$

where h and c are Planck's constant and the speed of light, respectively. The Onsager radius, a, is taken to be 7 Å. No significant differences in oscillator strength and $\Delta\mu$ are found. This suggests that the higher nonlinearity originates largely from the reduction in CT transition energy which is believed to be a result of the destabilization of the ground state through partial elimination of aromatic energy. The strong correlation and trade-off between β and the λ_{max} of the CT band is an recurring theme observed throughout our studies of the generic donor–conjugation–acceptor structures.[1,31] This property places a practical limit

(30) Mataga, N.; Kubota, T. *Molecular Interactions and Electronic Spectra*; Marcel Dekker: New York, 1970; Chapter 8.
(31) Cheng, L.-T.; Tam, W.; Feiring, A.; Rikken, G. L. J. A. *SPIE Proc.*

on the available nonlinearities of organic materials for harmonic generation applications in the blue and green region.

6. Cubic Hyperpolarizability. As in ref 1, the salient features of our THG measurement results on molecular cubic hyperpolarizability, γ, are a general dependence on conjugation length and a strong correlation with β. In addition, there are clear differences among the different conjugated structures. For the polyphenyls and α,ω-diphenylpolyynes, conjugation extensions lead to much weaker increase of γ in comparison with that of the α-phenylpolyenes and α,ω-diphenylpolyenes (see Table IV, VI, VII, and VIII). Much of the same structural considerations, such as torsional effect, bond alternation, and aromatic stabilizations, used for the discussion of β can be used to rationalize these differences in γ.

Conclusion

We have systematically investigated the conjugation dependences of the quadratic optical hyperpolarizability of organic molecules with EFISH and THG measurements. Over 100 compounds covering a wide range of structures have been studied in order to demonstrate the existence of systematic trends and illustrate the importances of different characteristics of the π system. Issues concerning the efficacies of various conjugation units, conjugation planarity, aromaticity and bond alternation, and electron localization and delocalization effects, as well as the conjugation length and end group dependences, were addressed.

Acknowledgment. We thank H. Jones (Du Pont), T. Hunt (Du Pont), and B. G. Tiemann (JPL) for expert technical assistance. We also thank Dr. G. R. Meredith (Du Pont) for valuable discussions throughout the preparation of this manuscript. The research described in this paper was performed, in part, by the Jet Propulsion Laboratory, California Institute of Technology, as part of its Center for Space Microelectronics Technology which is supported by the Strategic Defense Initiative Organization, Innovative Science and Technology Office, through an agreement with the National Aeronautics and Space Administration (NASA).

Registry No. *p*-$MeOC_6H_4CH{=}CHCN$, 14482-11-2; *p*-$Me_2NC_6H_4CH{=}CHCN$, 4854-85-7; *p*-$BrC_6H_4CH{=}CHCHO$, 49678-04-8; *p*-$MeOC_6H_4CH{=}CHCHO$, 24680-50-0; *p*-$Me_2NC_6H_4CH{=}CHCHO$, 20432-35-3; *p*-$MeOC_6H_4CH{=}CHCOCH_3$, 3815-30-3; $PhCH{=}CHNO_2$, 5153-67-3; *p*-$OHC_6H_4CH{=}CHNO_2$, 22568-49-6; *p*-$MeOC_6H_4CH{=}CHNO_2$, 5576-97-6; *p*-$Me_2NC_6H_4CH{=}CHNO_2$, 22568-06-5; *p*-$NO_2C_6H_4CH{=}CHNMe_2$, 136795-65-8; *p*-PhC_6H_4CN, 2920-38-9; *p*-$PhC_6H_4COCH_3$, 92-91-1; *p*-$PhC_6H_4NO_2$, 92-93-3; *p*-$Me_2NC_6H_4C_6H_4$-*p*-$SO_2(CH_2)_6OH$, 134249-49-3; *p*-$OHC_6H_4C_6H_4$-*p*-CN, 19812-93-2; *p*-$MeOC_6H_4C_6H_4$-*p*-$COCH_3$, 13021-18-6; *p*-$BrC_6H_4C_6H_4$-*p*-NO_2, 6242-98-4; *p*-$OHC_6H_4C_6H_4$-*p*-NO_2, 3916-44-7; *p*-$MeOC_6H_4C_6H_4$-*p*-NO_2, 2143-90-0; *p*-$NH_2C_6H_4C_6H_4$-*p*-NO_2, 1211-40-1; *p*-$Me_2NC_6H_4C_6H_4$-*p*-NO_2, 2143-87-5; *p*-$NH_2C_6H_4NO_2$, 100-01-6; *p*-$NH_2C_6H_4C_6H_4$-*p*-C_6H_4-*p*-NO_2, 38190-45-3; *p*-$NH_2C_6H_4C_6H_4$-*p*-C_6H_4-*p*-C_6H_4-*p*-NO_2, 118837-15-3; *p*-$MeOC_6H_4NO_2$, 100-17-4; *p*-$MeOC_6H_4C_6H_4$-*p*-C_6H_4-*p*-NO_2, 114253-99-5; *p*-$NH_2C_6H_4C{\equiv}CC_6H_4$-*p*-$SO_2Me$, 135043-09-3; *p*-$MeSC_6H_4C{\equiv}CC_6H_4$-*p*-$CO_2Me$, 135043-10-6; *p*-$NH_2C_6H_4C{\equiv}CC_6H_4$-*p*-$CO_2Me$, 119984-87-1; *p*-$MeSC_6H_4C{\equiv}CC_6H_4$-*p*-$COCH_3$, 135043-11-7; *p*-$NH_2C_6H_4C{\equiv}CC_6H_4$-*p*-$COCH_3$, 123770-68-3; *p*-$NH_2C_6H_4C{\equiv}CC_6H_4$-*p*-COPh, 135043-13-9; *p*-$MeSC_6H_4C{\equiv}CC_6H_4$-*p*-CN, 125138-98-9; *p*-$NH_2C_6H_4C{\equiv}CC_6H_4$-*p*-CN, 119984-85-9; *p*-$MeNHC_6H_4C{\equiv}CC_6H_4$-*p*-CN, 135043-12-8; *p*-$Me_2NC_6H_4C{\equiv}CC_6H_4$-*p*-CN, 54273-31-3; *p*-$BrC_6H_4C{\equiv}CC_6H_4$-*p*-NO_2, 15795-01-4; *p*-$MeOC_6H_4C{\equiv}CC_6H_4$-*p*-$NO_2$, 39082-40-1; *p*-$MeSC_6H_4C{\equiv}CC_6H_4$-*p*-$NO_2$, 119984-89-3; *p*-$NH_2C_6H_4C{\equiv}CC_6H_4$-*p*-$NO_2$, 7431-22-3; *p*-$MeNHC_6H_4C{\equiv}CC_6H_4$-*p*-$NO_2$, 101456-22-8; *p*-$Me_2NC_6H_4C{\equiv}CC_6H_4$-*p*-$NO_2$, 62197-66-4; *p*-$MeSC_6H_4C{\equiv}CC{\equiv}CC_6H_4$-*p*-CN, 119984-91-7; *p*-$NH_2C_6H_4C{\equiv}CC{\equiv}CC_6H_4$-*p*-CN, 119984-86-0; *p*-$MeSC_6H_4C{\equiv}CC{\equiv}CC_6H_4$-*p*-$NO_2$, 119984-90-6; *p*-$NH_2C_6H_4C{\equiv}CC{\equiv}CC_6H_4$-*p*-$NO_2$, 110175-15-0; *p*-$NH_2C_6H_4C{\equiv}CC{\equiv}CC{\equiv}CC_6H_4$-*p*-$NO_2$, 110175-16-1; *p*-$MeOC_6H_4CHO$, 123-11-5; *p*-$MeOC_6H_4CH{=}CHCH{=}CHCHO$, 49678-07-1; *p*-$MeOC_6H_4CH{=}CHCH{=}CHCH{=}CHCHO$, 72232-59-8; *p*-$Me_2NC_6H_4CHO$, 100-10-7; *p*-$Me_2NC_6H_4CH{=}CHCH{=}CHCHO$, 20432-36-4; *p*-$Me_2NC_6H_4CH{=}CHCH{=}CHCH{=}CHCHO$, 55298-77-6; *p*-$MeOC_6H_4CHC(CN)_2$, 2826-26-8; *p*-$MeOC_6H_4CH{=}CHCHC(CN)_2$, 136795-66-9; *p*-$Me_2NC_6H_4CHC(CN)_2$, 2826-28-0; *p*-$Me_2NC_6H_4CH{=}CHCH{=}CHCHC(CN)_2$, 129179-87-9; *p*-$Me_2NC_6H_4CH{=}CHCH{=}CHCHC(CN)_2$, 136822-54-3; *p*-$MeOC_6H_4CH{=}CHC_6H_4$-*p*-CN, 57193-97-2; *p*-$MeOC_6H_4CH{=}CHCH{=}CHC_6H_4$-*p*-CN, 136795-67-0; *p*-$MeOC_6H_4CH{=}CHCH{=}CHCH{=}CHC_6H_4$-*p*-CN, 136795-68-1; *p*-$BrC_6H_4CH{=}CHC_6H_4$-*p*-NO_2, 24325-71-1; *p*-$BrC_6H_4CH{=}CHCH{=}CHC_6H_4$-*p*-$NO_2$, 136795-69-2; *p*-$BrC_6H_4CH{=}CHCH{=}CHCH{=}CHC_6H_4$-*p*-$NO_2$, 136795-70-5; *p*-$MeOC_6H_4CH{=}CHC_6H_4$-*p*-$NO_2$, 4648-33-3; *p*-$MeOC_6H_4CH{=}CHCH{=}CHC_6H_4$-*p*-$NO_2$, 136795-71-6; *p*-$MeOC_6H_4CH{=}CHCH{=}CHCH{=}CHC_6H_4$-*p*-$NO_2$, 136795-72-7; *p*-$MeOC_6H_4CH{=}CHCH{=}CHCH{=}CHC_6H_4$-*p*-$NO_2$, 136795-73-8; *p*-$MeSC_6H_4CH{=}CHC_6H_4$-*p*-$NO_2$, 20101-50-2; *p*-$MeSC_6H_4CH{=}CHCH{=}CHC_6H_4$-*p*-$NO_2$, 136795-74-9; *p*-$Me_2NC_6H_4CH{=}CHC_6H_4$-*p*-$NO_2$, 2844-15-7; *p*-$Me_2NC_6H_4CH{=}CHCH{=}CHC_6H_4$-*p*-$NO_2$, 67309-70-0; *p*-$Me_2NC_6H_4CH{=}CHCH{=}CHCH{=}CHC_6H_4$-*p*-$NO_2$, 136795-75-0; *p*-$Me_2NC_6H_4CH{=}CHCH{=}CHCH{=}CHCH{=}CHC_6H_4$-*p*-$NO_2$, 136795-76-1; *o*-$MeOC_6H_4CH{=}CHCH{=}CHC_6H_4$-*o*-CN, 136795-77-2; *o*-$MeOC_6H_4CH{=}CHCH{=}CHCH{=}CHC_6H_4$-*o*-CN, 136795-78-3; *p*-$MeOC_6H_4CH{=}CHCH{=}CHC_6H_4$-*o*-CN, 136795-79-4; *p*-$MeOC_6H_4CH{=}CHCH{=}CHCH{=}CHC_6H_4$-*o*-CN, 136795-80-7; *o*-$MeOC_6H_4CH{=}CHCH{=}CHC_6H_4$-*p*-CN, 136795-81-8; *o*-$MeOC_6H_4CH{=}CHC_6H_4$-*o*-NO_2, 55801-78-0; *o*-$MeOC_6H_4CH{=}CHCH{=}CHC_6H_4$-*o*-$NO_2$, 136795-82-9; *o*-$MeOC_6H_4CH{=}CHCH{=}CHCH{=}CHC_6H_4$-*o*-$NO_2$, 136795-83-0; *p*-$MeOC_6H_4CH{=}CHC_6H_4$-*o*-$NO_2$, 112768-16-8; *p*-$MeOC_6H_4CH{=}CHCH{=}CHC_6H_4$-*o*-$NO_2$, 136795-84-1; *p*-$MeOC_6H_4CH{=}CHCH{=}CHCH{=}CHC_6H_4$-*o*-$NO_2$, 136795-85-2; *o*-$MeOC_6H_4CH{=}CHC_6H_4$-*p*-$NO_2$, 28915-66-4; *o*-$MeOC_6H_4CH{=}CHCH{=}CHC_6H_4$-*p*-$NO_2$, 136795-86-3; *o*-$MeOC_6H_4CH{=}CHCH{=}CHCH{=}CHC_6H_4$-*p*-$NO_2$, 136795-87-4; styrene, 100-42-5; biphenyl, 92-52-4; fluorene, 86-73-7; diphenylacetylene, 501-65-5; 2-cyanofluorene, 2523-48-0; 2-nitrofluorene, 607-57-8; 2-bromo-7-nitrofluorene, 6638-61-5; 2-methoxy-7-nitrofluorene, 54961-21-6; 2-dimethylamino-7-nitrofluorene, 19221-04-6; 1-(4-dimethylaminophenyl)-2-(5-nitrofuranyl)ethene, 136795-62-5; 1-(4-dimethylaminophenyl)-2-(5-nitrothienyl)ethene, 136795-63-6; 1-(4-dimethylaminophenyl)-3-(5-nitrofuranyl)-1,3-butadiene, 136795-64-7; 2-(4-methoxyphenyl)-5-(4-nitrophenyl)furan, 126739-60-4.

20 August 1999

ELSEVIER

Chemical Physics Letters 309 (1999) 315–320

CHEMICAL PHYSICS LETTERS

www.elsevier.nl/locate/cplett

Chiral 1,1È-binaphthyl-based helical polymers as nonlinear optical materials

Sven Van Elshocht [a,*], Thierry Verbiest [a], Martti Kauranen [a], Liang Ma [b], Hua Cheng [b], Kwon Y. Musick [b], Lin Pu [b], André Persoons [a]

[a] *KU Leuven, Laboratory of Chemical and Biological Dynamics, Catholic University of Leuven, Celestijnenlaan 200D, B-3001 Leuven, Belgium*

[b] *Department of Chemistry, University of Virginia, Charlottesville, VA 22901, USA*

Received 11 June 1999; in final form 2 July 1999

Abstract

We have studied the nonlinear optical properties of Langmuir–Blodgett films of several chiral 1,1È-binaphthyl-based helical polymers. We have studied the nonlinear optical properties and the quality of the Langmuir–Blodgett films. One of the compounds forms high-quality Langmuir–Blodgett films with a high nonlinear susceptibility that remains stable in time. We show that an important part of the nonlinear susceptibility is only allowed by the chirality of the film. © 1999 Elsevier Science B.V. All rights reserved.

1. Introduction

Nonlinear optics (NLO) has been recognized for several years as a field of research with important potential applications in optoelectronic devices [1,2]. Much work has been devoted to the identification of suitable materials. During the 1980s it became clear that organic materials (and especially polymers) could be useful for second- and third-order NLO applications. For second-order nonlinear optics, the material must be noncentrosymmetric on the molecular and macroscopic scales [3]. Noncentrosymmetry on the molecular scale is easy to achieve, for example by connecting an electron donor and acceptor by a one-dimensional π-conjugated bridge. On the other hand, macroscopic noncentrosymmetry has proven more difficult. Methods to achieve macroscopic noncentrosymmetry are electric-field poling [4], crystal growth [5], self-assembly, and deposition of Langmuir–Blodgett (LB) films [6,7]. An alternative approach is the use of chiral materials. Such systems are inherently noncentrosymmetric and can therefore be used for second-order nonlinear optics [8]. Chirality can also be used to advantage in crystal growth to prevent crystallization in a centrosymmetric group [9] and in Langmuir–Blodgett films to increase the nonlinear optical efficiency [10].

Binaphthyl monomers have been studied by Hicks et al. [11]. In this Letter, we study a series of chiral 1,1È-binaphthyl-based helical polymers (Fig. 1) and demonstrate that they can be successfully used to build high-quality LB films with good NLO properties. However, it is important to note that the study

* Corresponding author. Fax: +32-16-32-79-82; e-mail: sven.vanelshocht@fys.kuleuven.ac.be

0009-2614/99/$ - see front matter
PII: S0009-2614(99)00730-7

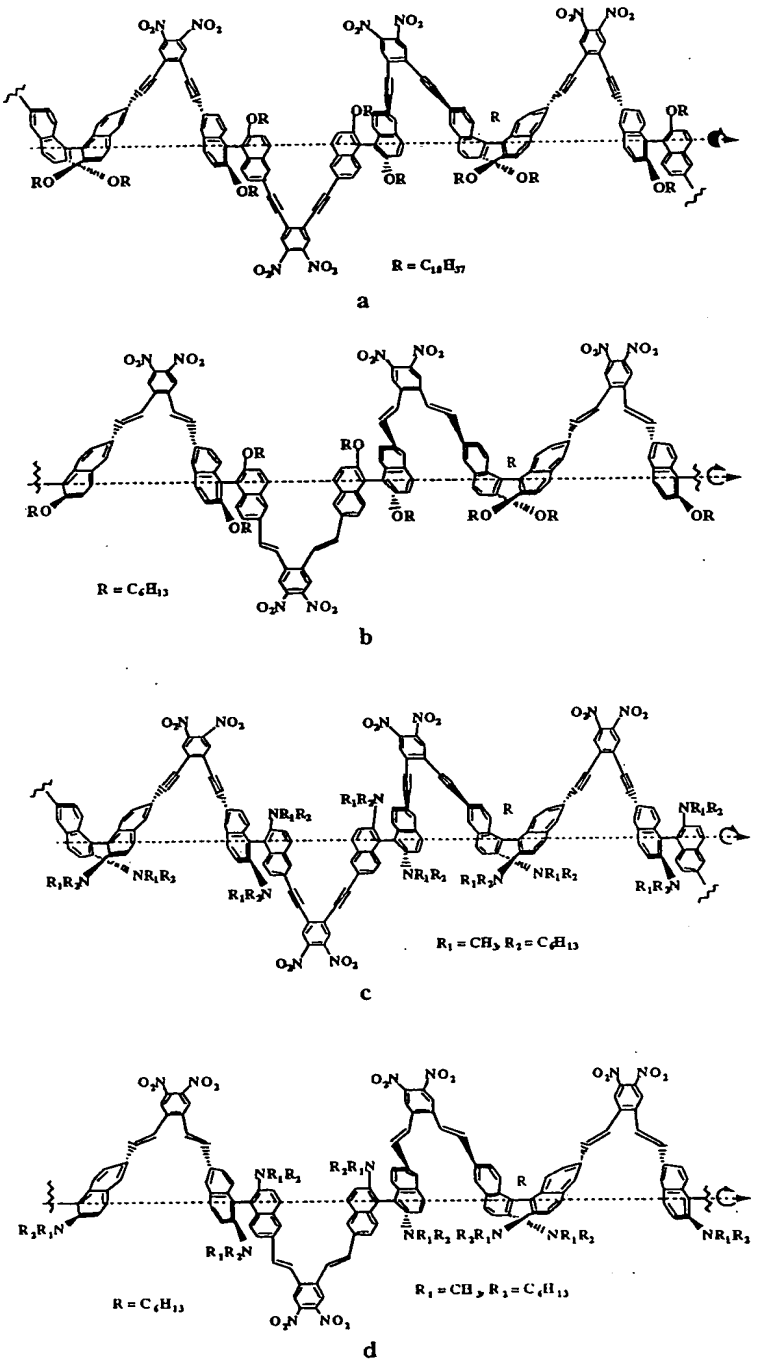

Fig. 1. Chemical structure of helical polymers a–d.

of the binaphthyls is not the main issue, but they were a tool to create large helical structures which are of importance in the field of chemical physics as mentioned above, and already have demonstrated interesting properties in linear and nonlinear optics [12,13].

2. Experimental

The polymers used in this study were prepared from chiral 1,1'-binaphthyl-based monomeric units and optimized for nonlinear optics by adding a π-conjugated bridge and electron donor and acceptor groups [14–16]. The monomer units can be considered as an ensemble of rigid electric-dipole units that form a propeller-like three-dimensional conformation due to the chirality of the binaphthyl units. Therefore, the chirality of these systems is derived from the main-chain configuration. All systems investigated were enantiomerically pure.

Surface pressure isotherms of the polymers were recorded by spreading dilute chloroform solutions of the polymers on the water subphase of a LB through (KSV minithrough). After complete evaporation of the solvent, the monolayer was compressed at a rate of 0.01 nm^2/(min repeat unit). The surface pressure isotherms of the four polymers investigated are shown in Fig. 2. All polymers show a rather featureless surface pressure isotherm. The surface pressure starts to rise at 0.40 and 0.48 nm^2 for polymers **a** and **b**, respectively, and 0.35 nm^2 for **c** and **d**. Polymers **b**, **c** and **d** clearly collapse at 45, 65 and 60 mN/m, respectively. The collapse could be visualy observed as the occurrence of long stripes on the surface. A film of polymer **a** on the other hand reaches an inflection point at 35 mN/m, where probably a double layer is formed, and collapses at 60 mN/m. The area per repeat unit, obtained by extrapolating the steepest slope of the isotherm to zero pressure, is between 0.25 and 0.35 nm^2 for all polymers.

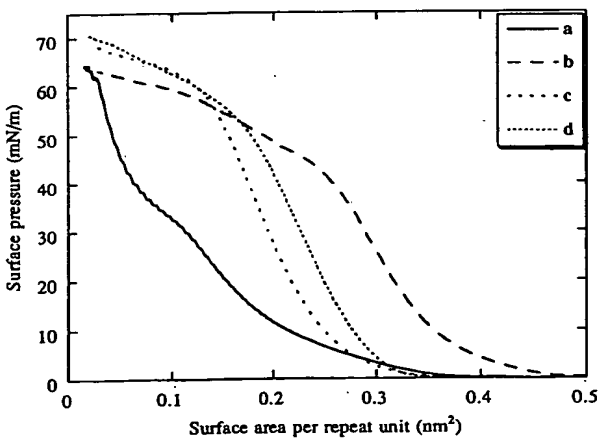

Fig. 2. Surface pressure/surface area isotherms of helical polymers **a**–**d**.

To construct multilayer LB films, the floating monolayers were compressed to a surface pressure of 10 mN/m for polymer **a**, 20 mN/m for **d** and **b**, and 30 mN/m for **c**. After 30 min of stabilization, the monolayers were transferred to hydrophobic glass slides (silanized with octadecyltrichlorosilane). Because of the high stiffness of the floating layers, only horizontal dipping could be used to transfer the floating layers to the glass substrates. LB films with thicknesses between 1 and 8 monomolecular layers were prepared. The transfer ratios were between 0.85 and 1.08, indicating that monomolecular layers were transferred to the glass slide.

The nonlinear optical properties of the materials were studied with second-harmonic generation (SHG). The second-harmonic response of the films was measured using a Q-switched Nd:YAG laser (10 ns, 50 Hz, 1064 nm) incident at 45° on the samples.

Films of **a**, **b** and **d** were of very good optical quality. The excellent quality was verified by observing that the second-harmonic signal increases quadratically as a function of the number of deposited layers. Deposition of **c**, on the other hand, resulted in films of poor optical quality. Large holes could be observed by the naked eye throughout the entire film. The quality of the LB films seems to benefit from the presence of double bonds in the monomer units and the presence of a long alkyl chain ($-C_{18}H_{37}$). These structural features probably give the polymer some degree of flexibility which improves film quality.

To analyze the nonlinear response in more detail, we studied its polarization dependence. The polarization of the fundamental beam was continuously varied by a quarter waveplate and the s- and p-polarized SH signals were detected in transmission or reflection. A detailed analysis of the experimentally obtained polarization patterns allows to determine all susceptibility components of the LB films [17,18]. The values of the susceptibility were calibrated using a quartz wedge ($d_{33} = 0.3$ pm/V) as in Ref. [19]. The symmetry of the LB film was also determined using SHG. The sample was irradiated with p-polarized fundamental light under 45° of incidence and the p-polarized SH was detected in transmission while rotating the samples about their surface nor-

mal. The shape of the rotation pattern is connected to the symmetry of the samples [20]. The symmetry of all films was found to be C_∞ with the surface normal as the ∞-fold rotation axis.

3. Results and discussion

The maximum SHG intensity from materials **a** and **b** was comparable but very weak. An additional problem with material **b** was the instability of the polymer when irradiated with the infrared laser light. The SHG signal decreased to 75% of its initial value within a few minutes. Films of the polymer **c**, on the other hand, showed a much stronger SHG efficiency, i.e., a factor of 50 higher compared to **a** and **b**. The higher efficiency of **c** can be attributed to the presence of the strong amino donor. However, as mentioned above the replacement of the sidegroup introduced a supplemental problem. The lack of the long alkyl chain had a negative impact on the quality of the LB films.

For **d** the $-N(CH_3)(C_6H_{13})$ sidegroup was kept but the triple bond, that connects the binaphthyl units, was replaced by a double bond. This modification greatly improved the film quality. A comparison of the SHG efficiency demonstrated that material **d** is 4 times more efficient than **c**, i.e., a total factor of 200 more efficient when compared to the original materials **a** and **b**. This can be explained by the strong resonantly enhanced signal from LB films of polymer **d**.

Structural changes as discussed above will not only influence the quality of the LB films and the NLO efficiency, but will give rise to changes in linear UV/VIS absorption spectra. Shifts in the main spectral features can be as much as a hundred nanometers (Fig. 3). Films of **c** and **d** have an absorption shoulder around 525 nm where **b** and **a** have an absorption shoulder around 425 nm. The second-harmonic wavelength 532 nm is close to the absorption shoulder of **c** and **d**. The nonlinear response of these materials is therefore expected to be resonantly enhanced.

Because of the low SHG efficiency of **a** and **b** and the poor film quality of **c**, we were only able to determine reliable values of the susceptibility components of films of **d**. From an analysis of the

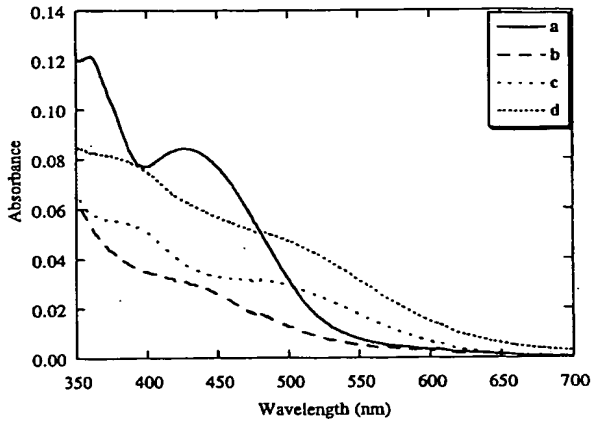

Fig. 3. UV–visible absorption spectra of helical polymers **a**–**d**.

polarization dependence of the SHG, we calculated the tensor components of the nonlinear susceptibility $\chi^{(2)}_{ijk}$. Since the film has C_∞ symmetry, the nonvanishing components ijk are zzz, $zxx = zyy$, $xxz = xzx = yyz = yzy$, $xyz = xzy = -yxz = -yzx$, where z is along the surface normal, and x and y are the in-plane coordinates. The absolute values of the susceptibility components are given in Table 1. Note that, in contrast to earlier work on polyisocyanides and polythiophenes [21,22], we saw no indication of magnetic contributions to the nonlinearity of the present materials.

The values of the susceptibility components, between 2 and 35 pm/V, although resonantly enhanced, are quite respectable for a polymer system that differs significantly in chemical structure from side-chain (see, e.g., Ref. [23]) polymers traditionally used in nonlinear optics. Furthermore, the high values of the xxz, zxx and zzz components suggest favorable ordering of the chromophoric parts of the polymer in the LB films, which is rather unexpected based on the chemical structure of the polymer. The chirality of the LB film is reflected by the presence of a nonnegligible xyz component of 2 pm/V.

Chirality also manifests itself in different SH efficiency when the films are irradiated with left- and right-hand circularly polarized light. Such circular-difference effects (CD) have been observed in other chiral LB films and can be quantified as [24]:

$$\frac{\Delta I}{I} = \frac{2(I_l - I_r)}{(I_l + I_r)}, \qquad (1)$$

Table 1
The absolute values of the second-order susceptibility components of helical polymer **d**, classification of the components as chiral or achiral

Second-order susceptibility component	Absolute value (pm/V)	Chirality classification
xyz	2	chiral
xxz	7	achiral
zxx	5	achiral
zzz	35	achiral

where I_l and I_r are the intensities of the second-harmonic light generated when the fundamental beam is left- and right-hand circularly polarized, respectively. For material **b** no meaningful result could be calculated because the SH signal decreased continuously due to instability of the material. For the other materials, all CD effects are between 25 and 60% [25], expressing the role of chirality in these films. No CD effects were observed for films of the racemic mixture of **c**.

Another virtue of the materials studied is the stability of the nonlinear response of the LB films. For example, the NLO efficiency of a 5-layer film of **d** was monitored for more than six months at room temperature and no decrease of the NLO efficiency was observed.

4. Conclusion

In conclusion, we have demonstrated that LB films of 1,1'-binaphthyl-based chiral polymers can have interesting NLO properties. High-quality LB films with good stability were prepared and their NLO properties analyzed. The high NLO efficiency shows the potential of these polymers as new NLO materials. The influence of chirality on the NLO properties was reflected by the presence of a nonnegligible *xyz*-susceptibility component and by the occurrence of extremely large CD-effects in the second-harmonic signals.

Acknowledgements

T.V. is a Postdoctoral Fellow of the Fund for Scientific Research-Flanders [FWO-V]. M.K. acknowledges support from the Academy of Finland. The research of S.V.E., T.V., and A.P. was supported by research grants from the Fund for Scientific Research-Flanders (FWO-V, No. G.0338.98 and 9.0407.98), from the Belgian government (No. IUAP P4/11), and from the University of Leuven (No. GOA/95/01). The work of L.M., H.C., K.Y.M., and L.P. was supported by the Department of Chemistry at University of Virginia, the Department of Chemistry at North Dakota State University, the National Science Foundation (DMR-9529805), the US Air Force (F49620-96-1-0360) and the Jeffress Memorial Trust.

References

[1] P.N. Prasad, D.J. Williams, Introduction to Nonlinear Optical Effects in Polymers and Molecules, Wiley, New York, 1992.
[2] Y.R. Shen, The Principles of Nonlinear Optics, Wiley, New York, 1984.
[3] R.W. Boyd, Nonlinear Optics, Academic Press, San Diego, CA, 1992.
[4] S. Miyata, H. Sasabe, Advances in Nonlinear Optics, vol. 4: Poled Polymers and Their Applications to SHG and EO Devices, Gordon and Breach, Singapore, 1997.
[5] Ch. Bosshard, K. Sutter, Ph. Prêtre, J. Hulliger, M. Flörsheimer, P. Kaatz, P. Günter, Advances in Nonlinear Optics, vol. 1: Organic Nonlinear Optical Materials, Gordon and Breach, Singapore, 1995.
[6] G. Roberts, Langmuir–Blodgett films, Plenum, New York, 1990.
[7] A. Ulman, An Introduction to Ultrathin Organic Films from Langmuir–Blodgett to Self-assembly, Academic Press, San Diego, CA, 1991.
[8] P.M. Rentzepis, J.A. Giordmaine, K.W. Wecht, Phys. Rev. Lett. 16 (1966) 792.
[9] J. Zyss, D.S. Chemla, Nonlinear Optical Properties of Organic Molecules and Crystals, vol. 1, Academic Press, Orlando, FL, 1987.
[10] T. Verbiest, S. Van Elshocht, M. Kauranen, L. Hellemans, J. Snauwaert, C. Nuckolls, T.J. Katz, A. Persoons, Science 282 (1998) 913.
[11] T. Petralli-Mallow, T.M. Wong, J.D. Byers, H.I. Yee, J.M. Hicks, J. Phys. Chem. 97 (1993) 1383.
[12] M.M. Bouman, E.E. Havinga, R.A.J. Janssen, E.W. Meijer, Mol. Cryst. Liq. Cryst. 256 (1994) 439.
[13] S. Van Elshocht, T. Verbiest, M. Kauranen, B.M.W. Langeveld-Voss, E.W. Meijer, A. Persoons, J. Chem. Phys. 107 (1997) 8201.
[14] L. Ma, Q.-S. Hu, D. Vitharan, C. Wu, C.M.S. Kwan, L. Pu, Macromolecules 30 (1997) 204.
[15] H. Sheng, L. Pu, Macromol. Chem. Phys. (in press).

[16] K.Y. Musick, Q.-S. Hu, L. Pu (in preparation).
[17] J.J. Maki, M. Kauranen, A. Persoons, Phys. Rev. B 51 (1995) 1425.
[18] M. Kauranen, J.J. Maki, A. Persoons, Proc. SPIE (Soc. Photo-Opt. Instrum. Eng.) 2527 (1995) 328.
[19] D. Roberts, IEEE J. Quantum Electron. 28 (1992) 2057.
[20] X. Zhuang, D. Wilk, L. Marruci, Y.R. Shen, Phys. Rev. Lett. 75 (1995) 2144.
[21] S. Van Elshocht, T. Verbiest, M. Kauranen, A. Persoons, B.M.W. Langeveld-Voss, E.W. Meijer, J. Chem. Phys. 107 (1997) 8201.
[22] M. Kauranen, T. Verbiest, E.W. Meijer, E.E. Havinga, M.N. Teerenstra, A.J. Schouten, R.J.M. Nolte, A. Persoons, Adv. Mater. 7 (1995) 641.
[23] W.M.K.P. Wijekoon, S.K. Wijaya, J.D. Bhawalkar, P.N. Prasad, T.L. Penner, N.J. Armstrong, M.C. Ezenyilimba, D.J. Williams, J. Am. Chem.Soc. 118 (1995) 4480.
[24] J.J. Maki, T. Verbiest, M. Kauranen, S. Van Elshocht, A. Persoons, J. Chem. Phys. 105 (1996) 767.
[25] A. Persoons, M. Kauranen, S. Van Elshocht, T. Verbiest, L. Ma, L. Pu, B.M.W. Langeveld-Voss, E.W. Meijer, Mol. Cryst. Liq. Cryst. 315 (1998) 93.

intensity of mass 51 ion at a high C_2H_4/CH_3OH ratio suggests that ethylene molecules have the greater opportunity to react with the protonated methanol ion in the presence of trace methanol. Thereafter the solvating ethylene molecules form the observed $(C_2H_4)_n(CH_3OH)H_3O^+$ ions. This sequence of peaks is observed throughout the entire cluster mass spectrum to the limit of our sensitivity.

Acknowledgment. This work was carried out with financial assistance from the Korea Standards Research Institute and the Korea S... fully acknowl... Alan L. Mack... ding the mani...

Push-Pull Porphyrins as Nonlinear Optical Materials

Kenneth S. Suslick,*,† Chin-Ti Chen,† Gerald R. Meredith,*,‡ and Lap-Tak Cheng‡

School of Chemical Sciences and Beckman Institute
University of Illinois at Urbana-Champaign
505 South Mathews Avenue, Urbana, Illinois 61801
Central Research and Development Department
The Du Pont Company, Experimental Station
P.O. Box 80356, Wilmington, Delaware 19880-0356

Received December 16, 1991
Revised Manuscript Received June 17, 1992

Due to their potential applications for optical communications, data storage, and electrooptical signal processing, molecules with nonlinear optical (NLO) properties have been extensively investigated.[1] As part of our interest in porphyrins and metalloporphyrins as photoresponsive[2] and field-responsive materials,[3] we have synthesized a series of "push-pull" porphyrins containing both donor and acceptor substituents and have examined their NLO properties. The enhancements in molecular hyperpolarizabilities in previous organic systems have relied on donor–acceptor interactions along one-dimensional pathways; our porphyrinic compounds are prototypes of donor–acceptor interactions in two dimensions.

Porphyrins with their large π-conjugated system provide a versatile synthetic base to create effective intramolecular charge transfer (CT). As shown in Figure 1, the difunctionalized tetraarylporphyrins with nitro groups (n) as electron acceptors and amino groups (a) as electron donors have been prepared. The synthesis of $H_2(an_3Por)$, $H_2(cis\text{-}a_2n_2Por)$, and $H_2(a_3nPor)$ does not involve the traditional crossed-condensation for multisubstituted porphyrins,[4] which are usually isolated only in low yields (<5%). Instead, $H_2(n_4Po4)$, $H_2(an_3Por)$, $H_2(trans\text{-}a_2n_2Por)$,

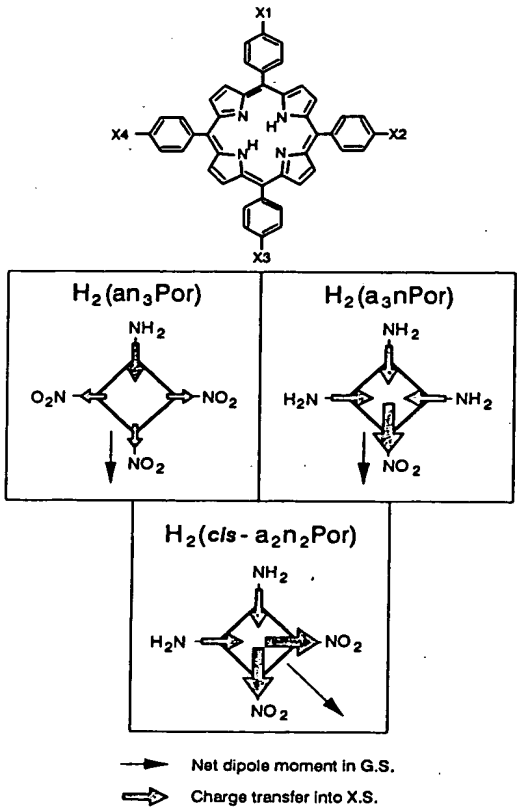

Figure 1. Structure, net dipole moment vectors, and charge-transfer transition vectors of push-pull porphyrins: $H_2(n_4Por)$, X1 = X2 = X3 = X4 = NO_2; $H_2(an_3Por)$, X1 = X2 = X3 = NO_2, X4 = NH_2; $H_2(trans\text{-}a_2n_2Por)$, X1 = X3 = NO_2, X2 = X4 = NH_2; $H_2(cis\text{-}a_2n_2Por)$, X1 = X2 = NO_2, X3 = X4 = NH_2; $H_2(a_3nPor)$, X1 = NO_2, X2 = X3 = X4 = NH_2; $H_2(a_4Por)$, X1 = X2 = X3 = X4 = NH_2; H_2TPP, X1 = X2 = X3 = X4 = H.

$H_2(cis\text{-}a_2n_2Por)$, $H_2(a_3nPor)$, and $H_2(a_4Por)$ were prepared by the partial reduction of the nitro groups of 5,10,15,20-tetrakis-(*p*-nitrophenyl)porphyrin[5] with 2.5 times the stoichiometric amount of $SnCl_2$. The reaction was performed under nitrogen in concentrated hydrochloric acid at 75 °C for 24 h. After the reaction was neutralized with concentrated ammonium hydroxide, the isolated solid mixture was placed in a Soxhlet apparatus and extracted with chloroform for 7 days. $H_2(an_3Por)$, $H_2(cis\text{-}a_2n_2Por)$, and $H_2(a_3nPor)$ were separated from each other by column chromatography in ~30% isolated yields each. They have been fully characterized by elemental analysis, TLC, and FAB-MS, UV–visible, FTIR, and ^1H NMR spectroscopies, as provided in the supplementary material. The optical spectra of these porphyrins are included in the supplementary material and show no absorbances at wavelengths greater than 680 nm.

The structural control of β, the second-order molecular hyperpolarizability, is well understood from both theoretical and experimental perspectives.[6] Organic molecules with strong electron donor and electron acceptor groups that are connected by a large conjugated π-electron system usually show high β values. Following this general rule, a variety of stilbenes, polyenes, and diazo molecules have been designed that have β values up

† University of Illinois at Urbana–Champaign.
‡ Du Pont Co.

(1) (a) Ulrich, D. R. *Mol. Cryst. Liq. Cryst.* **1990**, *189*, 3–38. (b) Khanarian, G., Ed. Nonlinear Optical Properties of Organic Materials II. *Proc. SPIE-Int. Soc. Opt. Eng.* **1989**, *1147*, 1–294. (c) Messier, J., Kajzar, F., Prasad, P. N., Ulrich, D. R., Eds. *Nonlinear Optical Effects in Organic Polymers*; Kluwer Academic Publishers: Dordrecht, The Netherlands, 1989. (d) Hann, R. A., Bloor, D., Eds. *Organic Materials for Nonlinear Optics*; Royal Society of Chemistry: London, 1989. (e) Prasad, P. N., Ulrich, D. R., Eds. *Nonlinear Optical and Electroactive Polymers*; Plenum: New York, 1988. (f) Heeger, A. J., Orenstein, J., Ulrich, D. R., Eds. *Nonlinear Optical Properties of Polymers*, MRS Symposium Proceedings; Materials Research Society: Pittsburgh, PA, 1988; Vol. 109.

(2) (a) Suslick, K. S.; Acholla, F. V.; Cook, B. R. *J. Am. Chem. Soc.* **1987**, *109*, 2812–3. (b) Hendrickson, D. N.; Kinnaird, M. G.; Suslick, K. S. *J. Am. Chem. Soc.* **1987**, *109*, 1243–4. (c) Suslick, K. S.; Watson, R. A. *Inorg. Chem.* **1991**, *30*, 912–9. (d) Suslick, K. S.; Watson, R. A.; Wilson, S. R. *Inorg. Chem.* **1991**, *30*, 2311–17.

(3) Suslick, K. S.; Chen, C.-T. *Proc. Am. Chem. Soc. Div. PMSE* **1990**, *63*, 272–6.

(4) (a) Ding, L.; Casas, C.; Etemad-Moghadam, G.; Meunier, B. *New J. Chem.* **1990**, *14*, 421–31. (b) Sun, Y.; Martell, A. E.; Tsutsui, M. *J. Heterocycl. Chem.* **1986**, *23*, 561–65. (c) Little, R. G.; Anton, J. A.; Loach, P. A.; Ibers, J. A. *J. Heterocycl. Chem.* **1975**, *12*, 343–9.

(5) Bettelheim, A.; White, B. A.; Raybuck, S. A.; Murray, R. W. *Inorg. Chem.* **1987**, *26*, 1009–17.

(6) (a) Marder, S. R.; Beratan, D. N.; Cheng, L.-T. *Science* **1991**, *252*, 103–6. (b) Prasad, R. N.; Reinharadt, B. A. *Chem. Mater.* **1990**, *2*, 660–9. (c) Chemla, D. S., Zyss, J., Eds. *Nonlinear Optical Properties of Organic Molecules and Crystals*; Academic Press: Orlando, FL, 1987; Vol.s 1 and 2. (d) Williams, D. J. *Angew. Chem., Int. Ed. Engl.* **1984**, *23*, 690–703. (e) Shen, Y. R. *The Principles of Nonlinear Optics*; Wily: New York, 1984. (f) Williams, D. J., Ed. *Nonlinear Optical Properties of Organic and Polymeric Materials*; ACS Symposium Series 233; American Chemical Society: Washington, DC, 1983.

0002-7863/92/1514-6928$03.00/0

Table I. Dipole Moments and EFISH Hyperpolarizabilities of Various Nitro/Amino Disubstituted Arenes and Tetraphenylporphyrins[a]

Compound	μ (10^{-18} esu)[a]	β (10^{-30} esu)[a]
I 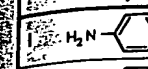	1.5[b]	0.55[b]
II 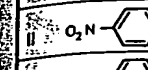	4.0[b]	1.9[b]
III 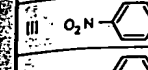	6.2[c] 7.8[d]	9.2[c] 10[d]
IV 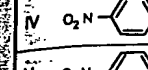	5.0 7.8[d]	24 24[d]
V 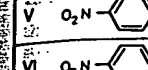	7.6[d]	16[d]
VI 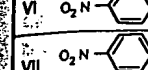	10[d]	11[d]
VII 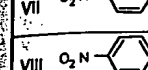	5.1	40
VIII 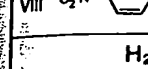	9	190 ± 50
$H_2(an_3Por)$		≤10
$H_2(cis\text{-}a_2n_2Por)$	7±1	30±10
$H_2(a_3nPor)$	5±1	20±10

[a] In $CHCl_3$. [b] Neat. [c] In acetone. [d] In NMP. [e] The probe wavelength was 1.91 μm, derived from H_2 Raman shifting of a 10 ns pulsed Nd:YAG laser (1.06 μm), as described in ref 14. Data for compounds I–VIII from ref 9.

to 1000 × 10^{-30} esu.[7] Phthalocyanines, which have a similar π-conjugated macrocyclic ring, have been predicted *theoretically* to have relatively large β values (165 × 10^{-30} esu) after they are unsymmetrically difunctionalized with four nitro groups and four amino groups.[8]

Table I compares the electric-field-induced second-harmonic generation (EFISH) measurements of our porphyrins (in $CHCl_3$ at 1.91 μm) with their two-dimensional conjugation to other linear, high β molecules.[9] The three porphyrins show moderately high β values. They are significantly smaller, however, then that of the tetraene VIII. The β value determined by the EFISH technique is a polarizability projection from the full β tensor: it is the vector component projected onto the molecular dipole. The β value is therefore expected to be diminished when the two directions differ significantly. Thus, in EFISH measurements, linear π-conjugated molecules have the advantage compared to those with nonlinear, but similar sized, π systems. The additional dimensionality of the π-conjugated system in a direction perpendicular to the principal molecular axis actually reduces the overall NLO response.[10] This explains the unexpected smaller β values being found for dinitrosostilbenes compared to nitrostilbenes.[11]

A similar view can also be applied to $H_2(an_3Por)$, $H_2(cis\text{-}a_2n_2Por)$, and $H_2(a_3nPor)$. As shown in Figure 1, the net dipole moment of $H_2(an_3Por)$ and $H_2(a_3nPor)$ is expected to be along the obvious mixed-substitution axis, while the moment f $H_2(cis\text{-}a_2n_2Por)$ is expected along the axis of the pyrrole N atoms, bisecting the pyrrole rings. The influence of off-moment substituents is clearly reduced or canceled in this situation by geometric factors. The behavior of β is somewhat different. Despite the similarity between the dipole moments of their ground states, $H_2(an_3Por)$ and $H_2(a_3nPor)$ are not equivalent in the charge-transfer behavior of their excited states. Donating NH_2 groups push substantially less charge into the conjugation system than the accepting NO_2 groups withdraw in the excited CT states. In $H_2(a_3nPor)$, charge is pushed into the total conjugation system by three donors and, in the excited CT state, pulled by one strong acceptor (shown schematically in Figure 1). The CT displacements are well aligned with the dipole axis and give a strong EFISH β value (20 × 10^{-30} esu). On the other hand, in $H_2(an_3Por)$, only one donor pushes charge into the macrocycle, while this charge is drained by three competing strong acceptors. In the competing CT displacements, only one of the acceptor's contributions is well aligned with μ. Thus, $H_2(an_3Por)$ displays a weaker EFISH β value (≤10 × 10^{-30} esu). This line of reasoning also explains the larger β value of $H_2(cis\text{-}a_2n_2Por)$ (30 × 10^{-30} esu).

It is important in considering the potential of push-pull porphyrins to note that tetraarylporphyrins have a less effective intramolecular CT due to the dihedral twist between phenyl rings and the plane of the porphyrin. Because of steric hindrance, the phenyl ring is expected to be out of the plane of porphyrin. The X-ray crystallographic structure[12] of H_2TPP has an average dihedral angle of 60°. The rotational barriers of the phenyl rings have been determined by NMR techniques[13] and are found to be relatively high, ranging from 11 to 17 kcal/mol. Theoretical calculations have shown that the β value will be reduced by about 50% due to this torsional angle.[10] This dihedral angle effect in polyphenyl systems is apparent from the decreasing β values[14] for IV, V, and VI in Table I. NMR studies indicate that the effects of phenyl substituents on tetraarylporphyrins are transmitted to the porphyrin π system by a combination of σ and π induction, rather than σ induction and π conjugation.[15] A similar conclusion can be drawn from the NMR data on these porphyrins.[16] Further evidence of inefficient CT in $H_2(an_3Por)$, $H_2(cis\text{-}a_2n_2Por)$, and $H_2(a_3nPor)$ can be found in their UV–visible spectra. The typical intramolecular CT absorption band occurs within the visible light region and depends on the size of π system. Its intensity can be comparable to that of the π–π* transitions of porphyrins, albeit broader.[17] The UV–visible spectra of these porphyrins, however, are dominated by the porphyrinic π–π* absorption bands and are similar in all six porphyrins (i.e., $H_2(n_4Por)$, $H_2(an_3Por)$, $H_2(trans\text{-}a_2n_2Por)$, $H_2(cis\text{-}a_2n_2Por)$, $H_2(a_3nPor)$, and $H_2(a_4Por)$). Since a CT band is relatively weak, we must conclude that the coupling of the donor and acceptor groups across the porphyrin ring is limited.

In conclusion, we have synthesized and isolated the first set of porphyrins with tailored quadratic NLO properties and have measured them by the EFISH technique. Though the molecular hyperpolarizabilities of these porphyrins are substantial, they are lower than one might expect for such large conjugation systems. Two factors reduce the efficacy of CT enhancement of EFISH β values in these compounds. First, EFISH is primarily sensitive to CT parallel to the permanent dipole moment, but here substantial CT in perpendicular directions competes. Second, the intramolecular CT transitions are relatively weak in tetraarylporphyrins due to the dihedral angle between phenyl groups and

(7) (a) Prasad, P. N.; Williams, D. J. *Introduction to Nonlinear Optical Effects in Molecules and Polymers*; Wiley: New York, 1991. (b) Bredas, J. L.; Chance, R. R. *Conjugated Polymeric Materials: Opportunities in Electronics, Optoelectronics, and Molecular Electronics*; Kluwer Academic Publishers: Dordrecht, The Netherlands, 1990.
(8) Li, D.; Ratner, M. A.; Marks, T. J. *J. Am. Chem. Soc.* **1988**, *110*, 1707–15.
(9) (a) Cheng, L.-T.; Tam, W.; Stevenson, S. H.; Meredith, G. R.; Rikken, G.; Marder, S. R. *J. Phys. Chem.* **1991**, *95*, 10631–10643. (b) Cheng, L.-T.; Tam, W.; Rikken, G.; Marder, S. R.; Stiegman, A. E.; Spangler, C. *J. Phys. Chem.* **1991**, *95*, 10643–10652.
(10) Leung, P. C.; Stevens, J.; Harelstad, R. E.; Spiering, M. S.; Gerbi, D. J.; Francis, C. V.; Trand, J. E.; Tiers, G. V. D.; Boyd, G. T.; Ender, D. A.; Williams, R. C. *Proc. SPIE-Int. Soc. Opt. Eng.* **1989**, *1147*, 48–60.
(11) Tiemann, B. G.; Marder, S. R.; Perry, J. W.; Cheng, L.-T. *Chem. Mater.* **1990**, *2*, 690–5.
(12) Sliver, S. J.; Tulinsky, A. *J. Am. Chem. Soc.* **1967**, *89*, 3331–7.
(13) Eaton, S. S.; Fishwild, D. M.; Eaton, G. R. *J. Am. Chem. Soc.* **1977**, *99*, 6594–9.
(14) Cheng, L.-T.; Tam, W.; Meredith, G. R.; Rikken, G. L. J. A.; Meijer, E. W. *Proc. SPIE-Int. Soc. Opt. Eng.* **1989**, *1147*, 61–72.
(15) Walker, F. A.; Blake, V. L.; McDermott, G. A. *Inorg. Chem.* **1982**, *21*, 3342–8.
(16) Suslick, K. S.; Chen, C.-T. Unpublished results.
(17) Ulman, A.; Willand, C. S.; Kohler, W.; Robello, D. R.; Williams, D. J.; Handley, L. *J. Am. Chem. Soc.* **1990**, *112*, 7083–90.

the porphyrin ring. We are currently examining amphiphilic derivatives of these porphyrins as Langmuir–Blodgett films and the macroscopic NLO properties of these assemblies.

Acknowledgment. This work was supported by the National Institutes of Health and by the Department of Energy (EDFG02-91ER45439) with a research assistantship (C.T.C.).

Supplementary Material Available: Spectroscopic and analytical data for $H_3(an_3Por)$, $H_2(trans\text{-}a_2n_2Por)$, $H_2(cis\text{-}a_2n_2Por)$, and $H_2(a_3nPor)$ (4 pages). Ordering information is given on any current masthead page.

Rapid Detection of ^{57}Fe NMR Chemical Shifts of Model Hemes: An Approximate Correlation between ^{57}Fe and ^{31}P Chemical Shifts of Fe(II) Porphyrins Bound to Phosphine Axial Ligands

Larry M. Mink, Kenner A. Christensen, and F. Ann Walker*

Department of Chemistry, University of Arizona
Tucson, Arizona 85721

Received March 30, 1992
Revised Manuscript Received June 15, 1992

The NMR chemical shift range of the ^{57}Fe nucleus is at least 12 000 ppm.[1-4] Therefore, ^{57}Fe NMR spectroscopy is potentially an extremely sensitive, direct probe of the electron density and asymmetry at the heme iron. However, the combination of low natural abundance (2.19%) and a low magnetogyric ratio makes the ^{57}Fe nucleus in natural abundance only 7.4×10^{-7} times as sensitive as the proton. Direct detection of ^{57}Fe resonances of model hemes and heme proteins[4-9] has therefore utilized isotopic enrichment of ^{57}Fe. Nevertheless, the direct detection of ^{57}Fe signals typically requires hours of NMR time and large volumes of enriched sample. Thus, indirect detection of ^{57}Fe rsonance frequencies is an attractive alternative method. La Mar and co-workers[10] showed some time ago that such double resonance techniques could allow the determination of ^{57}Fe chemical shifts of carbon monoxy complexes of heme proteins using ^{13}CO- and ^{57}Fe-enriches samples. Morishima[11] and Nozawa[12] have similarly determined ^{57}Fe chemical shifts using ^{15}N-enriched porphyrins. Koridze and co-workers[13] have utilized similar techniques, with ^{13}C as the observed nucleus, for ^{57}Fe-enriched ferrocenes and ferrocenyl cations, without ^{13}C enrichment. Benn and co-workers have utilized both ^{13}C[14] and ^{31}P[2,3] as the observed nucleus for investigating a number of ferrocenes[14] and phosphine-coordinated organometallic complexes of a number of low-γ metal nuclei.[2,3] The latter authors have also demonstrated the increased enhancement obtained by inverse 2D polarization transfer techniques.[2,3]

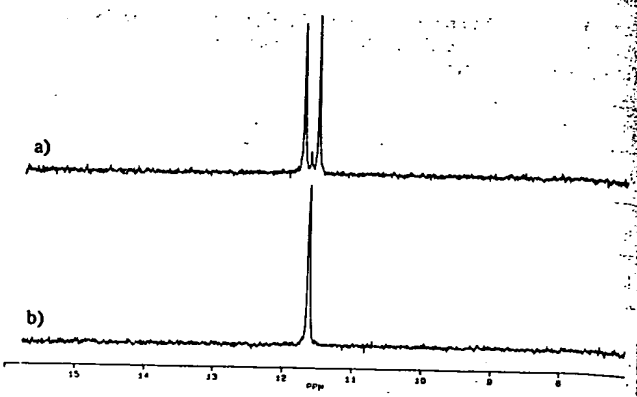

Figure 1. ^{31}P spectra of 95% ^{57}Fe-enriched $[(p\text{-}OCH_3)_4TPPFe(PMe_3)_2]$ at 25 °C in C_6D_6 (12 mM), recorded on a Bruker AM-500 spectrometer in the presence of broad band proton decoupling:[25] (a) off-resonance ^{57}Fe irradiation (128 acquisitions); (b) on-resonance ^{57}Fe irradiation, resulting in decoupling of the ^{31}P–^{57}Fe doublet (64 acquisitions). Chemical shifts are vs external 85% H_3PO_4; sample concentration was ~6 mM. Stepping through the ^{57}Fe frequency range around 16.2 MHz with a decoupling power of 0.5 W (bandwidth ~100 Hz) causes the ^{31}P doublet (J_{Fe-P} = 35–59 Hz) to collapse when the resonant frequency of ^{57}Fe is reached.

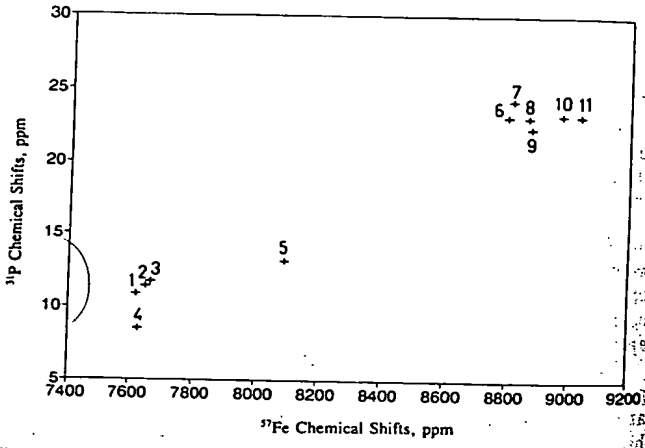

Figure 2. Correlation between ^{31}P and ^{57}Fe chemical shifts at 21 °C in C_6D_6, with ^{57}Fe shifts relative to external 90% $Fe(CO)_5$ in C_6D_6 and ^{31}P shifts relative to external 85% H_3PO_4: $[(p\text{-}Cl)_4TPPFe(PMe_3)_2]$ (1); $[TPPFe(PMe_3)_2]$ (2); $[(p\text{-}OCH_3)_4TPPFe(PMe_3)_2]$ (3); $[TPPFe(PMe)(CO)]$ (4); $[TPPFe(PMe_3)(n\text{-}BuNC)]$ (5); $[TPPFe(PMe_3)(n\text{-}BuNH_2)]$ (6); $[TPPFe(PMe_3)(PhCH_2SCH_3)]$ (7); $[TPPFe(PMe_3)(NMeIm)]$ (8); $[TPPFe(PMe_3)(4\text{-}NMe_2Py)]$ (9); $[TPPFe(PMe_3)(Py)]$ (10); $[TPPFe(PMe_3)(4\text{-}CNPy)]$ (11).

We have applied the 1D indirect method utilizing the sensitive ^{31}P nucleus as the detected signal to a series of model hemes of the type $[(RTPP)^{57}Fe(PMe_3)(L)]$[15-19] (RTPP = a symmetrical, R-substituted tetraphenylporphyrin, L = PMe_3, CO, isonitrile, aliphatic amine, imidazole, pyridine, or thioether). The coordination of one or two phosphine ligands to the axial positions of Fe(II) model hemes has allowed us to determine ^{57}Fe chemical shifts of new complexes by decoupling the ^{57}Fe–^{31}P doublet of enriched $^{57}Fe(II)$ porphyrins, as shown in Figure 1. While it might be expected that finding the proper ^{57}Fe frequency to

(1) Schwenck, A. *J. Magn. Reson.* **1971**, *5*, 376–389.
(2) (a) Benn, R.; Brenneke, H.; Frings, A.; Lehmkuhl, H.; Mehler, G.; Rufinska, A.; Wildt, T. *J. Am. Chem. Soc.* **1988**, *110*, 5661. (b) Benn, R.; Rufinska, A. *Magn. Reson. Chem.* **1988**, *26*, 893.
(3) Benn, R.; Brevard, C. *J. Am. Chem. Soc.* **1986**, *108*, 5622.
(4) Baltzer, L. *J. Am. Chem. Soc.* **1987**, *109*, 3479.
(5) Baltzer, L.; Becker, E. D.; Averill, B. A.; Hutchinson, J. M.; Gansow, O. *J. Am. Chem. Soc.* **1984**, *106*, 2444.
(6) Chung, J.; Lee, H. C.; Oldfield, E. *J. Magn. Reson.* **1990**, *90*, 148.
(7) Baltzer, L.; Landergren, M. *J. Chem. Soc. Chem. Commun.* **1987**, 32.
(8) Baltzer, L.; Landergren, M. *J. Am. Chem. Soc.* **1990**, *112*, 2804.
(9) Lee, H. C.; Gard, J. K.; Brown, T. L.; Oldfield, E. *J. Am. Chem. Soc.* **1985**, *107*, 4087.
(10) (a) LaMar, G. N.; Viscio, D. B.; Budd, D. L.; Gersonde, K. *Biochem. Biophys. Res. Comm.* **1978**, *82*, 19. (b) LaMar, G. N.; Dellinger, C. M.; Sankar, S. S. *Biochem. Biophys. Res. Comm.* **1985**, *128*, 628.
(11) Morishima, I.; Inabushi, T.; Sato, M. *J. Chem. Soc., Chem. Commun.* **1978**, 106–107.
(12) Nozawa, T.; Sato, M.; Hatano, M.; Kobayashi, N.; Osa, T. *Chem. Lett.* **1983**, 1289.
(13) Koridze, A. A.; Astakhova, N. M.; Petrovskii, P. V. *J. Organomet. Chem.* **1983**, *254*, 345–360.
(14) Benn, R.; Rufinska, A.; Kralik, M. S.; Ernst, R. D. *J. Organomet. Chem.* **1989**, *375*, 115–121.
(15) ^{57}Fe metal, 95% enriched, was purchased from New England Nuclear and inserted into the tetraphenylporphyrins as described previously.[16] The yields of TPP^{57}FeCl and the para-substituted-TPP^{57}FeCl derivatives were 80–90%, based on ^{57}Fe as the limiting reagent.
(16) Walker, F. A.; Huynh, B. H.; Scheidt, W. R.; Osvath, S. R. *J. Am. Chem. Soc.* **1986**, *108*, 5288–5297.
(17) Reduction of Fe(III) porphyrins was carried out by the method of Balch et al.;[18] mixed-ligand complexes were prepared by the method of Sodano and Simonneaux.[19]
(18) Balch, A. L.; Chan, Y.; Cheng, R.; LaMar, G. N.; Latos-Grazynski, L.; Renner, M. W. *J. Am. Chem. Soc.* **1984**, *106*, 7779–7785.
(19) Sodano, P.; Simonneaux, G. *J. Chem. Soc., Dalton Trans.* **1988**, 2615.

0002-7863/92/1514-6930$03.00/0